

# NGU



Norges geologiske  
undersøkelse  
Bulletin 398

Ole Graversen:  
Geology and Structural Evolution  
of the Precambrian Rocks of the  
Oslofjord-Øyeren Area,  
Southeast Norway

Universitetsforlaget 1984  
Trondheim - Oslo - Bergen - Tromsø



# NGU

## Norges geologiske undersøkelse

Geological Survey of Norway

---

*Norges geologiske undersøkelse* (Geological Survey of Norway), Leiv Eirikssons vei 39, Trondheim. Telephone: national (07) 92 16 11, International + 47 7 92 16 11. Postal address: Box 3006, N-7001 Trondheim, Norway.

Director: Dr. philos. *Knut S. Heier*

Bedrock Geology Division: div.director Dr. philos. *Peter Padget*

Superficial Deposits Division: div.director *Bjørn A. Follestad*

Geophysics Division: div.director *Inge Aalstad*

Geochemistry Division: div.director *Bjørn Bolviken*

The publications of *Norges geologiske undersøkelse* are divided into 2 series, *Bulletin* and *Skrifter*, each of which is issued as consecutively numbered volumes.

*Bulletins* comprise scientific contributions to the earth sciences of regional Norwegian, general, or specialist interest. The preferred language is English.

*Skrifter* first and foremost comprise geological map-sheet descriptions, but also include papers and reports of specialist or public interest of regional, technical, economic, environmental and other aspects of applied earth sciences. The *Skrifter* are issued in Norwegian, with an Abstract and Summary in English.

### EDITOR

Førstestatsgeolog Dr. *David Roberts*, Norges geologiske undersøkelse, P.O.Box 3006, N-7001 Trondheim, Norway.

### PUBLISHER

*Universitetsforlaget*, P.O.Box 2959, Tøyen, 0608 Oslo 6, Norway.

### DISTRIBUTION OFFICES

*Norway*: Universitetsforlaget, P.O.Box 2977, Tøyen, 0608 Oslo 6. *United Kingdom*: Global Book Resources Ltd., 109 Great Russell Street, London WC1B, 3ND.

*United States and Canada*: Columbia University Press, 136 South Broadway, Irvington on Hudson, New York 10533.

### EARLIER PUBLICATIONS AND MAPS

The most recent list of NGU publications and maps, 'Publikasjoner og kart 1879-1980', appeared in 1981. Copies can be obtained from the Publisher.

The most recent maps available from NGU are listed in the back cover.

### MANUSCRIPTS

From 1.1.1984 the NGU Bulletin and *Skrifter* series will be printed in a 2-column format as e.g. in *Norsk Geologisk Tidsskrift*. Contributors are asked to prepare their manuscripts in accordance with the 'Instructions to Authors' printed inside the back cover of NGU. A more comprehensive 'Instructions' for potential authors of NGU Bulletin and *Skrifter* papers will be issued during 1984.

# Geology and Structural Evolution of the Precambrian Rocks of the Oslofjord-Øyeren Area, Southeast Norway

OLE GRAVERSEN

Graversen, O. 1984: Geology and structural evolution of the Precambrian rocks of the Oslofjord-Øyeren area, Southeast Norway. *Nor. geol. unders. Bull.* 398, 1–50.

The area (1200 km<sup>2</sup>) described covers the northern part of a major thrust segment in the eastern subprovince of the Sveconorwegian orogenic belt along the southwestern margin of the Baltic Shield. The oldest rock unit is a supracrustal gneiss, which was later intruded by biotite gneiss (oldest), augen gneiss, a metatonalite/granite complex, and granitic orthogneiss (youngest). Four fold episodes, F<sub>0</sub>–F<sub>3</sub>, of regional importance have been distinguished. In the earliest regional fold structure (F<sub>0</sub>) the biotite gneiss occurs as the core of a large recumbent fold nappe enveloped by supracrustal gneiss. After this early fold episode the supracrustal gneiss was intruded by the augen gneiss, which forms a distinctive unit parallel to the biotite gneiss.

F<sub>1</sub> folds generally have subhorizontal NNE–SSW fold axes and are overturned to the east; the deformation is accompanied by medium- to high-grade amphibolite facies metamorphism and widespread anatexis. F<sub>2</sub> folds are superimposed on the F<sub>1</sub> folds nearly at right angles. The F<sub>2</sub> fold axes plunge at about 30° to the NW, and the E–W trending axial planes are inclined to the south. Medium-grade amphibolite facies metamorphism with renewed anatexis accompanied F<sub>2</sub>. During F<sub>2</sub> the western part of the area acted as a rigid block, while to the east, earlier structures were reoriented by the F<sub>2</sub> folds. The F<sub>3</sub> folds trend NNW–SSE with steep axial planes and rather shallow NNW-plunging fold axes. The deformation took place under medium- to low-grade amphibolite facies conditions, while retrogressive conditions in the greenschist-amphibolite transition facies occurred during the waning stages of this episode (F<sub>3</sub>’).

Granitic orthogneiss was intruded at around 1320 Ma between the F<sub>2</sub> and F<sub>3</sub> episodes, and the metatonalite/granite complex intruded shortly before F<sub>2</sub> (metamorphism) at around (?) 1500 Ma. These results indicate that only the youngest deformation (F<sub>3</sub>) took place in the Sveconorwegian orogeny. The major tectono-metamorphic evolution took place in pre-(Grenville-)Sveconorwegian times, and F<sub>1</sub> and F<sub>0</sub> presumably relate to a pre-1500 Ma deformation history.

*Ole Graversen, Institut for almen Geologi, University of Copenhagen, Øster Voldgade 10, DK-1350 København K, Denmark.*

## Contents

Introduction .....	3
Geological setting .....	3
Previous work .....	5
Aims and methods of the present work .....	5
Description of the main rock types .....	6
Supracrustal gneiss .....	6
Metaplutonic rocks intruding the supracrustal gneiss .....	10
Biotite gneiss .....	10
Meta-anorthosite/leucodiorite .....	14
Augen gneiss .....	15
Metatonalite/granite complex .....	16
Granitic orthogneisses .....	19
Amphibolites and metadolerites .....	20
Summary – relationships of metamorphism and structures .....	25
Geometrical and chronological analysis of the regional structure .....	26
Introduction .....	26
Major F <sub>3</sub> structures: the Mysen syncline, the Østensjø anticlinorium and the Østmarka syncline .....	27
Pre F <sub>3</sub> -structures in the Mjæren–Lyseren area .....	30
Supracrustal gneiss wedges in the granitic gneisses – Establishment of F <sub>1</sub> and F <sub>2</sub> structures .....	30

F <sub>1</sub> and F <sub>2</sub> folds in the Østmarka syncline .....	32
F <sub>2</sub> , F <sub>1</sub> and (?) F <sub>0</sub> structures outside the F <sub>3</sub> domain in the Bunnefjorden- Hallangspollen area .....	34
The Gjersjø dome .....	36
F <sub>0</sub> - The biotite gneiss-supracrustal gneiss nappe .....	38
Nesodden .....	40
Summary of the regional structure .....	40
Structural position of the metatonalite/granite complex .....	42
Correlation of the structural evolution in the Oslofjord-Øyeren area with that in adjoining areas in the Østfold and median segments .....	42
Correlation within the Østfold segment .....	42
Correlation between the Østfold and median segments .....	43
Discussions of the results and aspects of the regional geology .....	44
Structural considerations .....	44
Orogenic evolution .....	45
Acknowledgements .....	47
References .....	47

## Introduction

The area described in this paper is situated in southeast Norway and extends from Oslo southwards and eastwards into Akershus and Østfold counties. It includes the Nesodden peninsula in Oslofjorden to the west, and the Østmarka province between Bunnefjorden and Lake Øyeren to the east. The area was glaciated during the Pleistocene and the topographical relief is gentle with elevations from sea-level up to 300 m. Numerous lakes form part of the scenery in the area which is otherwise characterized by forests and farmland outside the urban areas.

## GEOLOGICAL SETTING

The Precambrian basement in southeast Norway and southwest Sweden is part of the Sveconorwegian province (Magnusson 1960) in the southwestern part of the Baltic Shield (Kratz et al. 1968). The Sveconorwegian province is the Scandinavian counterpart of the Grenville province of the Canadian Shield

(Wynne-Edwards & Hassan 1970, Wynne-Edwards 1972, Zwart & Dornsiepen 1978). Isotopic ages in the 1200–900 Ma range characterise the Sveconorwegian province (e.g. Magnusson 1960, Broch 1964, Verstevee 1975, Skiöld 1976, Pedersen et al. 1978, Wielens et al. 1980), and the deformation and metamorphism are referred to the Sveconorwegian (or Grenville-Sveconorwegian) orogeny. Within the Sveconorwegian province indications of the early history of the rocks are provided by a number of Rb/Sr whole rock ages of up to about 1800 Ma; these have been reported from southwest Sweden (Skiöld 1976, Welin & Gorbatshev 1976 a, b, 1978 a, b, c, d, Daly et al. 1979) and southern Norway (O'Nions & Baadsgaard 1971, O'Nions & Heier 1972, Verstevee 1975, Jacobsen & Heier 1978, Pedersen et al. 1978, Pedersen et al. 1979, Field & Råheim 1979 a, b, 1980, Wielens et al. 1980). The evolution of southwest Sweden has most recently been reviewed by Lundqvist (1979), Gorbatshev (1980) and Gorbatshev & Welin (1980); Berthelsen (1980) and Falkum & Petersen (1980) incorporated the evolution of southern Norway (Pedersen et al. 1978) and adjoining parts of Sweden in plate tectonic models culminating in the (Grenville-) Sveconorwegian orogeny.

The Sveconorwegian orogenic belt exhibits general N-S trends which to the east (in Sweden) cut across the older E-W trending Sveco-karelian structures. Berthelsen (1980) divided the Sveconorwegian belt into a western subprovince comprising the Precambrian of southern Norway west of the Kongsberg-Bamble region, and an eastern subprovince incorporating southeast Norway and southwest Sweden west of the Sveco-karelian orogenic belt (Rankama & Welin 1972, Lundqvist 1979) (Fig. 1). The eastern subprovince is bounded to the east by the Sveconorwegian front, along the central Swedish shear zone or Protogine Zone, and is divided into an eastern, a median and a western (Kongsberg-Bamble-Østfold) segment by major west-dipping thrusts (Berthelsen 1980, Hageskov 1980) (Fig. 1). The Kongsberg-Bamble-Østfold segment is further subdivided by the Oslofjord high-strain zone (Berthelsen 1980, Hageskov 1980) into the western Kongsberg-Bamble segment and the eastern Østfold seg-

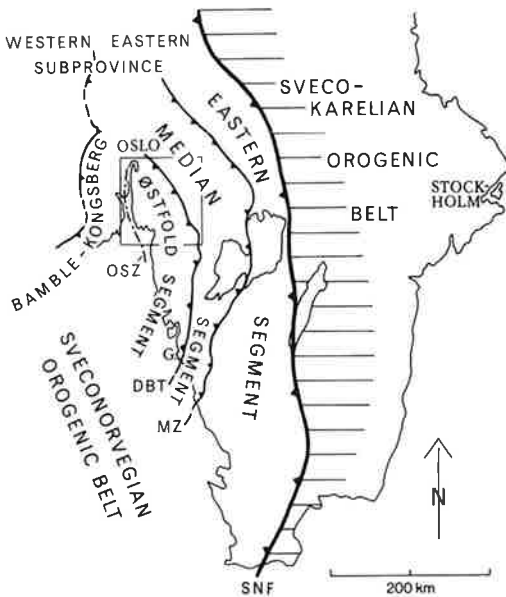
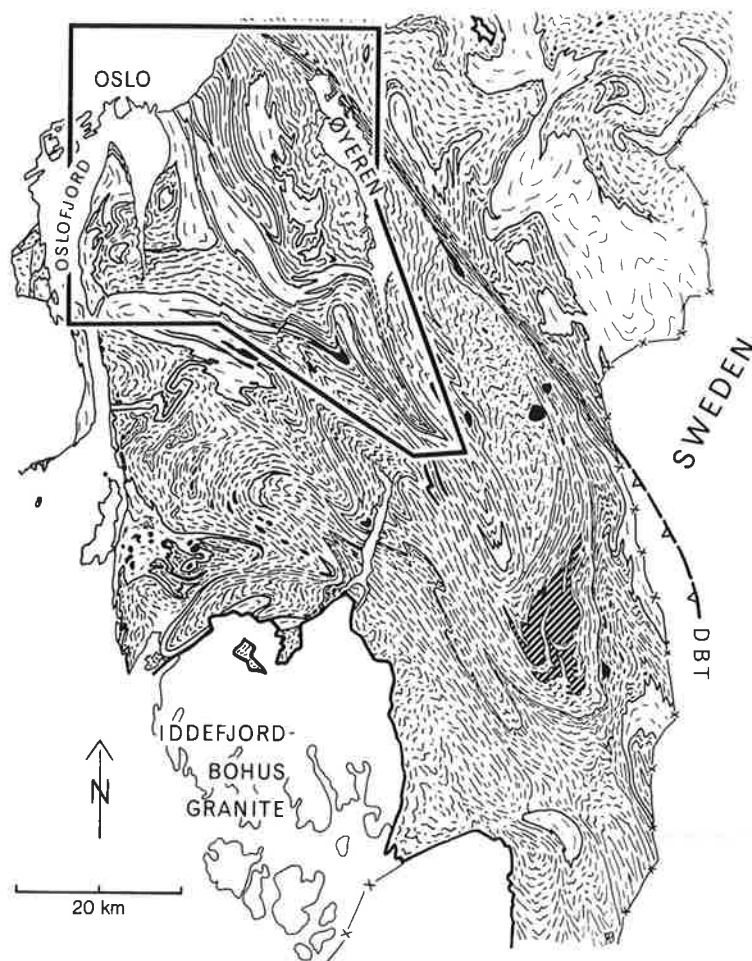


Fig. 1. Tectonic sketch of the eastern Sveconorwegian subprovince in southeast Norway and southwest Sweden (partly based on Berthelsen 1980). Frame indicates position of the Østfold region illustrated in Fig. 2. SNF: Sveconorwegian front, MZ: the Mylonite zone, DBT: Dalsland boundary thrust, OSZ: Oslofjord strain zone, G: Göteborg.

Fig. 2. Geological sketch map of the Østfold region, SE Norway, with location of the Oslofjord-Øyeren area indicated. Modified from a compilation by A. Berthelsen in Pedersen et al. (1978). DBT: Dalsland boundary thrust.



ment. The Østfold region (Pedersen et al. 1978) (Fig. 2) covers the northern (Norwegian) part of the Østfold segment and the adjoining parts of the median segment separated by the Dalsland boundary thrust (Berthelsen 1978).

The area described in this paper is situated within the Østfold region (Pedersen et al. 1978) and comprises the northern part of the Østfold segment (Fig. 2). In this segment the St. Le-Marstrand 'series' (Larsson 1956, Lundegårdh 1958) in Sweden forms a natural continuation of the supracrustal gneisses of the present area. These supracrustal gneisses are the oldest rocks recognized in the western segment; the subsequent evolution of the area is characterized by several periods of emplacement of tonalitic to granitic rocks separated

by intrusion of basic dykes. Major intrusion periods occur at 1600–1700 Ma, around 1500 Ma and 1400 Ma, between 1200 and 1300 Ma, and around 900–950 Ma (Skiöld 1976, Jacobsen & Heier 1978, Pedersen et al. 1978, Daly et al. 1979, Berthelsen 1980, Gorbatshev & Welin 1980, Hageskov & Pedersen 1980, Skjernaa & Pedersen 1982). The periods of intrusion were preceded and separated by orogenic episodes involving folding and amphibolite facies metamorphism accompanied by widespread migmatite formation.

The anorogenic Iddefjord-Bohus composite granite batholith (Pedersen et al. 1978, Berthelsen 1980, Gorbatshev 1980) with its widespread undeformed pegmatite dykes marks the close of the Sveconorwegian orogeny. Radiometric Rb/Sr whole rock ages of

the Iddefjord-Bohus granite vary between  $923 \pm 39$  Ma (Pedersen et al. 1978) and  $881 \pm 34$  Ma (Killeen & Heier 1975).

Towards the end of the Proterozoic the Sveconorwegian orogenic areas were peneplaned. Cambrian alum shale representing the Cambrian transgression is preserved in a small downfaulted area along Lake Øyeren (Holtedahl 1907). Palaeozoic sediments are also preserved in the downfaulted Oslo graben delimiting the area to the westnorthwest. Rocks forming part of the Permian magmatic province along the Oslo graben intrude the basement rocks as minor gabbroid (Oslo-essexite) plugs (Hageskov & Jorde 1980), and as dolerite and rhomb-porphry dykes.

#### PREVIOUS WORK

The precambrian bedrock southeast of Oslo has attracted little attention compared with the adjoining fossiliferous Palaeozoic strata and the rocks of the Oslo graben. The limited interest in the Precambrian terrain is reflected in the regional descriptions (Keilhau 1850, Kjerulf 1857, 1879, Barth 1960, 1963, Oftedahl 1974) and the regional geological maps (Kjerulf & Dahll 1858-65, Brøgger & Schetelig 1900, Holtedahl & Dons 1960) which provide little information about the Precambrian bedrock, with only a few granites distinguished from undifferentiated areas of gneiss. More detailed descriptions and maps are, however, available from Nesodden (Brock 1926, Gleditsch 1952) and Eidsberg (Rekstad 1921). Detailed mapping and structural analysis only became possible with the development of adequate methods (see e.g. Ramsay 1958 a, b, Berthelsen 1974) and production of modern, detailed photogrammetric maps (Økonomisk kartverk 1958).

Detailed mapping in the Moss area was started in 1965 (Berthelsen 1967); during the following years the area under study was extended through reconnaissance mapping and more detailed surveys by geology students. Since 1972 systematic mapping has been carried out by staff members of the Institut for almen Geologi, Københavns Universitet (Institute of General Geology, University of Copenhagen), through a formalized arrangement with Norges Geologiske Under-

søkelse. The results of this work, in simplified form, are incorporated in the new 1:1 M geological map of Norway (Sigmond et al. 1984). Detailed descriptions from restricted areas or papers focusing on subjects of special interest have been published by Berthelsen (1967, 1970, 1977, 1978), Graversen (1973, 1974, 1980), Graversen & Hageskov (1971), Hageskov (1972, 1978, 1980), Hageskov & Jorde (1980), Hageskov & Pedersen (1980), Skjernaa (1972) and Zetterstrøm (1974). In the Østfold region Pedersen et al. (1978) demonstrated repeated periods of intrusion from about 1800 Ma to around 1300 Ma, with the younger fold episodes postdating the 1300 Ma intrusions. Pedersen (1979) has suggested one deformation episode prior to  $1631 \pm 53$  Ma and another around 1500 Ma. In later description of areas in the western and eastern parts of the region (Hageskov 1980, Hageskov & Pedersen 1980, Skjernaa et al. 1979, Skjernaa & Pedersen 1982), it was concluded that the two or three major fold episodes recognized in these areas postdate intrusive periods at  $1320 \pm 22$  Ma and  $1277 \pm 20$  Ma, respectively; this implies that the major structures observed were all developed during the Sveconorwegian orogeny. This conclusion, however, is not supported by the present study.

#### AIMS AND METHODS OF THE PRESENT WORK

The area described here covers a complete section across the Østfold thrust segment formed during the Sveconorwegian regeneration of an old basement area. A broad account of the general geology is given, although special emphasis is laid on the structural framework in order to unravel the Sveconorwegian and pre-Sveconorwegian evolution.

The Precambrian bedrock in the area described is mainly composed of granitic gneisses with subordinate basic rocks. Distinctive key horizons are lacking, and in order to enable a structural analysis of the megascopic structures to be made, mapping of the sub-conformable granitic gneisses was carried out as lithostructural mapping (Berthelsen 1960 a). The gneiss *tectonostratigraphy* established in this way provides the basis for the structural analysis.

The major petrographic features of each mapping unit have been determined, and are described below. However, the main emphasis has been the establishment of a *teutonochronology* for each unit: a chronology of metamorphic evolution and migmatite formation relative to the structural evolution, contact relationships with adjacent units and the presence or absence of metabasite dykes.

The field mapping was based on 1:5,000 and 1:10,000 photogrammetric maps (Økonomisk kartverk 1958), while 1:50,000 mapsheets (Series M 711, 2-NOR edition) were used for the final compilation. The topographical relief is moderate (0–300 m), and the exposure is moderately good in regard to the extension of the rock units and the size of the structures. The compilation (Plate 1) was carried out by the author and included additional reconnaissance mapping. The field work was carried out during the summers 1968–76, and during this period the author spent 12½ months in the field.

In the description of the rocks, petrographic names follow the classification recommended by Streckreisen (1974). The metamorphic facies is of Barrovian type and its description is in accordance with Turner (1968).

In the petrographic descriptions, quartz, feldspar and other major rock-forming minerals are named first, followed by the minor constituents, usually listed in alphabetical order. The plagioclase An-content was determined optically by means of extinction angles in suitable sections (Trøger 1971). The mineralogical composition was determined through modal analysis of thin-sections of representative samples (Kalsbeek 1970). The textural descriptions follow the terminology of Becke (1904) as revised by Berthelsen (1960a).

Ages cited in the present paper are Rb–Sr whole rock ages, recalculated where necessary in accordance with the recommended standards of Steiger & Jäger (1977), using a decay constant of  $\lambda^{87}\text{Rb} = 1.42 \times 10^{-11} \text{ a}^{-1}$ .

## Description of the main rock types and their chronological significance

### SUPRACRUSTAL GNEISS

The supracrustal gneiss is the oldest rock unit in the area (Table 1). Rocks belonging to this unit can be traced to the south into Sweden (Fig. 2) where they join the St. Le-Marstrand 'series' (Magnusson 1958, Larsson 1956), which continues to the south to the Göteborg area in the Østfold segment (Fig. 1). In both Norway (Hageskov & Jorde 1980) and Sweden (e.g. Samuelsson 1980) these supracrustal gneisses were split up by a number of intrusive granitic bodies, the oldest of which now outcrop as continuous layers of orthogneiss.

The supracrustal gneiss is generally uniform over most of the area and is typically a grey, fine- to medium-grained, mainly psammitic gneiss with an overall granitic composition. The main minerals are quartz (40%), microcline (30%) and plagioclase ( $\text{An}_{30}$ ) (20%) which exhibit an interlobate eugranoblastic texture. Biotite is the dominant mafic mineral and gives the rock an open to disperse foliation. Kyanite, and more rarely sillimanite, occur in some places. Additional minor constituents include almandine-rich garnet, apatite, calcite, chlorite, epidote, muscovite, sphene, zircon, rutile and hematite. Sericite lenses occur abundantly in many areas; a few outcrops in the southwestern part of the area have revealed a core of only partly altered kyanite relics in the sericite lenses, and it is presumed that kyanite was a common constituent in alumina-rich parts of the supracrustal gneiss.

Subordinate quartzitic, semipelitic and pelitic layers varying from a few mm to tens of cm in thickness occur within the gneiss (Fig. 3), in addition to the layering that results from a varying mica content. Relict sedimentary structures and calc-silicate layers and lenses found within the supracrustal gneiss are described separately below.

The supracrustal gneiss has suffered anatectic transformation in several areas. Although the occurrence of veined and layered migmatite structures is quite common, the characteristic features noted above can usu-



Fig. 3. Field sketch of folded supracrustal gneiss showing alternating psammitic and pelitic layers. Ødegården, Kolbotn.



ally still be recognized. However, in some areas, anatectic transformation has destroyed most of the features of the supracrustal gneiss and nebulitic migmatite structures are developed; the presence of calc-silicate lenses as resistant xenoliths in the migmatite is then the only clue to the origin.

#### *Relict sedimentary structures*

Rhythmically layered supracrustal gneiss occurs as xenoliths in metatonalite at Nesodden in the western part of the area (Fig. 4). The layered rock shows a relict clastic texture with quartz grains set in a recrystallized matrix (Fig. 5) of either plagioclase or chlorite (in the dark layers). Microcline is present in some layers while other layers are dominated by plagioclase (oligoclase-andesine). Calcite occurs in small amounts throughout the rock

and clinzoisite-epidote is present in equilibrium with chlorite.

The various compositions of the different layers seem to reflect primary sedimentary differences and suggest an alternation of mainly psammitic layers with subordinate pelitic and quartzitic layers. Some layers appear to be graded and parts of the sequence could be interpreted as a layered turbidite sequence, although other interpretations are possible.

Where partly recrystallized, the metasediment has a hemigranoblastic saccharoidal (polygonal) texture with some recrystallized clastic quartz and plagioclase feldspar. However, in most cases the relict clastic fabric is completely destroyed in the supracrustal gneiss, and microcline, together with quartz and plagioclase, forms an interlobate eugranoblastic texture.



Fig. 4. Rhythmic layering in supracrustal gneiss. Nesodden, north of Søndre Spro brygge at Oslofjorden, west of Gardar.

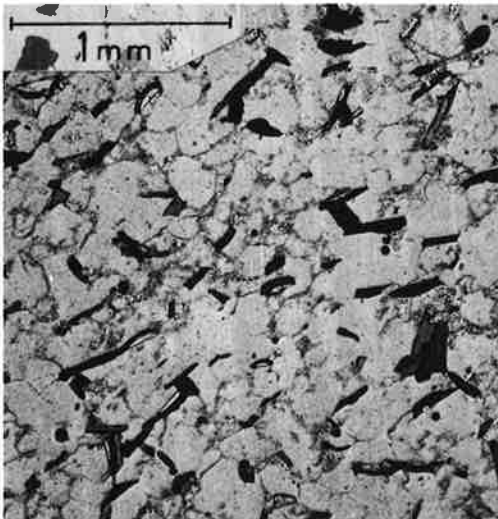


Fig. 5. Relict clastic texture in supracrustal gneiss; rounded quartz grains in matrix of partly altered plagioclase (clouded) together with biotite. Photomicrograph, plane polarized light. MM 15314. 350 m westsouthwest of Tangen school, northern Nesodden.

### *Calc-silicate layers and lenses*

Quartz-bearing calc-silicate lenses and layers 5–25 cm thick are found in the supracrustal gneiss (Fig. 6). A few outcrops demonstrate that some of the calc-silicate lenses were formed through boudinage of competent layers, but this does not exclude the possibility that some were calcareous nodules or concretions.

The calc-silicate lenses are composed mainly of labradorite and quartz (30%) with a granoblastic saccharoidal (polygonal) texture. The lenses may be zoned, in which case they exhibit a pink and sometimes spotted central part surrounded by a white rim; a dark intervening transitional zone may also occur. The spotted central part is characterized by poikiloblastic pyroxene (diopside enclosing quartz) surrounded by pink grossular-rich garnets. In the dark transitional zone, the pyroxene is replaced by amphibole, which in turn is replaced by biotite in the surrounding white rim.

Similar zoning in calc-silicate rocks has been described by Eskola (1922), in great detail by Hentschell (1943), and more recently, among others, by Mehnert (1968) from the Loftahammar region in southeast Sweden. The zoning is explained as reaction zones developed through transformation of impure limestone during metamorphism and granitisation (anatexis) in migmatitic areas. The limestone develops a reaction zone, thus forming armed relics (resisters) which are protected from further reaction with, and dissolution in, the surrounding rock.

### *Metamorphism and migmatization*

The mineral content of the supracrustal gneiss (quartz, microcline, plagioclase (An<sub>30</sub>), biotite, muscovite, kyanite, sillimanite) indicates amphibolite facies grade metamorphism. Along with metamorphism, the supracrustal gneiss has suffered at least two periods of migmatite formation.

Outcrops in the southwestern part of the area may contain two generations of relict kyanite and suggest a two-phase metamorphism that can be referred to the F<sub>1</sub> and F<sub>2</sub> fold episodes (Fig. 7). Kyanite of the first generation crystallized parallel to the main biotite foliation of the gneiss. This foliation

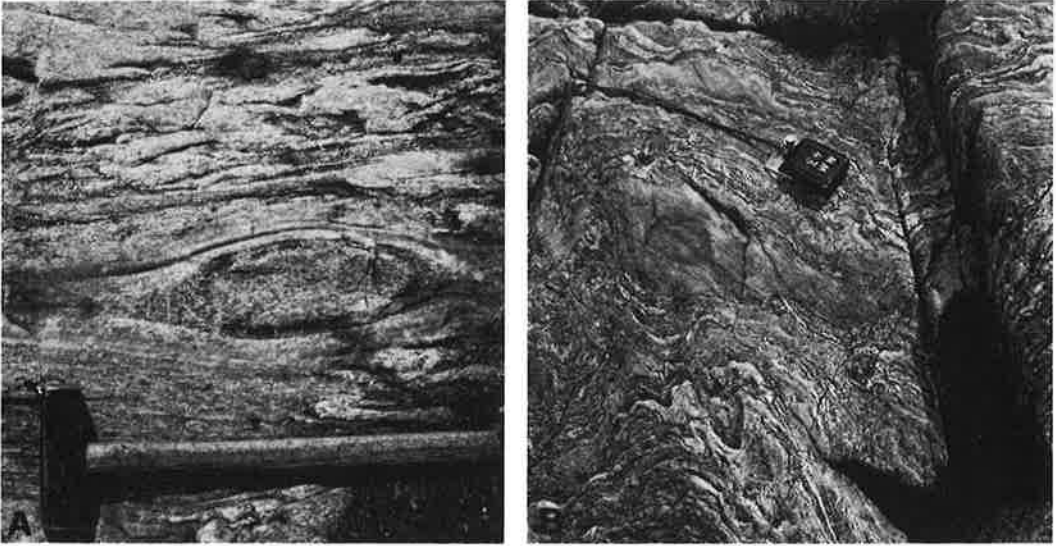


Fig. 6. (A) Zoned calc-silicate lens in supracrustal gneiss, Kolbotn. (B) Calc-silicate lens in strongly migmatized supracrustal gneiss. Nesodden, Bomannsvik brygge at Bunnefjorden, southsoutheast of Torvet.

was later folded, simultaneous with the development of a weakly developed new cleavage, during the  $F_2$  deformation. The older kyanite was often broken up and rotated together with the biotite, while the second generation of kyanite lies in superimposed schistosity planes. The late kyanites have overgrown the folded biotite and show no crushing. Some biotite possibly also recrystallized at this stage.

The early metamorphic phase reached sillimanite grade. This has been estimated from a few localities where both sillimanite (partly altered) and kyanite are overgrown by a later biotite foliation; in the same rock unaltered kyanite grains occur parallel with the foliation. This suggests that the sillimanite was formed together with the older kyanite of the first generation, and that during the subsequent ( $F_2$ ) metamorphism it was partly altered while kyanite remained stable.

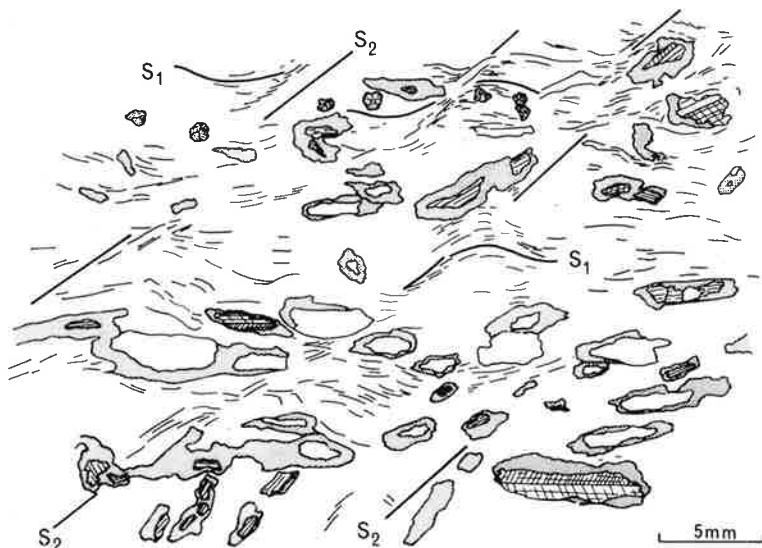
It is thus assumed that the highest P-T conditions were reached during  $F_1$ , where the sillimanite isograd was reached in some areas. During the subsequent  $F_2$  deformation, a medium-grade amphibolite facies metamorphism with kyanite prevailed.

The eastern area was overprinted by a low-grade amphibolite facies metamorphism dur-

ing  $F_3$ - $F_3'$ . Steep axial planes witness to strong lateral compression and the supracrustal gneiss commonly shows a recrystallized cataclastic development. Despite the intense shearing both garnet and kyanite have survived, often crushed and set in a matrix of deformed biotite which forms lensoid bodies (Fig. 8). These lenses and cataclastic feldspar grains occur in a recrystallized quartz matrix with minute shear zones outlined by fine-grained impurities and white mica. Altered but undeformed sillimanite(?) inclusions in crushed garnets (Fig. 8) in the eastern area are relics of the early metamorphism.

The oldest migmatite is characterized by layered (stromatic) and veined (phlebitic) structures. During  $F_2$  these structures were folded and new migmatitic veins were introduced parallel to the  $F_2$  axial planes. A subsequent period of migmatite formation is indicated in the eastern part of the area by pinch-and-swell pegmatitic veins cutting the folded stromatic structure (Fig. 9). The pinch-and-swell pegmatites are surrounded by a mafic biotite rim, are generally concentrated in shear zones and often follow the axial planes. This late migmatitization is less pronounced and may be ascribed to the  $F_3$  (or  $F_2$ ) deformation.

Fig. 7. Two generations of kyanite in supracrustal gneiss (MM 4050), south of Pollevannet. The older kyanite lies parallel to the folded  $S_1$  foliation. Kyanite of the second generation has crystallized in the superimposed  $S_2$  schistosity planes. Drawn from a thin-section.



In the southwestern area migmatites also reflect the two-stage metamorphism. Partly sericitized kyanite occurs in both the first and the second generation migmatic veins. The most thorough migmatization occurred during the  $F_1$  deformation and is consistent with the high P-T conditions (sillimanite grade) reached during this period.

#### METAPLUTONIC ROCKS INTRUDING THE SUPRACRUSTAL GNEISS

After deposition (and folding?), the supracrustal gneiss was intruded by several generations of granitic and basic plutonic rocks. The intrusive events were separated by major deformation episodes and the oldest metagranites now outcrop as continuous gneiss horizons, which outline the regional structure of the area. The basic rocks comprise several generations of dyke intrusion as well as larger basic bodies; these rocks have been transformed to a varying degree into garnet amphibolites, and are valuable as time markers in the tectonostratigraphic analysis.

In the following account the metaplutonic rocks are described in order of decreasing age: biotite gneiss, meta-anorthosite/leucodiorite, augen gneiss, metatonalite/granite complex and granitic orthogneisses. The metabasites are described subsequently.

#### BIOTITE GNEISS

The biotite gneiss delineates the main regional structure of the area; to the north it outcrops in up to 1 km-wide zones in the supracrustal gneiss, and to the south the outcrop widens to cover larger continuous areas (Plate 1).

The biotite gneiss is a rather homogeneous unit of monotonous grey augen gneiss of granitic composition. It is commonly migmatitic, showing a layered or veined structure parallel to the biotite foliation. Neosome veins also cut the main foliation (Figs 10 & 11).

The main minerals of the biotite gneiss are quartz (25%), microcline (40%), plagioclase ( $An_{30}$ ) (20%), biotite (10%) and garnet. The composite microcline augen are 2–4 cm long and 1–2 cm across. The augen are generally lensoid in shape, occasionally slightly lined, but an almost rectangular outline of the augen is found at a few localities. The biotite laths are parallel to a distinct foliation that bends around the augen. Garnets of cm size are also a characteristic constituent in some areas (Fig. 10).

The texture of the quartz-feldspar minerals is hemi-granoblastic with a grain size varying from 0.1–1.5 mm in the matrix and from 1–5 mm in the composite augen. Accessory minerals include apatite, muscovite, sphene, zircon and opaque minerals.

*Fig. 8.* Supracrustal gneiss (MM 18902) from the thrust zone southeast of Gjelleråsen, showing crushed and rotated garnets with inclusions of altered sillimanite(?) needles. The garnets are set in a biotite matrix. Photomicrograph, polars crossed with an  $80^\circ$  angle. The sillimanite(?) might be ascribed to the metamorphism accompanying the  $F_1$  deformation, and now occurs as inclusions in anhedral garnets crystallized during the  $F_2$  metamorphism. The euhedral inclusion-free garnet to the left may have grown during the  $F_3$  metamorphism.

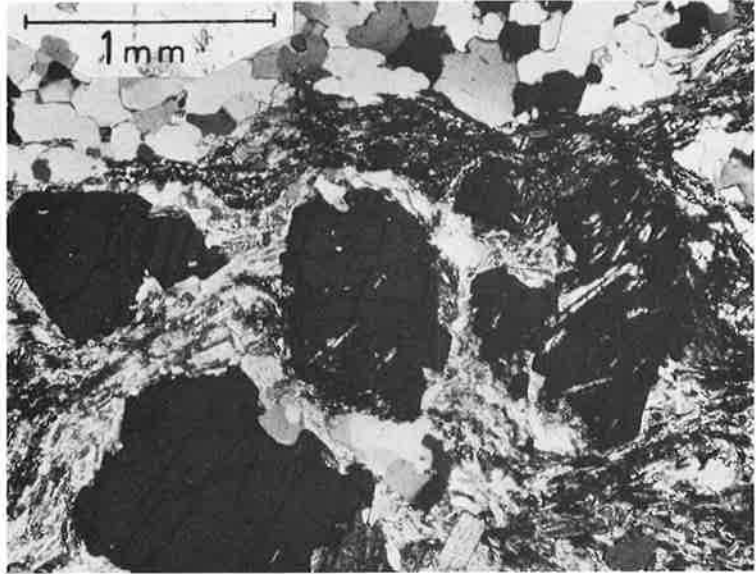


*Fig. 9.* Small-scale  $F_2$  Folding of ( $F_1$ ) stromatic migmatite structures in supracrustal gneiss, north of Lutvatnet. Later pinch-and-swell pegmatitic veins ( $F_3$ ) cut the folded structures sub-parallel with the axial planes.



### *Contact relationships and origin of the gneiss*

The contact between the biotite gneiss and the supracrustal gneiss is generally sharp and the foliation in the gneisses is nearly always parallel to the contact. At the contact the supracrustal gneiss generally rises above the biotite gneiss by virtue of its being more resistant to weathering, and the contact is marked by a scar in the topography.

The origin of the biotite gneiss is difficult to demonstrate as it has been repeatedly exposed to deformation and recrystallization under amphibolite facies conditions (see below), so that the nature of the primary contact has been destroyed. In the southwestern part of the area, different lithologies of the supracrustal gneiss are in contact with the biotite gneiss along the strike (B. Hageskov, pers. comm.) and at several localities within the biotite gneiss outcrop, a fine-grained gneiss closely resembling the surrounding supracrustal gneiss is found in 20–40 cm-thick layers or sheets; these sheets all show concordant contacts. Whether the contacts indicate an intrusive origin for the biotite gneiss (and a possible angular relationship being destroyed during later deformation), or whether they reflect a lateral variation during sedimentation of the supracrustal gneiss, cannot be decided because of the discontinuous nature of the exposure. However, lateral

facies variation in the supracrustal gneiss has not been observed elsewhere, thereby favouring the probability of an intrusive relationship. The exotic fine-grained gneiss sheets scattered in the biotite gneiss are, however, most probably xenoliths, suggesting an intrusive origin for this unit. This interpretation concurs with the homogeneous and granitic character of the biotite gneiss. On the other hand, the complex structural evolution, with possible initial nappe formation in the biotite gneiss-supracrustal gneiss nappe (see later) opens the possibility of thrusting along the contact as being responsible for a major discordance.

### *Folding, migmatization and metamorphic evolution*

The biotite gneiss was folded during four successive fold episodes of regional importance ( $F_0$ – $F_3$ ). The  $F_1$  and  $F_2$  fold episodes dominate the mesoscopic and macroscopic fold development in the western part of the area, and an interference pattern between these two fold systems in the biotite gneiss has been demonstrated through detailed structural work on refolded garnet amphibolites (Graversen 1973). During  $F_1$ , recumbent isoclinal folds developed with NNE-SSW trending axes, and these structures were later refolded by NW-plunging  $F_2$  folds which are the most



*Fig. 10.* Biotite gneiss with lensoid microcline augen from the southern Bunnefjorden area. Pegmatitic neosome veins formed during the  $F_2$  deformation along shear-zones cutting the main foliation. Small garnets are widespread.

common structures found (Fig. 18). Only the eastern part of the area was folded during  $F_3$  (Fig. 28).

The biotite gneiss generally displays a layered or veined migmatitic structure with leucosome veins parallel to the biotite foliation. This thorough migmatization occurred during  $F_1$ , while the migmatitic gneiss was folded during  $F_2$ . Small-scale intrafolial folds developed before the migmatization event may belong to  $F_0$ , or to the initial stages of  $F_1$ . Two types of later pegmatitic veins occur: 1) veins which cut the foliation are found along shear planes connected with small-scale flexures formed during  $F_2$  (Fig. 10); 2) randomly distributed accumulations of neosome material (Fig. 11) which developed in fissures and cavities resulting from dilation or boudinage (Fig. 11).

In the eastern part of the area (in the Østmarka syncline folded during  $F_3$ ), the patchy pegmatitic neosome pods cut both the old, intensely folded migmatitic schlieren ( $F_1$ ) and the pegmatitic veins which developed along cross-cutting shear planes ( $F_2$ ) (Fig. 11). The mesoscopic folds associated with the cross-cutting shear planes are governed by vertical  $F_2$  fold axes and were reoriented by the moderately NNW-plunging  $F_3$  Østmarka syncline. The migmatitic neosome patches were not further deformed and their formation is thus considered to be associated with  $F_3$ .

A three-stage metamorphic evolution of the biotite gneiss is also suggested by the garnets. Most garnets show no deformation and grow in late leucosome veins ( $F_2$ ,  $F_3$ ) as well as across the augen and layered leucosome veins of the first migmatitic phase (Fig. 10). In the paleosome (biotite gneiss) some garnets have been rotated around the youngest fold axis ( $F_2$ ) in the western area. This rotation is at some localities related to the development of a new foliation ( $S_2$ ) and with the folding (and recrystallization) of the previous  $S_1$ -foliation (Fig. 12). This points to a two-stage metamorphic evolution ( $F_1$ ,  $F_2$ ) separated by folding ( $F_2$ ). Poikiloblastic garnets surrounded by a rim of inclusion-free garnet also indicate successive stages of garnet growth; the present example may not include deformation between the two periods of garnet growth and might thus represent a third metamorphic event ( $F_3?$ ).

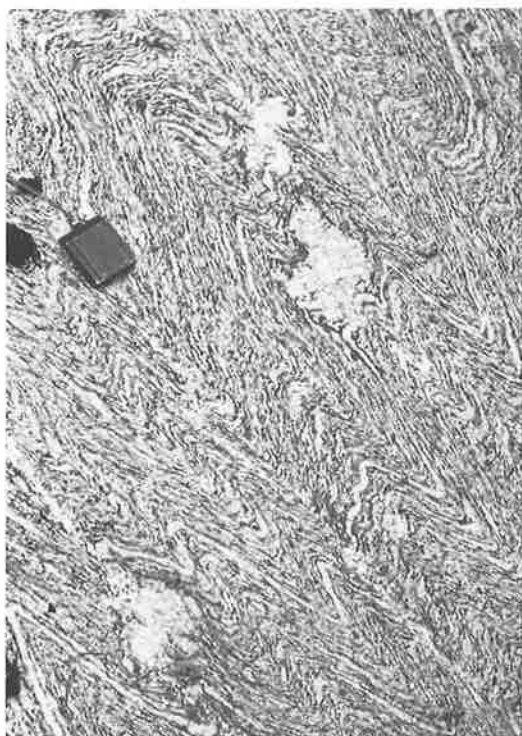


Fig. 11. Folded migmatitic biotite gneiss from Haukåsen in the Østmarka syncline. See text for further explanation.

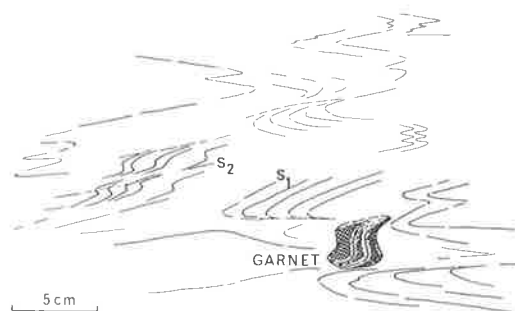


Fig. 12. Garnet with S-shaped inclusion trails in biotite gneiss from the southern Bunnefjorden area. The  $S_1$  biotite foliation was folded during  $F_2$ . A new foliation,  $S_2$ , is developed along shear-planes parallel to the axial planes of the  $F_2$  folds.

The metamorphic and migmatitic development appears to be coeval with the structural evolution. The main migmatite formation with leucosome veins parallel to the biotite foliation of the gneiss was formed in connection with the  $F_1$  deformation. During  $F_2$ , the  $F_1$  structures were folded and recrystallized and, in some cases, a new foliation developed

(S<sub>2</sub>, Fig. 12); the formation of migmatitic veins along shear planes which cross the S<sub>1</sub> foliation is connected with this F<sub>2</sub> deformation. The youngest neosome veins outcrop as homogeneous bodies cutting the earlier structures, and this migmatitic phase is linked to F<sub>3</sub>.

The mineral association (quartz, microcline, plagioclase (An<sub>30</sub>), biotite, muscovite) and migmatitic development of the biotite gneiss demonstrate medium- to high-grade amphibolite facies metamorphism. Even though the chemical composition of the biotite gneiss is not suited for exact determination of the metamorphic grade, the more intense migmatization during the first deformation suggests that the highest P-T conditions were reached at this time (kyanite-sillimanite grade ?), and that somewhat lower temperatures prevailed during the later F<sub>2</sub> and F<sub>3</sub> events (kyanite grade ?).

The biotite gneiss in the northeastern part of the area was retrogressively metamorphosed during F<sub>3</sub>-F<sub>3</sub>'. Plagioclase is strongly sericitized, while biotite is distorted and partly replaced by chlorite and prehnite. The garnets are slightly anisotropic but not recrystallized. It thus seems that low amphibolite-greenschist transition facies conditions prevailed during the last stages of the F<sub>3</sub> deformation; this retrograde metamorphism is linked to F<sub>3</sub>'.

At a later stage, unstrained muscovite grew across the secondary and the earlier formed minerals both in the eastern and the western part of the area. This demonstrates either that the metamorphism outlasted the regional deformation or that the area was subsequently metamorphosed under static conditions.

#### META-ANORTHOSITE/LEUCODIORITE

Several bodies of a distinctive white plagioclase gneiss with mafic schlieren, up to about 300 × 1500 m in size, have been mapped in the northern supracrustal gneiss on Nesodden and in the southwestern biotite gneiss (Plate 1); the latter occurrences have been described in more detail by Graversen (1980). The Nesodden meta-anorthosites were described as plagioclase-gedrite gneisses and garbenschiefer by Broch (1926) and interpreted as having a sedimentary origin. Broch (1926,

p. 171) has, however, also reported discordant contacts of a meta-anorthosite dyke (?) cutting the gneiss foliation. Because of their similar petrography and textures the Nesodden plagioclase-gedrite gneisses are here correlated with the intrusive meta-anorthosites to the south.

On weathered surfaces the meta-anorthosite has a mottled black and white appearance (Fig. 13). There is some variation in the proportion of mafic minerals and the way in which they are arranged, but in most outcrops the content ranges between 10 and 20%. The groundmass is composed of medium-grained massive plagioclase (An<sub>25-35</sub>). Most of the mafic minerals, fibrous amphibole, anthophyllite-gedrite and biotite, are usually concentrated in schlieren about 10 cm long and a few cm broad which exhibit a 'flame' or 'flaser-like' structure. Observations from localities showing little deformation suggest that the structure stems from an original cumulate texture with cumulus feldspar up to about 5 cm in size and mafic aggregates; on deformation the latter have become schlieren (Graversen 1980, Figs 8 and 9).

Plagioclase forms 75-95% of the rock, while fibrous amphibole, anthophyllite-gedrite and biotite together make up 5-25%; the accessory minerals include almandine-rich garnet, chlorite, muscovite, phlogopite, rutile, staurolite, zircon, hematite, ilmenite, magnetite, pyrite and pyrrhotite.

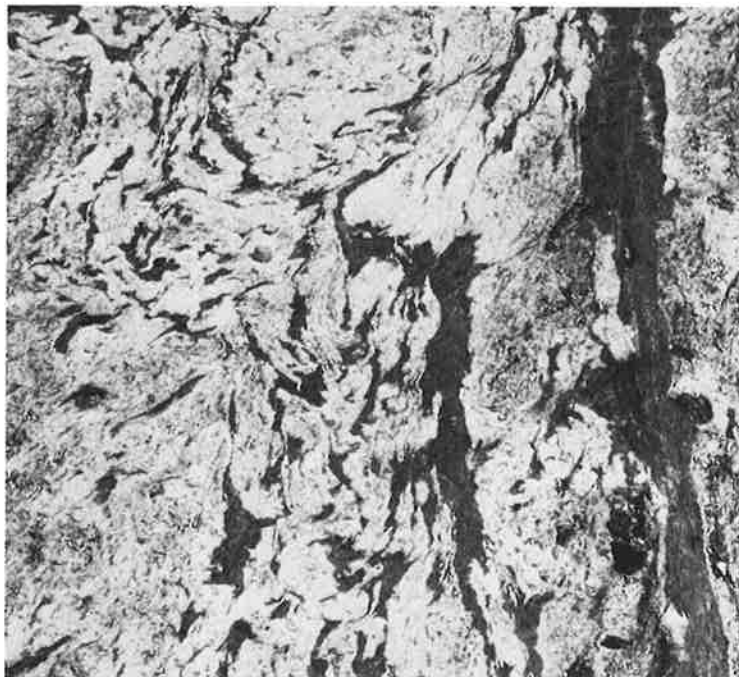
#### *Deformation and metamorphism*

Mesoscopically folded schlieren follow NW-plunging axes (F<sub>2</sub>) and suggest an earlier deformation (F<sub>1</sub>) as being responsible for the initial formation of the schlieren through deformation of the original cumulate texture. These considerations place the intrusion of the anorthosite/leucodiorite prior to the F<sub>1</sub> fold episode, and subsequent to the emplacement of the biotite gneiss.

The fibrous amphibole in the schlieren represents an early phase of recrystallization (F<sub>1</sub>?). Later, presumably during F<sub>2</sub>, subhedral to euhedral prismatic anthophyllite-gedrite crystals grew both in the mafic schlieren and in the plagioclase matrix. During a subsequent metamorphism, euhedral garnets, with



Fig. 13. Meta-anorthosite/leucodiorite with mafic bands and schlieren. Outcrop from the southern anorthositic bodies in the biotite gneiss southeast of Bunnelfjorden.



diameters up to 8 cm, have in some cases grown across the contact between the mafic schlieren and the plagioclase host, with no sign of later rotation. In the Nesodden meta-anorthosite, euhedral staurolite crystals have grown in the plagioclase matrix. The crystallization of euhedral garnet and staurolite indicates a late amphibolite facies grade metamorphism of the staurolite-kyanite zone. This development may be due to a metamorphism which outlasted either the  $F_2$ , or more likely the  $F_3$ , deformation. Garnet and mafic minerals may later be replaced by chlorite, indicating subsequent greenschist facies or greenschist-amphibolite transition facies conditions ( $F_3'$ ).

#### AUGEN GNEISS

Extensive outcrops of augen gneiss, enveloped by the supracrustal gneiss, occur in the Gjer-sjø dome, in the Østensjø anticlinorium and in the adjoining Mysen and Østmarka synclines where the augen gneiss follows the major structures outlined by the biotite gneiss (Fig. 23, Plate 1).

The augen gneiss has a coarser-grained and

more massive appearance than the supracrustal gneiss and the biotite gneiss. It is relatively resistant to erosion and usually forms higher ground than bordering rock units. The augen gneiss is a grey, weakly foliated migmatitic gneiss dominated by large microcline augen (Fig. 14). It has a granitic composition and the main minerals are quartz, microcline, plagioclase ( $An_{25-30}$ ), hornblende, biotite and almandine-rich garnet. The coarse and migmatitic character of the rock hinders any reliable modal analysis. Accessory minerals identified under the microscope include apatite, sphene, zircon and opaque minerals.

The large microcline augen are commonly up to 5 cm in length and may make up about 1/3 of the rock. The augen sometimes have a near-rectangular shape but are generally rounded or pointed at the ends (Fig. 14 A). Individual augen may be composite or single microcline grains. A subparallel arrangement of the augen and biotite in the matrix forms a rather weak foliation in the rock. The linear development of the augen is more pronounced, and in most cases is the only structure that can be recorded. Towards the contact with surrounding rocks, the augen gener-

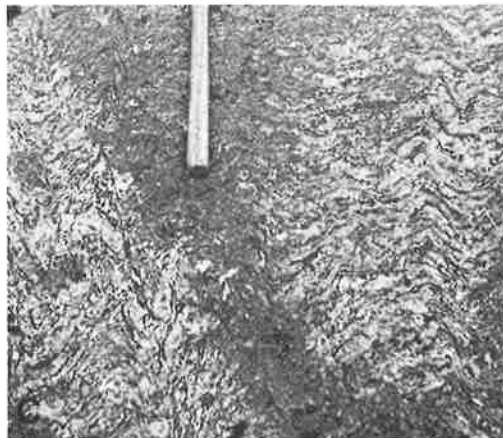
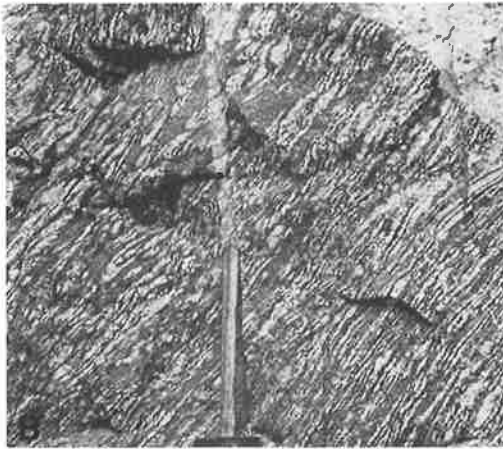
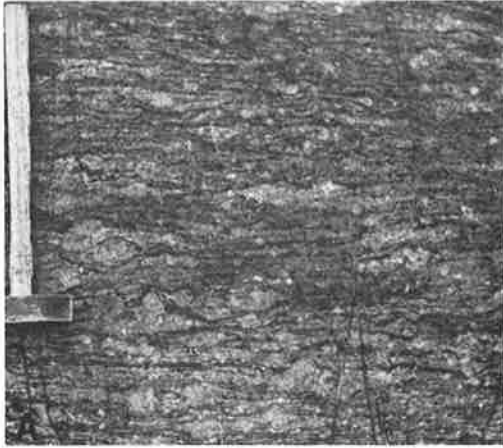


Fig. 14. Augen gneiss outcrops in the Østensjø anticlinorium. A) Foliated augen gneiss. B) Veined and layered migmatitic development of the augen gneiss. C) Folded migmatitic augen gneiss.

ally become completely destroyed and the rock is transformed into a well-foliated, banded gneiss. The foliation is parallel to the contact and to the foliation in the surrounding supracrustal gneiss.

#### *Metamorphism and migmatization*

The mineral paragenesis of the augen gneiss (see above), indicates amphibolite facies metamorphism. The augen gneiss is anatectic, generally displaying a veined or layered migmatitic structure (Fig. 14 B & C). The leucosome is characterized by quartz and plagioclase, often found in the pressure shadow zone at the end of larger microcline augen. The microfabric is hemi-hetero-granoblastic with sinuously curved grain boundaries. Late distortion and even crushing of some grains is an additional characteristic feature.

The leucosome veins are sometimes folded on a mesoscopic scale (Fig. 14 C); folding and recrystallization clearly took place after the migmatization (Mehnert 1968).

#### *Origin, relative age and deformation of the augen gneiss*

The granitic composition, homogeneous nature, and the presence of xenoliths of supracrustal gneiss 1–2 m across (Fig. 15), all suggest that the augen gneiss is of intrusive origin. The augen gneiss appears to have been intruded later than the biotite gneiss, since anorthositic rocks and garnet amphibolites which abundantly intrude the latter are not found in the augen gneiss. The interpretation of the regional structures (see later) also suggests that the augen gneiss was intruded later than the emplacement of the biotite gneiss but participated in the major  $F_1$  to  $F_3$  deformations.

It seems likely that the migmatization occurred during  $F_1$ , and the later amphibolite facies recrystallization during  $?F_2$ . The late deformation of the rigid gneiss may be ascribed to  $F_3$ – $F_3'$ .

#### METATONALITE/GRANITE COMPLEX

In the northern part of the area large volumes of tonalitic and granitic rocks were intruded into the supracrustal gneiss. The in-

Fig. 15. Xenoliths of supracrustal gneiss in migmatitic augen gneiss. Gjersø dome west of Kolbotn.



trusive rocks show a variable but weak foliation and are sometimes lineated. The main constituents of the metatonalite are quartz, plagioclase ( $An_{30-35}$ ) and biotite, while the colour index is 20–25. The metagranite is composed largely of quartz, microcline and plagioclase ( $An_{20}$ ); biotite is less important and the colour index is around 5.

Compared with the biotite gneiss and the granitic augen gneiss, the metatonalites and metagranites have a fresher appearance, and are not restricted to a specific structural level in the supracrustal gneiss. The mapping indicates that the contacts cut the foliation in the supracrustal gneiss discordantly, and that the tonalitic rocks contain xenoliths of supracrustal gneiss from dm scale to mappable size (100–200 m). The tonalitic and granitic rocks were intruded between the  $F_1$  and  $F_3$  fold episodes, possibly prior to the  $F_2$  fold episode.

The outcrops are concentrated in two main areas; the eastern Østmarka area where only tonalitic rocks occur, and a western area around the Gjersjø dome which is characterized by the occurrence of both tonalitic and granitic rocks (Plate 1). In the Østmarka area, the metatonalites are situated in the supracrustal gneiss *below* the augen gneiss in the tectonostratigraphic sequence, whereas in the western area the tonalitic and granitic rocks are intruded into the supracrustal gneiss *above* the biotite gneiss.

The Østmarka metatonalite area has been studied mainly by Christian Mohr (University of Copenhagen) and his detailed map was generously placed at the author's disposal. Only the northwestern part was mapped by the present author.

The description of the metatonalite/granite complex which follows is mainly based on the Nordstrand-Sømarka area east and north of the Gjersjø dome where fresh and clean outcrops, exposed during the building activity in the newly extended suburb areas around Oslo, enable clear and detailed observations to be made.

On weathered surfaces, both the metagranite and the metatonalite are whitish or grey in colour and the difference between them can be so small that if both types are not present in the same outcrop they are liable to be indistinguishable in badly exposed areas. This difficulty also affects estimates of their relative proportions and their areal distribution. Generally, both types occur within a relatively small area and no distinction between the two has been made on the map.

The *metatonalite* is a dark, medium-grained massive rock. Biotite is the dominant dark mineral and constitutes an open foliation in the rock. Quartz and feldspar occur in small augen that may be lineated and sometimes flattened parallel to the foliation. The minerals identified in thin-section are quartz (33%), plagioclase ( $An_{30-35}$ ) (40%) and biotite (20%), together with accessory amounts of almandine-rich garnet, apatite, chlorite, muscovite, sericite, sphene, zircon and opaque minerals. The texture is characterized by composite plagioclase augen, generally up to 5 mm in size, set in a finer grained (0.2–2 mm) quartz-plagioclase matrix. The plagioclase grains in the augen may be up to 1 mm across and show a granoblastic polygonal texture. The texture of the quartz and plagioclase grains in the augen may be up to 1 mm across and show a granoblastic polygonal

texture. The texture of the quartz and plagioclase in the matrix is granoblastic. The plagioclase is andesine with albite twins in nearly all grains while combined Carlsbad-albite twins are also common.

The *metagranite* is a whitish grey, medium- to coarse-grained rock. The first impression is that of a more massive rock than the metatonalite, but this is mainly due to the low (5%) biotite content; however, both quartz and feldspar are elongated and flattened parallel to the open biotite foliation. The microscopically identified minerals are quartz (30%), microcline (35%), plagioclase (An<sub>20</sub>) (30%) and biotite, together with accessory almandine garnet (?), apatite, calcite, chlorite, epidote, muscovite, sericite, zircon and opaque minerals. The compositional variation expressed by the microcline/plagioclase ratio is rather variable and ranges from about 1:1 to 5:1.

The age relationships between the tonalitic and the granitic phase are rather obscure. The contact between the two is always sharp (Fig. 16). The foliations of both rocks are parallel and generally show a large angle with the contact, thus indicating that the foliation

must have developed simultaneously in both rocks during a post-intrusion deformation. However, the fact that only the metatonalite contains xenoliths of supracrustal gneiss suggests that this phase is somewhat older, and that the granite later preferentially intruded the tonalite.

The metatonalite/granite complex was emplaced after the F<sub>1</sub> deformation. This is indicated by dykes of the tonalite as well as the granite, which cut both the regional foliation and the main migmatization of the supracrustal gneiss (formed during the F<sub>1</sub> deformation), and by the fact that the tonalite intrudes migmatitic augen gneiss.

Rb–Sr reference ages of 1525 and 1480 Ma have been obtained by Pedersen (1979) and Pedersen et al. (1978) from whole rock analyses of metatonalite and metagranite sampled between Kolbotn and Nordstrand in the Nordstrand–Sørmarka metatonalite/granite area. The ages may reflect a metamorphic episode around 1500 Ma shortly after the emplacement of the rocks (Pedersen 1979).

#### *Deformation and metamorphism of the metatonalite/granite complex*

The metatonalite/granite complex reacted as a competent body during deformation and only few mesoscopic folds have been observed. The regional structures around Østensjøvannet in the northern part of the Østensjø anticlinorium (Fig. 24) demonstrate that the complex was folded during the last major (F<sub>3</sub>) deformation (Plate 2 section XVII–XIX).

The small metatonalite area which outcrops along the southeastern part of the Gjersjø dome (in the northern part of Gjersjøvannet, Plate 1), is situated in a major open fold ascribed to the F<sub>2</sub> fold episode (Plate 3). This fold is furthermore believed to be responsible for the refolding and culmination of the N–S trending F<sub>1</sub> fold which forms the Gjersjø dome. The weak development of the superimposed F<sub>2</sub> fold and the well preserved nature of the F<sub>1</sub> fold is in striking contrast to the fold development in the surrounding areas. It is thought probable that the restricted development of F<sub>2</sub> folds in this area is due to the competent Nordstrand–Sørmarka me-



Fig. 16. Contact between metagranite (right) and metatonalite with xenoliths of supracrustal gneiss. East of Østensjøvannet.

tatonalite/granite body to the north and east acting as a shield during the  $F_2$  deformation. According to this supposition, the metatonalite/granite complex was in existence during  $F_2$ , and was thus intruded between the  $F_1$  and  $F_2$  fold episodes.

The metamorphosed tonalite and granite exhibit amphibolite facies parageneses (see above). In some samples the biotite is strained and bent around both the garnets and the feldspar augen, and may also be partly replaced by or intergrown with chlorite. Idiomorphic epidote has overgrown the biotite-chlorite laths. This metamorphic retrogression seems to be connected with sericitization of the plagioclase and recrystallization of the quartz. Late growth of muscovite has also been observed.

The late retrogression involves the crystallization of chlorite, sericite, epidote and albite, which characterize greenschist or greenschist-amphibolite transitional facies conditions during the last  $F_3$ - $F_3'$  deformation. The preceding deformation under amphibolite facies conditions has been responsible for the weak foliation and subordinate migmatite formation along transecting shear planes resembling the second ( $F_2$ ) period of migmatization in the supracrustal gneiss and the biotite gneiss. The amphibolite facies conditions were probably imposed during the  $F_2$  and/or possibly the  $F_3$  deformation.

#### GRANITIC ORTHOGNEISSES

To the south and west the area is bounded by poorly foliated granitic orthogneisses (metagranites) which cut the contacts of the previously described major units, with the exception of the augen gneiss (Plate 1). A correlation between the orthogneisses and the augen gneiss has previously been proposed by Graversen & Hageskov (1976) and Hageskov & Jorde (1980); this view, however, is no longer favoured by the present author.

The relation between the western orthogneisses on Nesodden and the southern orthogneiss area is unclear as only few and scattered exposures exist in the transitional boundary area between Hallangpollen and Årungen. In the following, a brief account of the two areas is presented.

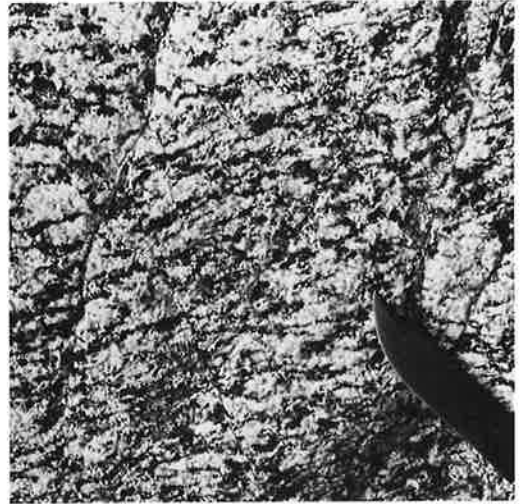


Fig. 17. Amphibole-biotite metagranite from the southern orthogneiss area east of Tomter.

#### *The southern orthogneiss area*

The orthogneiss zone trending WNW-ESE along the southern boundary of the area (Plate 1) consists mainly of even-grained, poorly foliated hornblende-biotite metagranites. They are generally medium- to fine-grained, although coarser varieties do occur (Fig. 17). The orthogneisses have a granitic composition and both microcline- and plagioclase ( $An_{25-30}$ )-rich varieties occur. Hornblende and biotite together make up about 15% of the rock. Minor constituents include almandine-rich garnet, apatite, epidote, sphene zircon and opaque minerals. The hornblende is commonly replaced by biotite; both hornblende and biotite may be replaced by epidote. In addition, single grains of twinned and zoned epidote also occur as a characteristic minor constituent in the orthogneisses.

The orthogneiss can be seen on a large-scale map (Plate 1) to take up a structural position in continuation of the augen gneiss in the Mysen syncline southeast of Lyseren. However, in contrast to the augen gneiss unit, the orthogneiss appears to cut the biotite gneiss/supracrustal gneiss contact discordantly (Plate 1, Fig. 23). Although the exposure south of Ski is rather poor, detailed mapping and structural interpretation of the biotite gneiss/supracrustal gneiss contact has revealed a set of  $F_2$

folds that are not shared, but on the contrary are cut off by the orthogneiss unit (Plate 2 section XV, Plate 3). If these observations are correct, the southern orthogneisses must postdate the  $F_2$  deformation and are thus considerably younger than the augen gneiss in the Østensjø anticlinorium and the Mysen syncline, which were folded during both the  $F_1$  and the  $F_2$  fold episodes.

The orthogneisses exhibit amphibolite facies parageneses with subsequent recrystallization in greenschist-amphibolite transitional facies. It is suggested that amphibolite facies conditions were reached during the  $F_3$  deformation and that the downgrading of the rocks took place during the  $F_3'$  fold episode. In contrast to the augen gneiss and older units, these orthogneisses have not been exposed to anatexis subsequent to their emplacements.

#### *The western orthogneisses on Nesodden*

The western granitic orthogneisses on Nesodden are the northern continuation of the Moss-Filtvet orthogneiss complex mapped to the south by B. Hageskov (Hageskov & Jorde 1980, Hageskov & Pedersen 1980). A granitic augen gneiss constitutes the southern area on Nesodden, while the northern area consists of a fine- to medium-grained, poorly foliated aplitic granite (Plate 1).

Hageskov & Jorde (1980) correlate the augen gneiss around Garder in the central part of the Nesodden peninsula with the granitic augen gneiss from the western orthogneiss complex. This correlation, however, is not supported by the present results. The contact of the western orthogneisses against the supracrustal gneiss (including the metatonalite/granite complex, Fig. 23) indicates a possible primary intrusive relationship with discordant contacts; this applies especially to the contact between the supracrustal gneiss and the metatonalite/granite complex which always occurs together with the supracrustal gneiss outside the orthogneiss areas (Plate 1). The Gardar augen gneiss is deformed by superimposed  $F_1$  and  $F_2$  antiforms (Plate 3), while the orthogneisses to the west apparently do not share these structures. In the southern Bunnefjorden-Hallangspollen area,  $F_2$  folds are cut by

the western orthogneiss (Fig. 27, Plate 3). It is suggested, therefore, that the western orthogneiss complex was intruded after the  $F_2$  fold episode. The orthogneisses thus appear to have a young structural age in both areas, and were most probably intruded between the  $F_2$  and  $F_3$  fold episodes.

The granitic augen gneiss in the southwestern orthogneiss area is part of the Moss-Filtvet augen gneiss which has yielded a Rb-Sr whole rock isochron age of  $1320 \pm 22$  Ma (Hageskov & Pedersen 1980), viewed as the age of intrusion and in the present context indicating a lower age limit for the  $F_2$  deformation. These conclusions, however, are not in agreement with Hageskov & Pedersen (1980), who state that the emplacement of the Moss-Filtvet complex predates all the major fold episodes (N-S and E-W trending structures) that outline the regional structures in the area.

#### AMPHIBOLITES AND METADOLERITES

Metabasites of several generations occur widely distributed in the gneisses; only the larger bodies are shown on the map (Plate 1). The metabasites belong principally to two main groups: an old group of concordant garnet amphibolites intruded before the  $F_1$  fold episode, and a group of younger cross-cutting metadolerites and metagabbro bodies which were intruded between the  $F_1$  and  $F_3$  fold episodes. The younger group can sometimes be divided into two separated by the  $F_2$  deformation.

The *garnet amphibolites* and *oldest metadolerites* are generally fine-grained and are essentially composed of hornblende and oligoclase feldspar. Accessory minerals include apatite, biotite, chlorite, epidote, almandine-rich garnet, sphene and opaque minerals. The hornblende is generally oriented parallel to the  $F_2$  fold axes, plunging at around  $30^\circ$  to the northwest. Larger hornblende grains and garnet may be poikilitic with numerous quartz inclusions. Quartz may also be present as interstitial grains and constitute up to 10% of some samples. The plagioclase is commonly saussuritised, while the amphibole is occasionally replaced by epidote and chlorite.

In the *youngest metadolerites*, plagioclase laths or the recrystallized equivalents can still be recognized and outline an original (sub)ophitic texture. The garnets in this group are subhedral and generally occur in irregular aggregates, a feature that can be observed as a cauliflower structure on weathered surfaces. The mineral parageneses, mimetic ophitic textures and subhedral garnet aggregates suggest recrystallization under static (?) conditions of the amphibolite facies. These conditions probably prevailed in the southwestern part of the area during the last deformation ( $F_3$ ) outside the main deformation area to the east.

#### *Refolded garnet amphibolites (old group)*

Concordant garnet amphibolites are restricted to the supracrustal gneiss and biotite gneiss where they outcrop as continuous layers 10 cm–1 m thick. They occur abundantly over large areas and constitute a characteristic feature (up to 20%) of the gneisses.

The garnet amphibolites are fine- to medium-grained with red cm-sized almandine-rich garnets (Graversen & Hageskov 1971, Fig. 9). A faint biotite-amphibole foliation is parallel to the contacts and to foliation in the surrounding gneiss. The amphibole is generally lineated parallel to the  $F_2$  fold axes.

In the southwestern part of the area the biotite gneiss reveals continuous outcrops of tight to isoclinally folded and refolded amphibolite horizons (Fig. 18 a). The structural interpretation (Fig. 18 b) demonstrates  $F_1$  folds refolded during the  $F_2$  deformation. A more complete picture of these outcrops and a more thorough discussion of the interpretation is given by Graversen (1973) and Graversen & Hageskov (1971).

Although the majority of the garnet amphibolites show no mesoscopic  $F_1$  folds, the repeated folding which they have undergone is demonstrated here by the existence of an older internal foliation within the garnets in contrast to the later developed external texture.

The garnet amphibolites occur both in the supracrustal gneiss and in the biotite gneiss and are interpreted as former dolerite dykes or sills. They were intruded prior to the  $F_1$

fold episode but their relationships to  $F_0$  (see later) are unknown. The mineral parageneses and structural evolution demonstrate repeated amphibolite facies metamorphism during the  $F_1$  and  $F_2$  fold episodes, in agreement with the metamorphic evolution of the supracrustal gneiss and the biotite gneiss.

#### *Cross-cutting metadolerites (younger groups)*

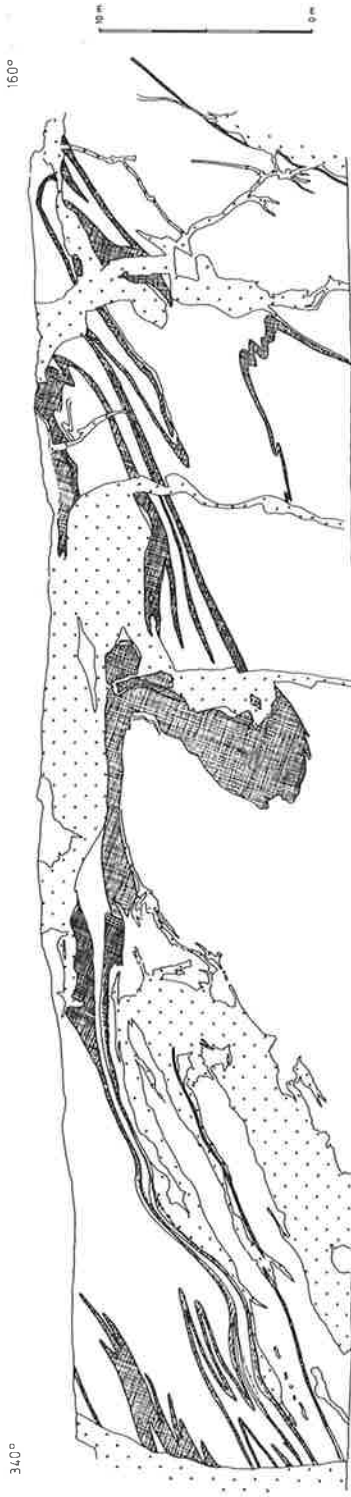
Metadolerites which cross-cut the regional foliation are found in all the gneiss groups. The dolerites have undergone amphibolite facies metamorphism and may also be folded and boudinaged, although they do not exhibit the intense  $F_1$  folding demonstrated by the old group of concordant garnet amphibolites. The metadolerites were intruded between the  $F_1$  and  $F_3$  fold episodes. At several outcrops it is possible to distinguish two generations. The major structural and metamorphic evolution suggests two main phases of younger dolerite intrusions separated by the  $F_2$  fold episode.

#### *Metadolerites in the metatonalite/granite complex*

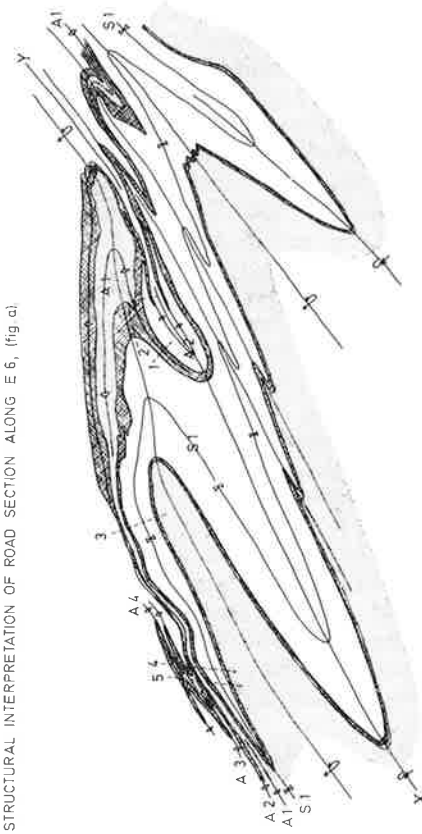
Metadolerites in the metatonalite/granite complex occur as dykes, agmatitic bodies and minor net-veined intrusions. The dykes range up to a few metres in width but are generally less than a metre wide. Apophyses and chilled margins are commonly preserved and, in a few cases, rotated xenoliths of the wall rock are present (Fig. 19). Some dykes cut the  $S_2$  foliation in the host rock and are found both in the tonalitic and the granitic varieties of the metatonalite/granite complex. Although recrystallization and growth of almandine-rich garnet under amphibolite facies conditions is characteristic, relict feldspar phenocrysts and an ophitic texture may still be identified outside the main area folded during  $F_3$ . It is suggested that these metadolerite dykes intruded between the  $F_2$  and  $F_3$  fold episodes.

A few agmatitic metabasites are found in the tonalitic part of the complex (Fig. 20). They outcrop as zones up to a metre wide veined by the surrounding tonalitic material. The metabasite fragments are angular and their mutual relationships demonstrate that

a) FIELD SKETCH OF ROAD SECTION ALONG E 6,  
25 KM SOUTH OF OSLO.



b) STRUCTURAL INTERPRETATION OF ROAD SECTION ALONG E 6, (fig. a).



c) PROFILE J. F.

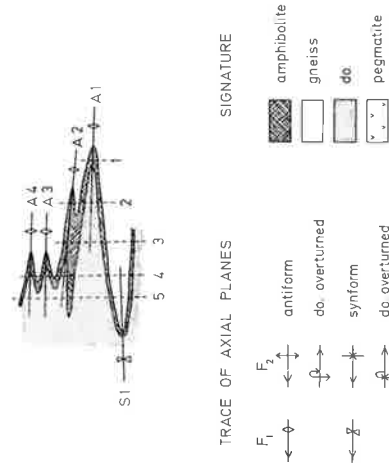


Fig. 18. Outcrop pattern and structural interpretation of refolded garnet amphibolites (oldest group) in biotite gneiss. Location of the outcrop is indicated in Fig. 27 A.

E-71 OC





Fig. 19. Metadolerite dyke cutting foliated metatonalite in the northern Østmarka metatonalite area. The metatonalite contains xenoliths of supracrustal gneiss.

they must have been brecciated more or less in situ, possibly from an originally unbroken dolerite dyke. Some of the larger doleritic lumps, even in the central part of the agmatite, exhibit a finer grained margin against the tonalitic material, which can be interpreted as a chilled margin and suggests that the original intrusive dyke was itself back-veined by the host rock. This would imply that these doleritic rocks must have been intruded into the tonalite when it was sufficiently cooled to enable the formation of joints which served as pathways for the magma. During the cooling of the dyke, however, the surrounding tonalite was locally remelted and subsequently involved the partly solidified dolerite. The agmatitic metabasites were intruded between  $F_1$  and  $F_2$  dated by the intrusion of the metatonalite/granite complex.

Any immediate distinction between agmatitic metadolerites and dykes as time markers must, however, be viewed with reservation, as the development of agmatitic metadolerites in this context depends on the temperature of the tonalite at the time of intrusion. If the temperature gradient was uniform – which would be unexpected in rela-

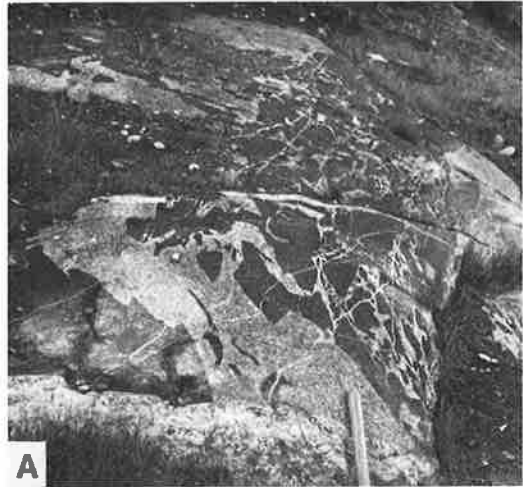
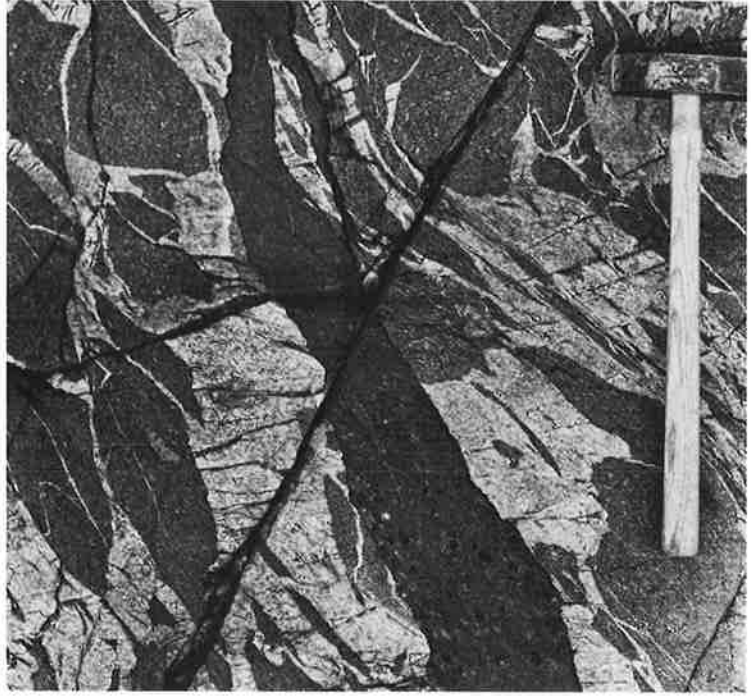


Fig. 20. Agmatitic metadolerite dykes outcropping in the augen gneiss southeast of Nøkle vannet.

tion to the present erosion level – agmatitic dykes at low levels might outcrop as normal dykes at higher levels. It is thus difficult to estimate the extent to which different dykes, including agmatitic dykes, may correspond in age.

Where an agmatitic dolerite is cut by a metadolerite dyke (Fig. 21), it is, however, possible to distinguish two main generations of basaltic magma emplacement: an early intrusion prior to the  $F_2$  deformation exhibiting an agmatitic nature, and also later intrusions outcropping as normal dykes.

Fig. 27. Metadolerite dyke cutting partly deformed agmatitic metadolerite in metatonalite. Nesodden, 50 m south of Torvik brygge at Bunnefjorden, northeast of Torvet.



#### *Metadolerites outside the metatonalite/granite complex*

Metadolerites in the older gneisses generally show characteristics of intrusion under cratogenic conditions. Metadolerites with a preserved, but recrystallized, ophitic texture may have been intruded between the  $F_2$  and  $F_3$  fold episodes. Older metadolerites outside the metatonalite/granite complex often show conspicuous boudinage with a NW-plunging axis ( $F_2$ ). Amphibolite facies metamorphism and NW-plunging amphibole lineation are additional characteristic features of these metadolerites; these indicate intrusion prior to the  $F_2$ , and presumably subsequent to the  $F_1$  deformation as they also, in places, cut the foliation in the surrounding gneiss.

#### *Larger metabasite intrusions*

Large metabasite intrusions crop out in the southeastern part of the area around Solbergfoss and Vågvannet along the lower, southern and eastern contact zone between the augen gneiss/orthogneiss and the supracrustal gneiss. Further to the northnorthwest, narrow, elongate metabasite bodies occur along

the thrust zone between the Østensjø anticlinorium and the Østmarka syncline (Plate 1).

The metabasites are generally dark, monotonous amphibolites, and several generations seem to occur. Northwest of Lyseren an amphibolite body is deformed by megascopic  $F_2$  folds (Fig. 25), demonstrating that at least some larger metabasites were intruded prior to the  $F_2$  deformation.

In the Vågvannet area the metabasite preserved ophitic textures and at several localities it is possible to demonstrate repeated magma intrusion. The Vågvannet and, very probably, the Solbergfoss metabasites were intruded between the  $F_1$  migmatization (Fig. 22) and the last,  $F_3'$ , deformation event (Fig. 24).

The southern metabasite bodies associated with the granitic orthogneiss around Solbergfoss include coarse-grained metagabbro which exhibits a magmatic layering in some areas. In addition, several deformed, agmatitic metabasites outcrop with a fine-grained aplitic granite. The close association of agmatitic metabasite, aplitic granite and the orthogneiss suggests a mutual connection, and if this is so

the age of the Solbergfoss metabasite complex may be useful in determining the age of the orthogneiss.

Agmatitic metabasites which outcrop in the orthogneiss in the western limb of the southern  $F_3'$  synform (Fig. 24) have been sheared and recrystallized to form biotite gneiss/schist fragments. The rocks in this area show no marked lineation, and this could indicate intrusion of the metabasite between the  $F_2$  and  $F_3'$  deformation. On the other hand, a NW-plunging lineation in the Solbergfoss area situated in the hinge zone of the southern  $F_3'$  synform may be connected with either the  $F_2$  folding and/or the  $F_3$ - $F_3'$  folding. However, a definite age is at present difficult to establish.

#### SUMMARY - RELATIONSHIPS OF METAMORPHISM AND STRUCTURES

The metamorphic evolution of the area is characterized by repeated episodes of amphibolite facies metamorphism. The mineral parageneses (see above) belong to the amphibolite facies of Barrovian type (Turner 1968).

Although the occurrence of diagnostic alumina-silicates is scarce, and information as to their time of crystallization in relation to the deformation episodes restricted, it is still possible to suggest a general correlation between folding, metamorphism and migmatite formation from  $F_1$  onwards. The migmatitic developments permit distinction of three main periods of migmatite formation related to the deformation episodes.

The most thorough migmatization occurred during  $F_1$ . This migmatitic development was simultaneous with the early crystallization of sillimanite and/or kyanite and indicates medium- to high-grade amphibolite facies metamorphism, reaching sillimanite grade at least in parts of the area.

During  $F_2$  kyanite remained stable. A new biotite foliation is sometimes present in the gneisses associated with rotation of  $F_1$  garnets and development of an amphibole lineation in amphibolites. A second generation of pegmatitic leucosome veins developed along axial planes of minor folds during this ( $F_2$ ) deformation, and is distinct from, and separates, the migmatitic schlieren which developed during the  $F_1$  and  $F_3$  fold episodes. A me-



Fig. 22. Raft of migmatitic supracrustal gneiss in metabasite from the Vågvanet metabasite area. Ytre Enebakk east of Vågvanet.

dium-grade amphibolite facies metamorphism with kyanite accompanied the  $F_2$  deformation.

Recrystallization during  $F_3$  affected the whole area, although only the eastern part was severely affected by macroscopic folding. Amphibolite facies conditions still prevailed, as demonstrated by scattered migmatitic accumulations, and crystallization of amphibole and idiomorphic garnet porphyroblasts across older structures in the southwestern part of the area. The growth of idiomorphic staurolite porphyroblasts in meta-anorthosite is ascribed to this period and indicates recrystallization under medium to low amphibolite facies conditions.

$F_3'$  is characterized by the widespread occurrence of epidote, and chlorite that may partly replace biotite, hornblende and garnet; this demonstrates retrogressive conditions during waning metamorphism. Intensive mylonitization affected the rocks in the eastern

part of the area. Early formed garnets partly survived this deformation, although they are commonly rotated and partly crushed. Biotite-chlorite aggregates are common in the partly recrystallized mylonite texture. Greenschist-amphibolite transitional facies conditions prevailed.

Late crystallization of muscovite across earlier formed textures is a characteristic feature throughout the area. This demonstrates either that the last metamorphism outlasted the regional deformation, or that the area was metamorphosed under static, low-grade conditions at an even later stage.

## Geometrical and chronological analysis of the regional structure

### INTRODUCTION

The regional structure of the area described is outlined by stratiform bodies of biotite gneiss and augen gneiss emplaced into older supracrustal gneiss. The outcrop pattern is governed by three well defined fold episodes, and possibly a fourth ( $F_0$ ), which have been traced throughout the area. The individual folds and their suggested correlations are shown on the structural map (Plate 3) and the accompanying cross sections (Plate 2). A structural stereogram of the contact between the supracrustal gneiss and the biotite gneiss is shown in Plate 4.

The structure of the area is dominated by folds which plunge into the northwest and

northeast quadrants, with a maximum of fold axes plunging about  $30^\circ$  NW (to NNW) (Plate 3). NE-plunging folds are overrepresented in the stereograms, as structures which deviated from the dominant NW-plunging structures were preferentially measured in the field. In general, the orientation of  $\pi$ -axes is in agreement with fold axes and lineations measured in the same area.

The regional analysis of the area involves folds of kilometre size, evident only on the scale of the map. The fold mechanism observed in mesoscopic folds of outcrop size appears to comprise both buckling and shearing, and it appears that shearing followed initial buckling. The large-scale structures probably originated in the same way, and it is assumed that the large folds were developed in a cylindrical manner (Turner & Weiss 1963) forming prominent linear structures. The orientation of fold axes and refolding relationships have therefore been important tools in the geometrical analysis in respect of extrapolation and correlation of folds developed at different levels. The low topographical relief does not allow analysis using structural contours (Berthelsen 1960 b).

The geometrical analysis of the structures is mainly based on the tectonostratigraphic sequence observed in the Gjersjø dome and in the major  $F_3$  synforms (Fig. 23). The central augen gneiss in the Gjersjø dome is surrounded by supracrustal gneiss with a layer of biotite gneiss marking the outer shape of the dome. This succession is also found in the  $F_3$  synforms to the east where the augen gneiss is, in addition, underlain by supracrustal gneiss:

<i>Gjersjø dome:</i>	<i>Mysen syncline:</i>	<i>Østmarka syncline</i>
supracrustal gneiss		supracrustal gneiss
biotite gneiss	biotite gneiss	biotite gneiss
supracrustal gneiss	supracrustal gneiss	supracrustal gneiss
augen gneiss	augen gneiss	augen gneiss
	supracrustal gneiss	supracrustal gneiss

In the following account synforms and anti-forms are described as synclines and anticlines with respect to this succession, which permits discussion also of inverted folds.

The rock sequence, or tectonostratigraphic succession, is intruded by rocks of the meta-tonalite/granite complex in the upper and lower supracrustal gneiss, while abundant

bodies of metabasites occur in the lowest supracrustal gneiss close to the augen gneiss contact (Plate 1). However, none of these rock units form significant parts of the tectonostratigraphic succession used to decipher the major structures, and they are not shown on the simplified tectonostratigraphic map (Fig. 23). The tectonostratigraphy given

above is valid between Bunnefjorden and Øyeren and forms the basis for the geometrical analysis and interpretation of the structural evolution. In the following outline and detailed descriptions the youngest structures are described first, followed by a progressive unravelling of the older structures.

In the eastern part of the area, major  $F_3$  folds with moderately NW- to NNW-plunging fold axes dominate the outcrop pattern (Fig. 24). These young structures refold older folds ( $F_2$ ,  $F_1$ ,  $F_0$ ), occurring now as inconsistently oriented minor folds on the flanks of the  $F_3$  folds (Fig. 30).

The influence of the  $F_3$  fold episode decreases to the west and southwest, where the outcrop pattern is dominated by interference between the  $F_1$  and  $F_2$  fold systems. The trend of the axial planes of the  $F_2$  folds is here mainly E-W, with fold axes plunging about  $30^\circ$  to the NW. The  $F_1$  folds, originally trending NNE-SSW with subhorizontal axes, now plunge at moderate angles towards the northeast quadrant. The Gjersjø dome is an outstanding example of superimposition of  $F_1$  and  $F_2$  antiforms.

It is possible that the supracrustal gneiss and biotite gneiss were folded together during an  $F_0$  fold episode prior to the intrusion of the augen gneiss. The assumption of the existence of an early  $F_0$  structure (the biotite gneiss-supracrustal gneiss nappe, Fig. 29) could explain why the biotite gneiss does not appear on Nesodden west of Bunnefjorden; this implies that the supracrustal gneiss above the biotite gneiss is equivalent to that below (Fig. 23), and would require a revision of the tectonostratigraphic succession.

The vertical cross sections (Plate 2) that accompany the geological and structural maps (Plates 1 and 3) have been constructed at intervals of 2.5 km. The general orientation is SW-NE (from left to right), such that the sections are viewed in the general direction of plunge, to the northwest. Fold hinges from the map are projected into the sections according to the local orientation of fold axes. During construction of the  $F_3$  synclines, a plunge angle of  $15-20^\circ$  was used. Minor  $F_1$  folds (the Sølvdobla syncline and anticline, SS and SA), plunging south on the eastern flanks of major  $F_3$  synclines (the Østmarka

and Mysen synclines), thus rise when followed northnorthwest in the general direction of plunge (Plate 2, section XI-XIX). It must also be borne in mind that when older folds are refolded by younger folds, the hinge zones of the younger folds relative to a particular horizon may be elevated (or lowered) along the plunge direction; this is seen in Plate 2, section X-XII, where the hinge zones of the Vågvannet (VS) and Holåsen (HS)  $F_2$  synclines and adjacent anticlines (GA and PA) have been elevated when traversing the  $F_1$  Sølvdobla syncline and anticline (SS and SA). This mutual relationship is also illustrated in Plate 4.

#### MAJOR $F_3$ STRUCTURES: THE MYSEN SYNCLINE, THE ØSTENSJØ ANTICLINORIUM AND THE ØSTMARKA SYNCLINE

The largest structures in the eastern part of the area were formed during the last main fold episode ( $F_3$ ). The augen gneiss outlines two conspicuous synforms; the Mysen syncline to the southeast and the Østmarka syncline between Øyeren and Bunnefjorden. The Østensjø anticlinorium separates the synclines, but as it has been modified by shearing it is less obvious on the map. These folds trend NNW-SSE, controlled by axes plunging NW to NNW at moderate angles.

In the Mjæren-Lyseren area south of the eastern metatonalite complex, the Mysen syncline and the southern part of the Østensjø anticlinorium are deformed by flexure. This late deformation episode is referred to as  $F_3'$  (Fig. 24).

In addition to the augen gneiss, the *Mysen and Østmarka synclines* are outlined by the structurally more complex outcrops of biotite gneiss in the fold cores. The biotite gneiss separates the intermediate and high-level supracrustal gneisses and the trace of the  $F_3$  axial plane is drawn through the major hinge zones from the lowest to the highest tectonostratigraphic levels (Plates 2 and 3).

In the *Østensjø anticlinorium*, the outcrop pattern of the dominating augen gneiss is governed by relatively flatlying, undulating fold axes. The general NW to NNW plunge is reversed in two minor depressions, one through Østensjøvannet to the north, and

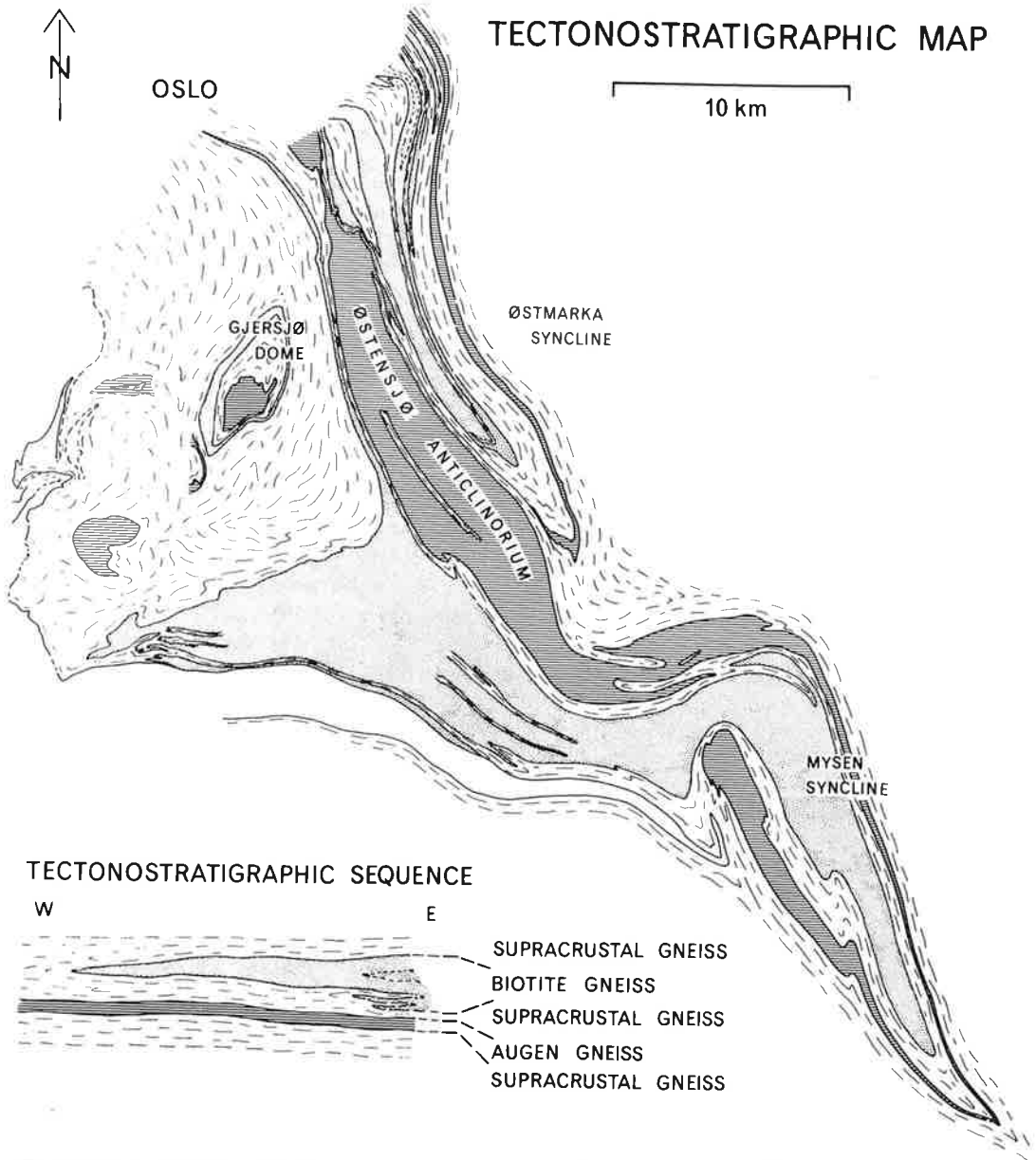


Fig. 23. Tectonostratigraphic map. The map is based on the tectonostratigraphic sequence established prior to the intrusion of the metatonalite/granite complex; the latter is omitted for simplicity and replaced by supracrustal gneiss. Major faults are also omitted.

another southwest of Vågvannet in the southeast; these are related to the late  $F_3'$  flexure.

There is a pronounced symmetry around the depression to the north centered on the Østensjø anticline (ØA) on the western flank of the anticlinorium (Plate 3). This anticline

is correlated to the southeast with the young ( $F_3$ ) anticline on Meieriåsen in the Mjæren-Lyseren area (Fig. 24). The adjacent syncline (LS) to the north on Meieriåsen lies on a parallel course through the NNW-plunging wedge of supracrustal gneiss along Lake Langen (LS Plate 2, section XIII), continuing

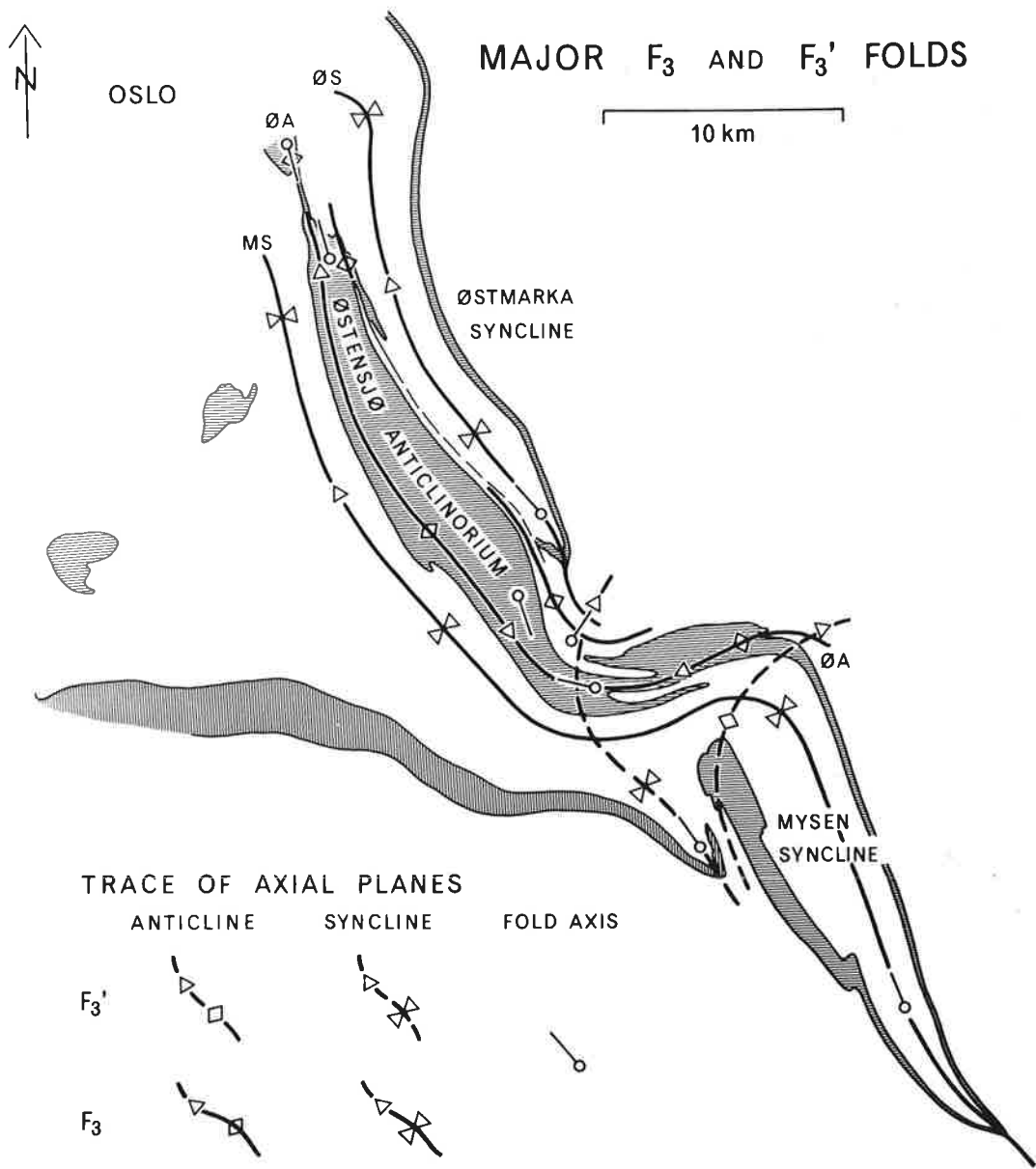


Fig. 24. Major F<sub>3</sub> and F<sub>3</sub>' folds. The trace of the axial plane of Østmarka-Meieriåsen anticline (ØA) is shown in the Østmarka anticlinorium. MS: Mysen syncline, ØS: Østmarka syncline.

northnorthwest to the area west of Nøklevannet (Plate 3).

The eastern part of the anticlinorium is poorly defined. The easternmost anticline around Sølvdøbla is extremely flattened and the augen gneiss limb, also common to the Østmarka syncline, is disrupted by intense

shearing. West of the eastern anticline and east of Østmarka anticline and Langen syncline, another anticline and syncline fold pair occurs (Plate 3). The southern termination of this fold pair towards Vågvannet is somewhat obscure; at the augen gneiss-supracrustal gneiss contact the folds may be concealed in

Vågvannet, or they might be disrupted, or die out.

The major  $F_3$  structures re-fold older folds ( $F_2, F_1, F_0$ ), which now outcrop as imper-sistent smaller structures on the flanks of the  $F_3$  folds.

#### PRE $F_3$ -STRUCTURES IN THE MJÆREN-LYSEREN AREA

Around Mjæren and Lyseren, south of the eastern metatonalite complex, the otherwise simple Mysen syncline ( $F_3$ ) exhibits a complicated outcrop pattern (Plates 1 and 3). Here, the major  $F_3$  syncline has an E-W trend, and the northern flank is complicated by thickening of the augen gneiss together with major and minor folds incompatible with the major  $F_3$  structures in the adjoining areas. The outcrop pattern is in addition disturbed by cross-cutting steep faults and large amphibolite bodies which intrude the supracrustal gneiss (Fig. 25 A).

In order to facilitate the structural analysis, the displacements on the faults have been eliminated, and the amphibolites have been omitted. The simplified map (Fig. 25 B) shows a number of westward-plunging folds with the traces of their axial planes. The antiform-synform fold pair (LS, ØA) on Meieriåsen, to the east of the lower (northern) augen gneiss-supracrustal gneiss contact, follows the *normal* tectonostratigraphic succession (augen gneiss above the lowest supracrustal gneiss). This structure is therefore treated as an anticline-syncline fold pair on the flank of the major  $F_3$  Mysen syncline in the Østensjø anticlinorium (Plate 3, Plate 2, section VII).

In contrast, the western synform (VS)-anti-form fold pair on the northern (lower) contact around Mjæren, shows *inverted* tectono-stratigraphic relations (augen gneiss plunging below the lowest supracrustal gneiss), and these WNW-plunging folds are treated as an *inverted* anticline-syncline pair (Fig. 25 C). To the south on the *upper* augen gneiss-supracrustal gneiss contact, a similarly inverted and westward-plunging syncline and anticline (GA) occur; these structures are also reflected by the supracrustal gneiss and biotite gneiss to the east, even though the relationship is somewhat disturbed by minor folds.

The inverted structures do not accord with the geometry of the adjacent  $F_3$  folds and must be older ( $F_2$ ). The two sets of older folds ( $F_2$ ) may, however, represent one syncline-anticline fold pair refolded by the younger ( $F_3$ ) folds on Meieriåsen. The outcrop of the supracrustal gneiss wedge in the augen gneiss would then take the form of superimposed synforms from the two fold systems, the ideal shape being an arrowhead-shaped outcrop pattern (Fig. 25 C).

The inverted (and refolded) syncline-anticline (VS-GA) fold pair ( $F_2$ ) is situated on the northeast flank of the Mysen syncline. Since the older folds plunge to the west with a steeper angle than the neighbouring  $F_3$  folds, it is to be expected that they will outcrop with normal stratigraphic relations on the southwest flank of the Mysen syncline (Plate 2, sections VIII-IX).

The transecting minor folds eliminated in Fig. 25 C are incompatible with both the early ( $F_2$ ) and the young ( $F_3$ ) folds; they are regarded as minor folds accompanying the late  $F_3$ ' flexure of the Mysen syncline in this area.

#### SUPRACRUSTAL GNEISS WEDGES IN THE GRANITIC GNEISSES - ESTABLISHMENT OF $F_1$ AND $F_2$ STRUCTURES

Wedge-shaped outcrops of supracrustal gneiss occur both in the augen gneiss and in the biotite gneiss. These wedges are up to 7 km long and 250 m across and their contacts are parallel with the foliation in the surrounding rocks. The broad end of the wedges is always to the west and northwest, the general plunge direction. These wedges seem not to be accidental xenoliths in the orthogneisses, but are part of a regular fold system consistent with the surrounding structures and the tectonostratigraphic sequence. Similar wedges of supracrustal gneiss in the augen gneiss in the Mjæren-Lyseren area (Fig. 25) and along the northern part of Langen in the Østensjø anticlinorium (Plate 3) have been considered to form synclinal structures. This interpretation is in accordance with the orientation of the fold axes and places the supracrustal gneiss at the upper augen gneiss-supracrustal gneiss contact.

On both flanks of the Østensjø anticlinorium ( $F_3$ ), the upper augen gneiss-supra-



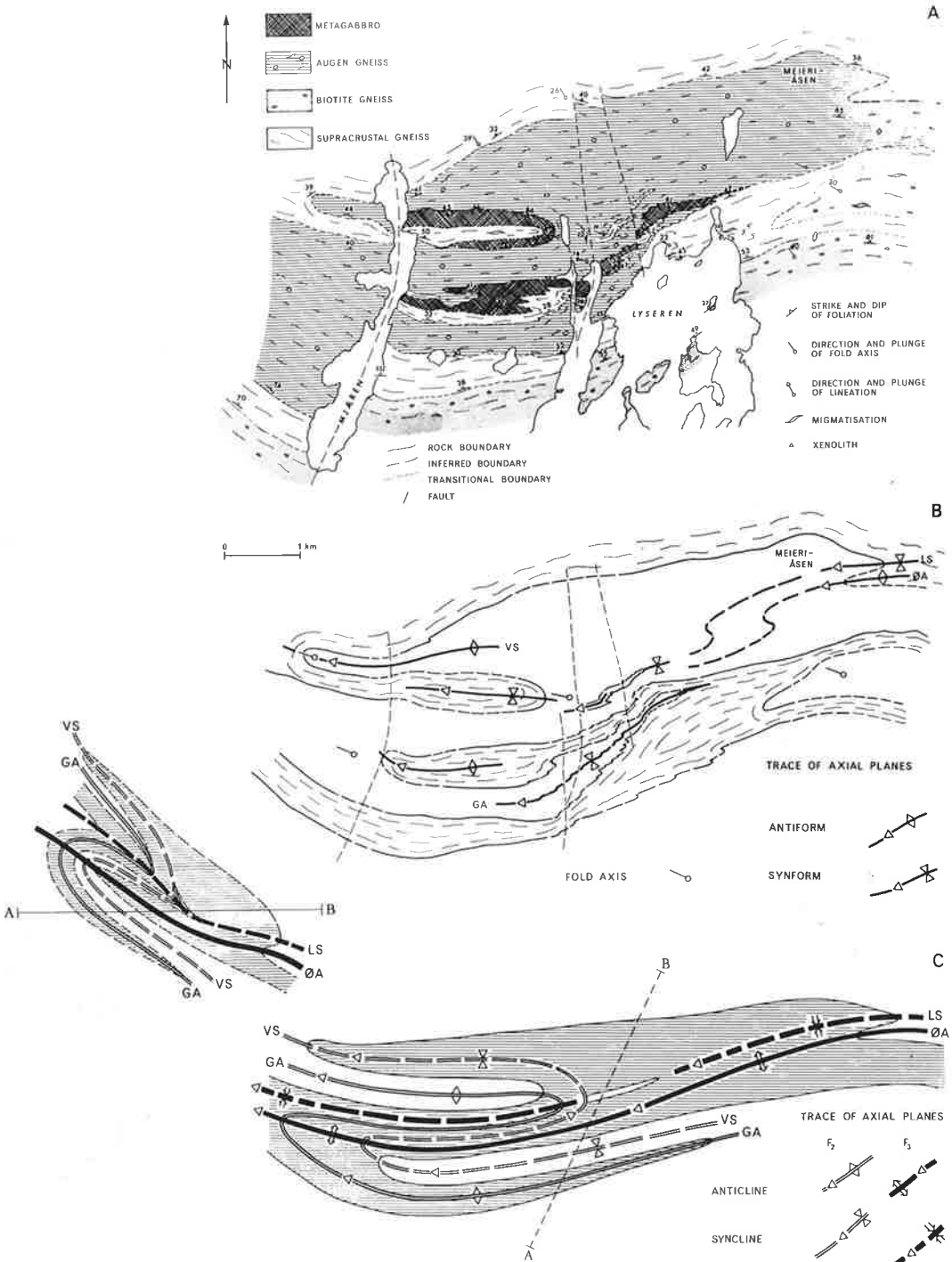


Fig. 25. Interpretation of the Mjæren-Lyseren area. A) Geological map. Location is indicated in Plates 1 and 3. B) Simplified map with major folds indicated. The metagabbro is omitted, and displacements on the faults reconstructed. C) Interpretation and correlation of major folds. The minor folds present in B) and eliminated from this outline were formed during the  $F_3$ ' deformation. VS: Vågvannet syncline, GA: Gjersjø anticline, LS: Langen syncline, ØA: Østensjø anticline.

crustal gneiss contact shows folds which are inconsistent with this major structure. On the western flank of the anticlinorium, a SSE-plunging antiform-synform fold pair outcrops with normal stratigraphic relationships at Pongen (south of the Langen supracrustal gneiss wedge). In contrast, a NNW-plunging synform-antiform fold pair around Sølvdobla is found on the eastern limb north of the Langen supracrustal gneiss wedge with *inverted* tectonostratigraphic relationships (Plate 1). However, the fold pairs on both flanks may also be correlated and viewed as a single anticline-syncline fold pair refolded by the ( $F_3$ ) anticlinorium (Fig. 26). The broad end of the supracrustal gneiss wedge in the  $F_3$  syncline through Langen is then situated where the older syncline is refolded by the younger ( $F_3$ ) structures. The supracrustal gneiss wedge is therefore interpreted as an arrowhead-shaped interference pattern composed of superimposed synclines (Plate 3 and Fig. 26). This is consistent with the split of the northern broad end of the wedge.

The original trend of the older Pongen-Langen-Sølvdobla structure prior to the  $F_3$  deformation was probably NNE-SSW, whereas the refolded ( $F_2$ ) structure from the Mjæren-Lyseren area probably had NW-SE trends; the two sets of older (pre- $F_3$ ) structures cannot be correlated.

The two wedge-shaped outcrops of supracrustal gneiss in the biotite gneiss southeast of Nærevannet are tentatively treated as NW-plunging synclines, similar to the supracrustal gneiss outcrop in the augen gneiss, and consistent with the observed fold axes. The northern syncline (VS) (supracrustal gneiss wedge) then occupies the predicted position on the southwestern flank of the Mysen syncline (MS) ( $F_3$ ) of the refolded and right-way-up equivalent of the inverted  $F_2$  syncline from the Mjæren-Lyseren area (Plate 2, sections IX-XI, Plate 3).

The southern WNW-plunging syncline (supracrustal gneiss wedge) on Holåsen (HS) is parallel to that to the north and is also thought to be of  $F_2$  age (Fig. 26). These synclines then occur at the upper biotite gneiss-supracrustal gneiss contact at the highest tectonostratigraphic level. The southern syncline is correlated to the southeast with the syn-

cline around Mørkved which developed in the lower part of the tectonostratigraphic sequence on the southwest limb of the Mysen syncline (Plates 2 & 3).

Taking into account the cut-off of the assumed  $F_2$  supracrustal gneiss synclines in the biotite gneiss, a possible refolded syncline would then have to be an older ( $F_1$ ) originally NE-SW-trending syncline. The extension of the Pongen-Sølvdobla structure (SA, SS) into this area reveals (at a higher tectonostratigraphic level) the expected  $F_1$  syncline (Plate 2, section XI, Plate 3). The continuation of the  $F_1$  structure towards the NE at this high level is found in the Østmarka syncline, which was later refolded during the  $F_3$  deformation (Fig. 26, Plate 4). The expected continuation of the  $F_1$  fold pair (SA, SS) southeast of the Holåsen syncline has not been verified on account of poor exposure.

The divergent trends of the refolded pre- $F_3$  structures in the Østensjø anticlinorium and Mysen syncline can now be explained as two older intersecting fold systems ( $F_1$  &  $F_2$ ). The interpretation of the wedge-shaped supracrustal gneiss outcrops as superimposed synclines seems to be justified by the fact these structures are of different ages, and the folds involved in each case are also found at other tectonostratigraphic levels than the one in question.

#### $F_1$ AND $F_2$ FOLDS IN THE ØSTMARKA SYNCLINE

Megascopic folds of the  $F_1$  and  $F_2$  fold systems are outlined by biotite gneiss which crops out in the core of the NNW-plunging  $F_3$  Østmarka syncline (Plates 2 & 3).

On the *upper* biotite gneiss-supracrustal gneiss contact in the *eastern* limb, the biotite gneiss outcrops in the core of a SE-plunging anticline (SA) around Plassen in the northern part of the area (Fig. 26 B, Plates 1 & 3). This fold and the adjoining syncline to the northeast have normal tectonostratigraphic relationships (the biotite gneiss plunges below the upper supracrustal gneiss). These folds may be correlated with the refolded  $F_1$  folds in the Østensjø anticlinorium at Pongen and Sølvdobla via the *inverted* NNE-plunging syncline-anticline fold pair north of Bindings-

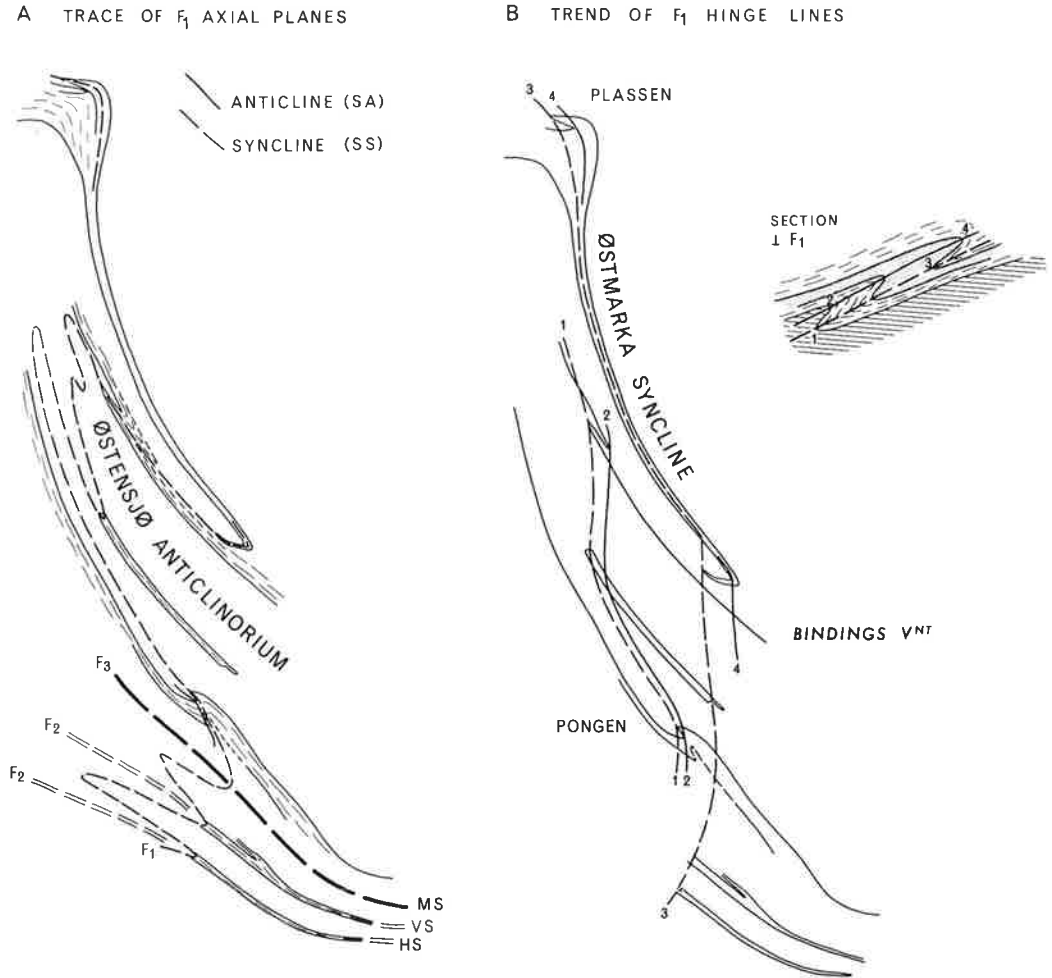


Fig. 26. Correlation of F<sub>1</sub> folds across the F<sub>3</sub> Østensjø anticlinorium. A) Trace of F<sub>1</sub> axial planes. B) Trend of F<sub>1</sub> hinge lines. Symbols in the F<sub>1</sub> section according to Fig. 23. SA: Sølvdobla anticline, SS: Sølvdobla syncline, VS: Våg vannet syncline, HS: Holåsen syncline, MS: Mysen syncline.

vatnet, which reappears to the south on the western limb of the major F<sub>3</sub> syncline (Fig. 26, Plate 2, section XIV, Plate 4).

The corresponding F<sub>1</sub> folds on the lower biotite gneiss-supracrustal gneiss contact south of Sølvdobla (Fig. 26 A) are sheared off or strongly compressed against the Østensjø anticlinorium along the western flank of the Østmarka syncline (Plate 2, section XVI, Plate 3).

Rocks of the metatonalite/granite complex outcrop around Nøklevannet as a north-plunging synform in the biotite gneiss on the western limb of the Østmarka syncline (Plate

1, NS in Plates 2 (section XIX) and 3). Large xenoliths of supracrustal gneiss (10–100 m across) are frequent, and exposures at the contacts against the biotite gneiss show that supracrustal gneiss occurs as a 0.5–1 m-wide screen separating the metatonalite/granite complex from the biotite gneiss. These observations concur with the relationships found west of the Østensjø anticlinorium in a symmetrical position, and indicate that the synform is a (supracrustal gneiss) syncline at the upper biotite gneiss-supracrustal gneiss contact (Fig. 23). The synform is thus placed at the same tectonostratigraphic level as the su-

pracrustal gneiss around Lutvannet to the east in the core of the Østmarka ( $F_3$ ) syncline (ØS), and must be linked to the latter through an intervening anticline in the biotite gneiss (NA in Plate 2, section XIX). This correlation is also suggested by the folded foliation in the biotite gneiss indicating a NNW-plunging antiform.

The folds in question are internal folds in the biotite gneiss on the western limb of the Østmarka syncline and must therefore be older than the  $F_3$  syncline itself. The refolded  $F_1$  structures in this limb show inverted tectonostratigraphic relationships, and the (supracrustal gneiss) syncline, which is now occupied by rocks of the metatonalite/granite complex, is considered to be of  $F_2$  age. These ( $F_2$ ) folds in the western limb of the Østmarka syncline are thus responsible for the thickening of this limb relative to the eastern one. As the present trend of the  $F_2$  structures in question is caused by refolding in the  $F_3$  Østmarka syncline (Fig. 28), this interpretation corresponds with a northward extension of the  $F_2$  fold system found to the south.

The internal folds of the Østmarka syncline mentioned above have been explained as  $F_1$  and  $F_2$  folds, and both are refolded by the major  $F_3$  syncline. However, the tight to isoclinal folds in the biotite gneiss on the eastern limb cannot be placed into this system of superimposed folds.

#### $F_2$ , $F_1$ and (?) $F_0$ STRUCTURES OUTSIDE THE $F_3$ DOMAIN IN THE BUNNEFJORDEN-HALLANGSPOLLEN AREA

The influence of the youngest deformation ( $F_3$ ) decreases to the west. South of the Gjer-sjø dome, the foliation is generally E-W trending with a moderate northerly dip (Plate 1). The complicated outcrop pattern revealed by detailed mapping around Bunnefjorden in the southwestern part of the area is shown on Fig. 27 A. The structural interpretation of this area is based on a simplified map showing biotite gneiss outcrops surrounded by supracrustal gneiss; displacements on later faults have been readjusted and the uncertain occurrence of biotite gneiss southwest of Pollevannet omitted (Fig. 27 B).

WNW- and NW-plunging folds are the most common mesoscopic structures in the

area, but folds plunging to the east and north-east also occur (Plate 3, stereogram c). The isolated wedge-shaped outcrops of supracrustal gneiss, together with the development of two predominant axial directions, suggest an interpretation similar to that for the supracrustal gneiss wedges in the biotite gneiss to the east (southeast of Nærevannet). Thus, the narrow outcrops of supracrustal gneiss which are outlined in the biotite gneiss are shown as ( $F_2$ ) synclines (BS and FS in Fig. 27 B). An older ( $F_1$ ) refolded syncline (KS), crossed by the younger folds and responsible for the closed outcrop pattern, is suggested by the split western end of the supracrustal gneiss wedges. The outcrop pattern can be interpreted as the result of an old NNE-SSW trending ( $F_1$ ) syncline being refolded by E-W trending, NW-plunging ( $F_2$ ) folds (Fig. 27 B).

The  $F_1$  syncline (KS) around Knardal on the upper biotite gneiss-supracrustal gneiss contact to the north is correlated with the  $F_1$  synclinal structure described above, being refolded by the northern  $F_2$  anticline (BA) (Fig. 27 B). This  $F_2$  anticline lies parallel to and north of the  $F_2$  syncline through the supracrustal gneiss at Bekkevol (BS), and both  $F_2$  folds developed on the upper biotite gneiss-supracrustal gneiss contact to the west around Bjerke. It follows from this interpretation that the superimposed synclines in the isolated outcrops of supracrustal gneiss are developed at the upper biotite gneiss-supracrustal gneiss contact (Fig. 27 B).

The anticline separating the superimposed  $F_2$  synclines in the supracrustal gneiss at Bekkevol and Fossen is counterbalanced to the southwest on the *lower* biotite gneiss-supracrustal gneiss contact by the presumably east-plunging anticline (FA). It is followed to the south by an east-plunging syncline correlated with the southern  $F_2$  syncline (FS) around Fossen on the upper augen gneiss-supracrustal gneiss contact along section line A-B on the map in Fig. 27 B. The complicated outcrop pattern of the E plunging syncline on the lower contact is caused by refolding of the old ( $F_1$ ) structure generating schrein B axes (Sander 1948) during the  $F_2$  deformation (section A-B, Fig. 27 B).

The system of NNE-SSW-trending  $F_1$  folds superimposed by the predominant E-W-trending  $F_2$  folds plunging to the NW is con-

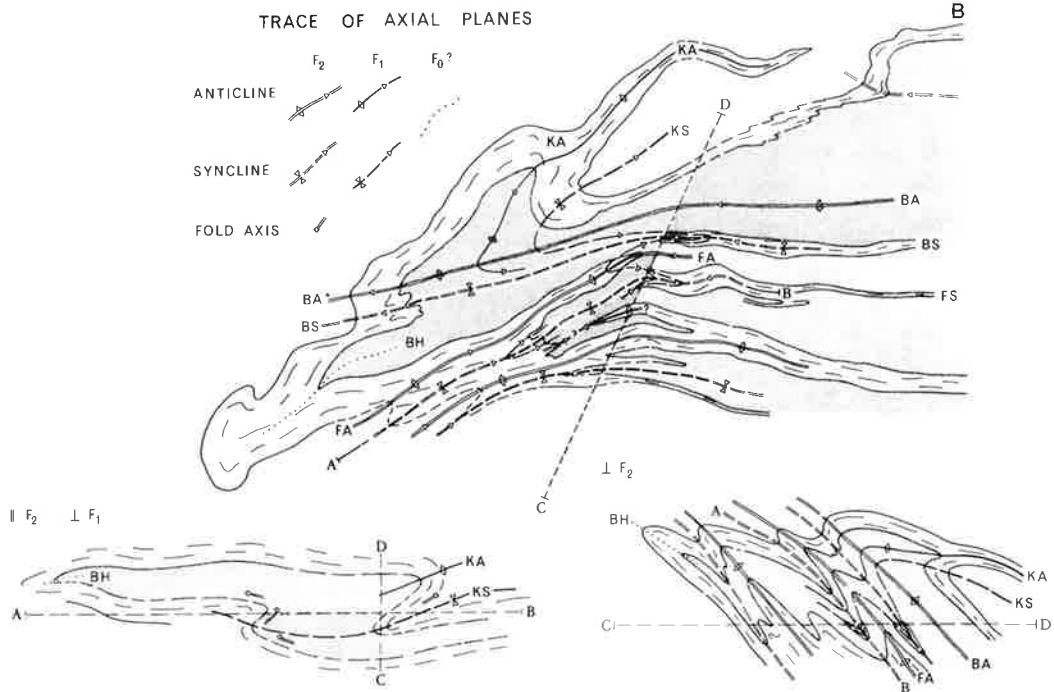
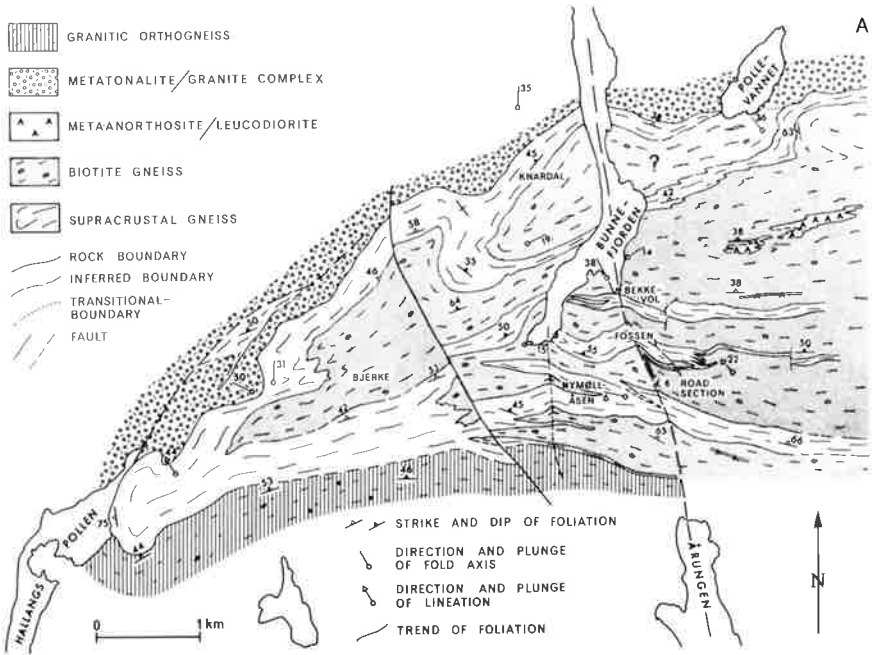


Fig. 27. Interpretation of the Bunnefjorden-Hallangspollen area. A) Geological map. Location is indicated in Plates 1 & 3. B) Interpretation and correlation of major folds. The questionable occurrence of biotite gneiss westsouthwest of Pollevannet is omitted together with the cross-cutting faults. BH: Bjerke-Haukåsen recumbent folds, KA: Kolbotn anticline, KS: Knardal syncline, BA: Bekkevoll anticline, BS: Bekkevoll syncline, FA: Fossen anticline, FS: Fossen syncline.

firmed on a mesoscopic scale in a road section along highway E 6 (Fig. 27 A); here garnet amphibolites in the biotite gneiss show a similar structural pattern (Fig. 18, and Graveresen 1973).

When the system of parallel  $F_2$  folds is extended to the south (and east) on the lower biotite gneiss-supracrustal gneiss contact (Fig. 27 B), a possible depression ('?') with sub-horizontal fold axes marks the limit of the E-plunging  $F_2$  structures. To the east the trace of the  $F_2$  axial planes (BA, BS, FA, FS), controlled by the strike of the foliation, fits with the NW-plunging anticline-syncline fold pairs of the same order on the lower biotite gneiss-supracrustal gneiss contact on Bjørnåsen (FA, FS) and southwest of Lyseren (BA, BS) (Plate 3 and Fig. 28).

This correlation establishes a natural extension and continuation of the already established  $F_2$  folds (HS, PA, VS, GA) north of Bjørnåsen (southeast of Nærevann) on the upper biotite gneiss-supracrustal contact (Plate 2, sections X–XV). Likewise, the earlier established folds find their natural counterparts to the west and northwest on the upper biotite gneiss-supracrustal gneiss contact around Pollevannet and Langhus along the northern border of the main biotite gneiss area (Plate 3, Fig. 28).

The westernmost extension of the biotite gneiss northeast of Hallangspollen marks the transition from the *lower* biotite gneiss-supracrustal gneiss contact to the *upper* one which is marked with a dotted line (BH) on the map and section A–B of Fig. 27 B. It is uncertain whether this probably NNE-plunging western limitation of the biotite gneiss represents a thinning-out of an intrusive granitic sheet, but the folded foliation in the transition zone points to a repetition of the supracrustal gneiss and biotite gneiss. If this assumption is correct, it implies a revision of the tectonostratigraphy through correlation of the supracrustal gneiss below and above the biotite gneiss.

Both the  $F_1$  and the  $F_2$  structures may be correlated across the biotite gneiss (section C–D, Fig. 27 B) which must consequently have been intruded and most probably folded on a large scale ( $F_0?$ ) (section A–B, Fig. 27 B) prior to the  $F_1$  deformation.

The broad exposure of the biotite gneiss

in the main area to the south around Ski and Nærevannet (Plate 1) is best explained through extensive repetition, mainly controlled by  $F_2$  folds superimposed on a relatively thin granitic sheet (biotite gneiss) thinning-out to the west (Fig. 28). To the east, the  $F_2$  folds become increasingly involved in the  $F_3$  Mysen syncline and the foliation turns to a NW-SE orientation (Fig. 28). The thin biotite gneiss layer extending to the north-northwest along the Østensjø anticlinorium there finds a natural position on the eastern limb of the Mysen syncline. The limited thickness of this limb reflects the original thickness of the granitic (biotite gneiss) sheet, as is also seen to the southwest in the Hallangspollen-Bunnefjorden area (Fig. 27 B, section A–B). The thickness of the biotite gneiss layer exposed in the Gjersjø dome corresponds with this interpretation.

Although the exposure south of Ski is limited, the granitic orthogneiss along the southern border of the biotite gneiss/supracrustal gneiss outcrop appears to be discordant (Plate 1 and Fig. 27 A); the folds established along the adjacent southern biotite gneiss/supracrustal gneiss contact do not involve the granitic orthogneiss. If these considerations are correct, the granitic orthogneiss must post-date the  $F_2$  deformation and cannot be correlated with the granitic augen gneiss to the east and north which was folded during both the  $F_1$  and  $F_2$  fold episodes.

#### THE GJERSJØ DOME

In the description of the Gjersjø dome, Zetterstrøm (1974) leaves the interpretation of the dome-forming mechanism to future regional interpretation, but points to either a diapiric mode of formation as propounded by Wegmann (1930), or to formation through superimposed folding (Ramsay 1962).

The dome has an overall NNE-SSW orientation; the contacts generally dip to the west or northwest. A number of minor NW-plunging folds (especially along the northern augen gneiss-supracrustal gneiss contact) and the larger NW-plunging antiformal around Gjersjøen to the southeast affect the general NNE-SSW elongation. It seems most probable that the dome was formed through interference of an old ( $F_1$ ) E-verging anticline

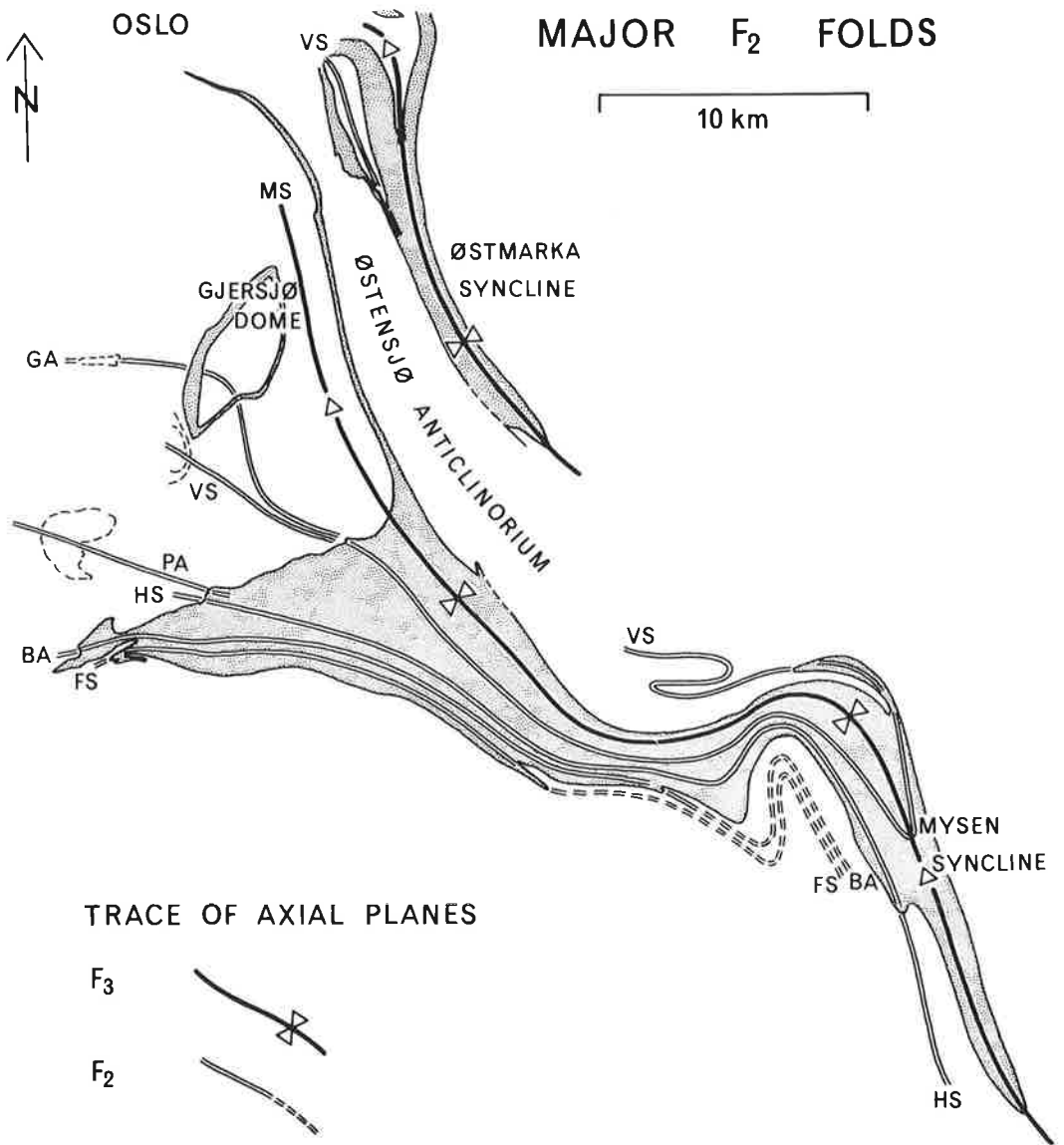


Fig. 28. Outcrop pattern of the biotite gneiss with correlation of major F<sub>2</sub> folds. NS: Nøklevannet syncline, GA: Gjersjø anticline, VS: Vågvannet syncline, PA: Pøllevannet anticline, HS: Holåsen syncline, BA: Bekkevoll anticline, FS: Fossen syncline.

trending NNE-SSW and a younger (F<sub>2</sub>) NW-plunging and roughly E-W-trending anticline (Plate 3).

This interpretation and the actual position of the dome corresponds with the structural development to the south and east. The older anticline (the Kolbotn anticline, KA) of the Gjersjø dome seems to be an F<sub>1</sub> structure and can be correlated to the south with the F<sub>1</sub>

anticline in the southern Bunnefjorden area; both these structures are of similar size and have similar trends. The superimposed younger anticline (the Gjersjø anticline, GA) is an F<sub>2</sub> structure. The trace of the axial plane through Gjersjøen is governed by the foliation in the surrounding gneiss, and correlated with the NW-plunging syncline-anticline fold pair on the upper biotite gneiss-supracrustal gneiss

contact around Langhus (Plate 3). This connects the Gjersjø dome with the inverted  $F_2$  structures in the Mjæren–Lyseren area (GA, VS) via the equivalent structures on a higher tectonostratigraphic level on the southwestern limb of the  $F_3$  Mysen syncline (Plate 2, Plate 3, Fig. 28). The position of the Gjersjø dome west of the  $F_3$  Mysen syncline is in agreement with the symmetrical repetition of the tectonostratigraphic succession to the east in the Østensjø anticlinorium.

The interpretation of the structures in the supracrustal gneiss area south and west of the Gjersjø dome is uncertain as marker horizons are either absent or only partly exposed. The augen gneiss southwest of the dome may be an extension of the augen gneiss from the dome, an  $F_1$  anticline refolded by an open WNW-plunging  $F_2$  syncline (?VS) (Plate 3). This interpretation is partly in agreement with Zetterström (1974) who, however, interpreted this structure as a basin. The present interpretation is shown in Plate 2, section XVI, where the augen gneiss is a natural link between the Gjersjø dome and the Gardar granite on Nesodden.

#### $F_0$ - THE BIOTITE GNEISS-SUPRACRUSTAL GNEISS NAPPE

The existence of a fold episode prior to the  $F_1$  deformation which was responsible for structures that do not fit the three main fold systems ( $F_3$ ,  $F_2$  and  $F_1$ ), has been discussed for the Bunnefjorden–Hallangspollen area, and was also suggested by structures occurring in the eastern limb of the Østmarka syncline.

In the Hallangspollen area, it was suggested that the westward extension of the biotite gneiss was arrested in an early N- to NNE-plunging reclined fold ( $F_0$ ). This view is supported by the westward thinning of the biotite gneiss in the eastern limb of the Mysen syncline to the northnorthwest (around Akershus in the Oslo area), and by the fact that the biotite gneiss does not outcrop on Nesodden although the lower level augen gneiss is exposed in a refolded anticline structure around Gardar (Plate 1). The westernmost outcrops of the biotite gneiss thus follow a NNE-SSW-trending zone (fold axis?) through Bunnefjorden (Fig. 29).

In the eastern limb of the Østmarka syncline, the internal structures on the lower biotite gneiss/supracrustal gneiss contact are shown as isoclinal synclines (Plate 2, section XIX, Plate 3, Fig. 29). Although this interpretation follows the tectonostratigraphic analysis, there is still some doubt as to its correctness as these structures do not fit any of the three previously described main fold episodes which build up the rest of the area.

The augen gneiss on the eastern limb does not show any folds that can be correlated with these structures, and an  $F_3$  or younger age for the folds in question is not possible. Nor is a correlation with the second ( $F_2$ ) fold episode possible, as  $F_2$  folds which outcrop in the eastern limb of an  $F_3$  syncline would show inverted stratigraphic relations. Even if the structures outlined by the biotite gneiss are regarded as inverted synclines plunging south as antiformal structures, they are not repeated in the western limb of the Østmarka syncline, and the argument that they might be sheared off against the Østensjø anticlinorium is excluded by the fact that they do not occur further south in the Mysen syncline. The  $F_1$  folds in the eastern  $F_3$  syncline limb show normal stratigraphic relations in south-plunging folds immediately to the west around Plassen on the upper biotite gneiss/supracrustal gneiss contact, which also makes correlation with  $F_1$  folds doubtful.

A north-plunging isoclinal fold within the biotite gneiss between Lutvannet and Haukåsen (Plate 1), however, makes a reasonable structural continuation of the possible folds on the lower contact. This fold is marked by a layer of supracrustal gneiss within the biotite gneiss and is shown as a north-plunging syncline in accordance with the structures to the east (Plate 3, Fig. 29). These isoclinal structures thus seem to predate the three main fold systems ( $F_1$ – $F_3$ ) which govern the outcrop pattern through most of the area.

Through elimination of the  $F_1$ – $F_3$  structures, correlation of the pre- $F_1$  structures in the biotite gneiss from the southwestern and northeastern parts of the area is put forward in the pre- $F_1$  cross-section of Fig. 29. An interpretation in favour of folding as being responsible for the pre- $F_1$  structures now appears most appropriate as the folded layer of supracrustal gneiss in the augen gneiss west



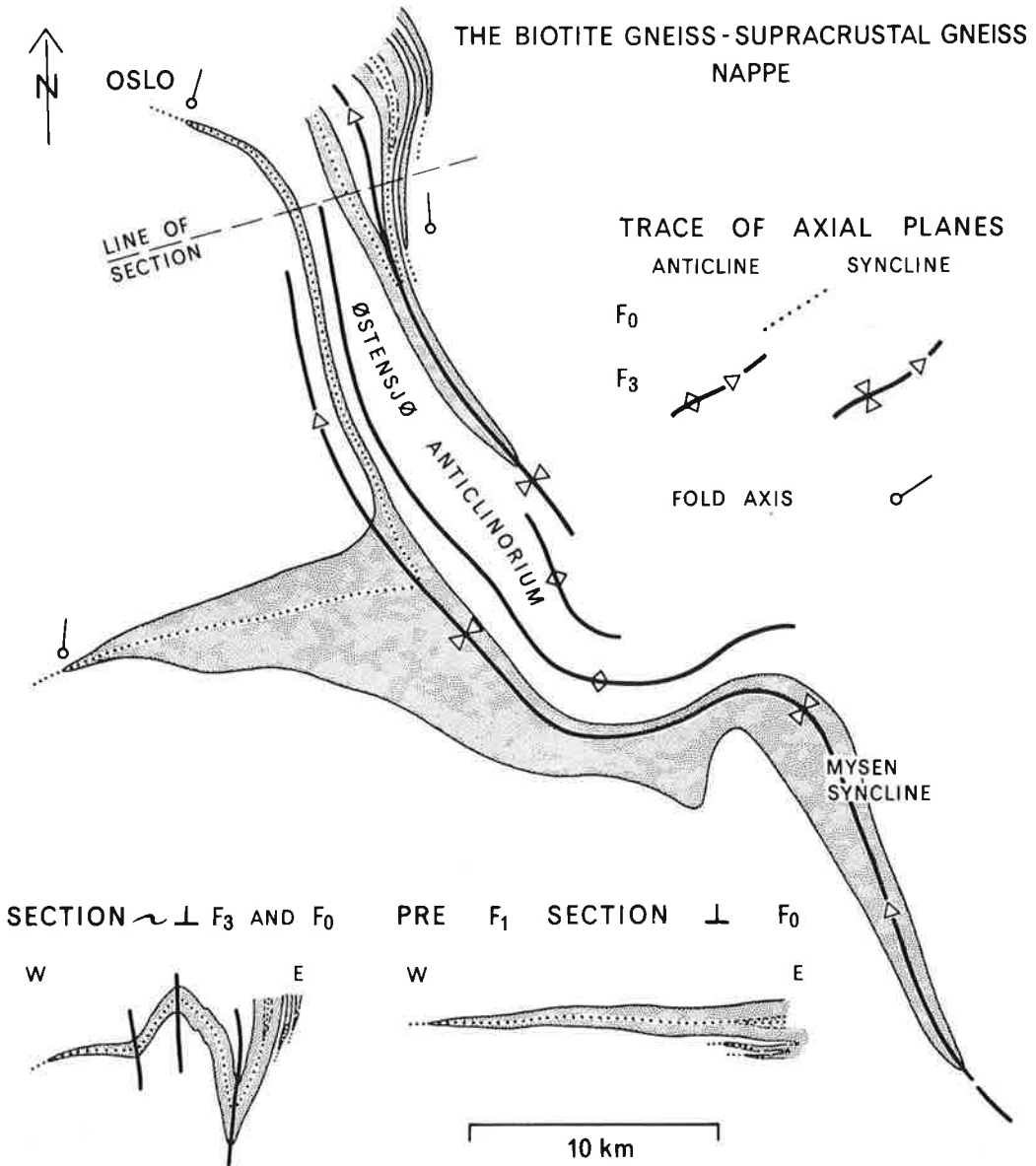


Fig. 29. The biotite gneiss - supracrustal gneiss nappe. Interference pattern between the F<sub>0</sub> biotite gneiss-supracrustal gneiss nappe and major F<sub>3</sub> folds. F<sub>1</sub> and F<sub>2</sub> folds have been partly eliminated.

of Haukåsen to the northeast corresponds to the termination of the biotite gneiss to the west. Furthermore, the closures in question are all parallel and follow a flat north-plunging axis. The pre-F<sub>1</sub> structures are therefore given the status of a separate fold phase and are referred to as F<sub>0</sub>.

The previously suggested revision of the tectonostratigraphic succession is thus main-

tained, and the supracrustal gneiss above the biotite gneiss can be correlated with the supracrustal gneiss below. The interpretation put forward places the biotite gneiss in the core of an early (F<sub>0</sub>) fold nappe, the biotite gneiss-supracrustal gneiss nappe, extending westwards and with an unknown root zone somewhere in the east.

## NESODDEN

As the biotite gneiss is lacking on Nesodden, the tectonostratigraphic sequence established east of Bunnefjorden no longer holds (Fig. 23). However, the structural evolution may still be interpreted along lines similar to those for the area east of Bunnefjorden (Plate 3). The lunar-shaped outcrop pattern of the gneissic augen granite around Gardar may thus be explained as an old ( $F_1$ ) NNE-SSW-trending anticline superimposed by a younger E-W-trending ( $F_2$ ) anticline plunging to the northwest. To the north, the Gardar granite can be linked to the arrowhead-shaped augen gneiss (granite) at Torvet through the older ( $F_1$ ) anticline, brought to outcrop level again by a later E-W-trending ( $F_2$ ) anticline.

Both E-W-trending ( $F_2$ ) anticlines on Nesodden can be linked to the area east of Bunnefjorden through correlation with the  $F_2$  anticline (GA) of the Gjersjø dome to the north, and (probably) with the anticline (PA) to the south in the biotite gneiss area (Plate 3, Fig. 28). The older ( $F_1$ ) anticline on Nesodden likewise forms a natural westward extension of  $F_1$  structures developed to the east (Plate 2, section XVI).

## SUMMARY OF THE REGIONAL STRUCTURE

Interpretation of the structural framework is mainly based on the tectonostratigraphic succession and the interaction and correlation of individual folds that have been separated into the regionally developed superimposed fold systems. Consequently, it is generally not possible to judge the relative age of individual folds in a single outcrop. Furthermore, the widespread correlation of separated folds presupposes a cylindrical development of the folds on a kilometre scale – an assumption that has not been definitely established. However, the successful application of this assumption might in itself be supporting evidence for a cylindrical development of the folds.

Four fold episodes,  $F_0$ – $F_3$ , of regional importance have been distinguished (Figs 30 & 31, Plate 4). The fold style of the individual systems shows great variation and the outcrop pattern within a single system may depend on competence differences between the individual folded layers.

Interpretation of the earliest, recognizable fold system ( $F_0$ ) of regional importance is based on the interpretation of the biotite gneiss unit as the core of a large fold nappe enveloped by a supracrustal gneiss. It is a recumbent structure extending from the east for 20–30 km and terminating to the west with a N–S trending axis. On the lower limb minor folds occur (Fig. 31). The traces of the ( $F_0$ ) axial planes in the biotite gneiss are shown in Fig. 29.

The intrusion of the augen gneiss between the  $F_0$  and  $F_1$  episodes (it is not affected by the  $F_0$  deformation) may mark a major time interval. The tectonostratigraphic sequence established at this stage formed the basis for the structural analysis (Figs 23 & 30).

The  $F_1$  fold system is characterized by sub-horizontal fold axes and NNE-SSW-trending folds overturned to the east (Fig. 31). Folds which outcrop close to the augen gneiss are of larger dimensions and less compressed than corresponding folds at higher levels, reflecting the higher competence of the augen gneiss. The ESE-verging folds, with an amplitude of around 2 km and wavelengths between 2 and 10 km, are in striking contrast to the tectonic style of the biotite gneiss-supracrustal gneiss nappe (Fig. 31), and perhaps confirm a major break between the  $F_0$  and  $F_1$  fold episodes.

$F_2$  folds are superimposed on the  $F_1$  folds nearly at right angles. The characteristic E-W trend of the trace of the  $F_2$  axial planes is seen in the west outside the main area of the  $F_3$  deformation (Fig. 28). The  $F_2$  fold axes plunge around  $30^\circ$  to the NW, and axial planes are inclined to the south (Fig. 31). The style of the  $F_2$  folds is similar to that of the  $F_1$  major folds, and the folds are of about the same dimensions.

During the  $F_3$  deformation the western part of the area acted as a rigid block, while to the east earlier structures were reoriented by the  $F_3$  folds. The  $F_3$  fold system is characterized by a few major folds with rather flat ( $15^\circ$ ) NNW-plunging fold axes (Fig. 31). The  $F_3$  folds trend NNW-SSE with steep axial planes; the amplitude of the major folds is 6–7 km, about twice that of the wavelength. The  $F_3$  folds are thus of greater dimensions than the  $F_1$  and  $F_2$  folds which outcrop on the limbs of the superimposed  $F_3$  fold structures.

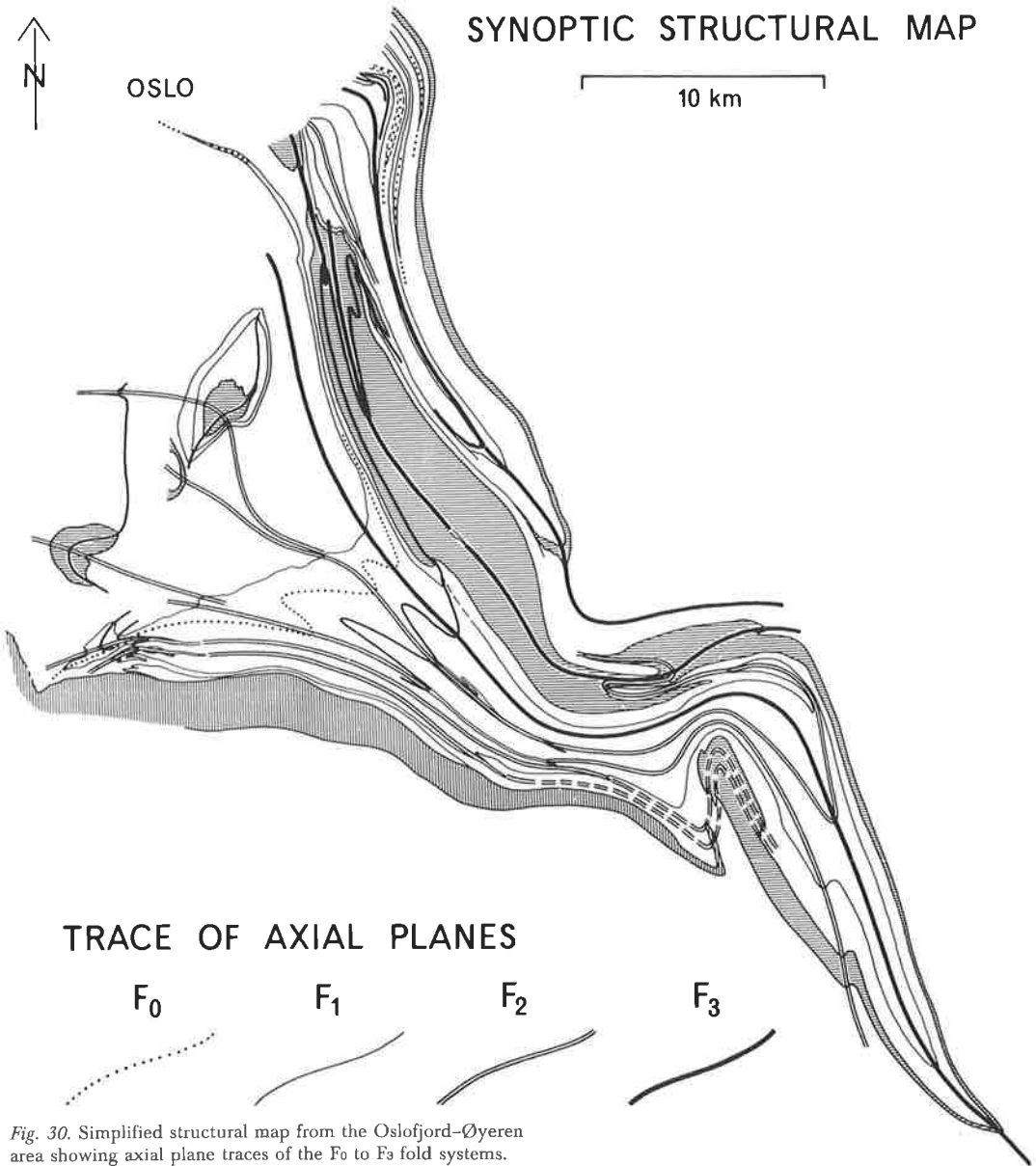


Fig. 30. Simplified structural map from the Oslofjord-Øyeren area showing axial plane traces of the F<sub>0</sub> to F<sub>3</sub> fold systems.

Strong lateral compression during the F<sub>3</sub> deformation is indicated by the amplitude/wavelength ratio (2:1) of the F<sub>3</sub> folds and by the pronounced rotation of the axial planes of the earlier folds into a subparallel orientation with the F<sub>3</sub> axial planes. Furthermore, the western limb of the Østmarka syncline is extremely flattened and partly sheared out.

A simplified map of the biotite gneiss out-

crop, partly omitting the F<sub>1</sub> and F<sub>2</sub> folds, demonstrates that the main outcrop pattern of the area is actually governed by superposition of the major F<sub>0</sub> and F<sub>3</sub> folds, which are thus more important than the F<sub>1</sub> and F<sub>2</sub> folds (Fig. 29). In this connection it also becomes clear that the bend of the F<sub>3</sub> (and older) folds in the Mjæren-Lyseren area is a late flexure. This late flexure is designated F<sub>3</sub>' (Fig. 24).

### STRUCTURAL POSITION OF THE METATONALITE/GRANITE COMPLEX

The metatonalite/granite complex has been omitted in the geometrical analysis although the rocks exhibit a deformation pattern formed during the  $F_3$  and  $F_2$  fold episodes. The Nordstrand-Sørmarka complex in the central part of the area was intruded after the  $F_1$  deformation. During the  $F_2$  deformation rocks of this complex were folded in the Gjer-

sjø dome, at the same time apparently acting as a competent rock unit which left the major  $F_1$  fold in the Gjersjø dome relatively unaffected. During the  $F_3$  deformation, the Nordstrand-Sørmarka complex was folded in the Østensjø anticlinorium to the north (Plate 2, section XIX), although the  $F_3$  fold system was arrested to the west in this complex which acted as a competent shield protecting the older structures to the west and southwest.

To the eastnortheast, the Østmarka metatonalite complex parallels the  $F_3$  folds and to the south the complex terminates in the core of the late  $F_3$ ' flexure (Fig. 32). The metatonalite complex may have acted as a competent body during the lateral E-W compression which during the latest stages was 'pushed' into the earlier formed steep  $F_3$  folds, indirectly causing the  $F_3$ ' flexure and thus the present varied orientation of the  $F_3$  axial planes. The shear zone northeast of the Østmarka metatonalite complex may then be ascribed to intense movement in the supra-crustal gneiss which gradually terminated in the eastern border zone of the competent body. This northeastern shear zone is part of the Dalsland boundary thrust (Skjernaa 1972, Berthelsen 1978) which delimits the Østfold segment to the east (Figs 1, 2 & 32).

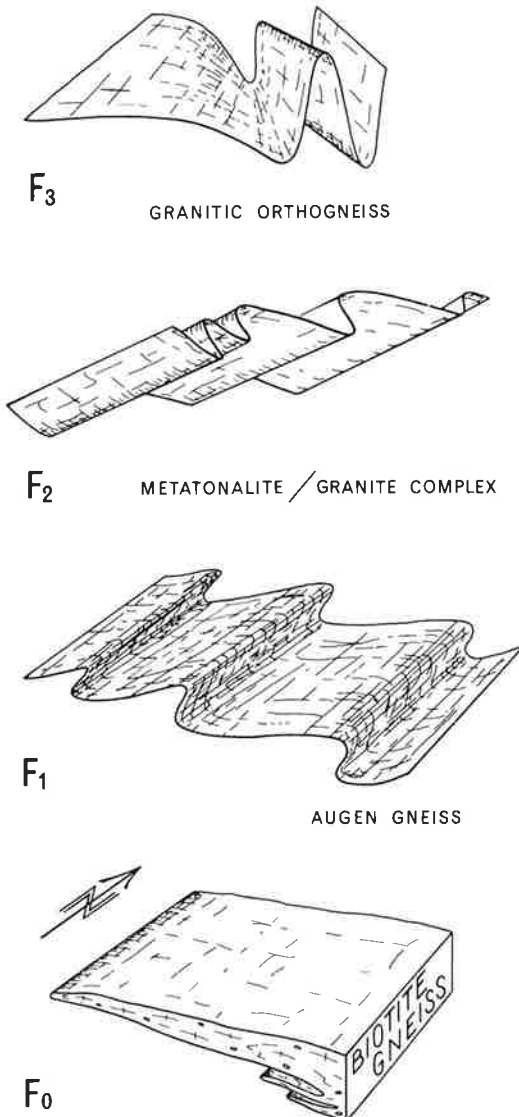


Fig. 31. Outline of the regional fold systems developed during the  $F_0$  to  $F_3$  deformation episodes. Rock units indicate relative positions of intrusive episodes.

### Correlation of the structural evolution in the Oslofjord-Øyeren area with that in adjoining areas in the Østfold and median segments

#### CORRELATION WITHIN THE ØSTFOLD SEGMENT

Within the Østfold segment, detailed mapping south (Hageskov & Pedersen 1980, Hageskov 1980) and southeast (Marker 1977, 1979) of the Oslofjord-Øyeren area has revealed a structural and metamorphic development which is in many ways similar to the evolution presented in this paper. However, a number of inconsistencies are apparent.

### *The Linnekleppen area*

The structural events of the Linnekleppen area (Marker 1977, 1979), 30 km southeast of the Oslofjord-Øyeren area, demonstrate that the  $F_1$  to  $F_3$  fold episodes of the two areas can be directly correlated; each fold phase shows similar characteristics in respect of trends of fold axes, structural style, vergence and magnitude of the structures. The original orientation of the  $F_1$  folds in the Linnekleppen area was not evaluated in great detail by Marker (1977), but if the effect of the major  $F_3$  folds is compensated by symmetrical opening of the fold around the ( $F_3$ ) axial plane, then the presumed  $F_1$  folds are found to be overturned to the east and to have N-S oriented axes; this corresponds to the conditions established in the Oslofjord-Øyeren area. A possible pre- $F_1$  history is suggested by the discordant relationship between the Linnekleppen intrusive complex (which was folded during the  $F_1$  deformation) and the surrounding supracrustal gneiss intercalated with biotite gneiss.

In both areas identical high-amphibolite facies conditions were reached during the  $F_1$  deformation, while during the subsequent  $F_2$  and  $F_3$  fold phase, medium-grade amphibolite facies conditions prevailed.

### *The southwest Østfold area*

An outline of the structural evolution covering the Oslofjord-Øyeren area and the adjoining area to the south (the southwest Østfold area) was presented by Graversen & Hageskov (1976). In this southern area (Hageskov 1980, Hageskov & Pedersen 1980), the structural evolution is characterized by older folds with N-S-trending axial surfaces, which were refolded by younger E-W-trending folds overturned to the south and with fold axes plunging to the W or WNW. These folds were subsequently reoriented to the east, parallel to the eastern margin of the Østfold segment along the Daland boundary thrust (Graversen & Hageskov 1976, Hageskov 1980). The metamorphism accompanying the oldest deformation is characterized by high-amphibolite facies while middle- to low amphibolite facies conditions prevailed during the following deformations (Hageskov

& Pedersen 1980). Since these deformation phases show structural and metamorphic characteristics similar to those of the  $F_1$  to  $F_3$  deformations of the Oslofjord-Øyeren area to the north, correlation of the deformation phases of the two areas seems probable.

Although the age relationships of the intrusive granitic gneisses and their host rocks in the two areas seem to be the same, a major discrepancy arises in respect of their structural age. According to Hageskov & Pedersen (1980, Table 1) all orthogneisses of granitic to tonalitic composition in the western Østfold area were emplaced subsequent to an old deformation following the deposition of the supracrustal gneiss (greywackes), but *prior* to development of N-S-trending folds ( $\sim F_1$ ). The Moss-Filtvet orthogneiss in the southern area is equivalent to the granitic orthogneiss in the Oslofjord-Øyeren area, and in both areas they are the youngest of the granitic intrusions. The geological evolution and structural model established to the north incorporates the intrusion of this orthogneiss between the  $F_2$  and  $F_3$  fold episodes. However, viewed from the south (Hageskov & Pedersen 1980), the same orthogneiss unit was apparently emplaced prior to the N-S-trending folds ( $\sim F_1$ ).

### CORRELATION BETWEEN THE ØSTFOLD AND MEDIAN SEGMENTS

The eastern demarcation of the Oslofjord-Øyeren area described in this paper is the Dalsland boundary thrust (Skjernaa 1972, Berthelsen 1977) which separates the Østfold segment from the median segment (Figs 1 and 2). The Dalsland boundary thrust is ascribed to the Dalsland deformation (Dalslandian) (Berthelsen 1978) which is the youngest deformation in the Sveconorwegian orogeny (Berthelsen 1980). The preceding major fold episodes,  $D_3$  and  $D_2$  (equivalent to Østfoldian and Värmlandian folding in Berthelsen (1978)), and a major metamorphic event during  $D_1$  all influence the 1277 Ma old red orthogneisses in the Rømskog-Aurland-Høland area (Skjernaa & Pedersen 1982); these deformation episodes are also included in the Sveconorwegian orogeny by Skjernaa et al. (1979), Berthelsen (1980) and Skjernaa & Pedersen (1982).

The  $F_3'$  deformation in the Oslofjord-Øyeren area described here is related to the late thrusting and can be correlated with the Dalsland deformation and  $D_4$  in the median segment. The earlier  $F_3$  and the  $D_3$  and Østfold deformations in the two areas are parallel, and both are cut by the Dalsland boundary thrust; folds belonging to these deformations can also be correlated. The Värmland and  $D_2$  deformation in the median segment is characterized by folds which are overturned to the south and have E-W to SE-NW-trending fold axes (Berthelsen 1977, 1978, 1980, Skjernaa & Pedersen 1982). Although this trend also characterizes the  $F_2$  folds in the Oslofjord-Øyeren area, an immediate correlation is questionable. In the median segment, the Värmland deformation post-dates the 1277 Ma red orthogneisses (Rømskog gneiss) (Skjernaa et al. 1979, Berthelsen 1980, Skjernaa & Pedersen 1982) while the  $F_2$  deformation (? 1500 Ma) in the Østfold segment predates the 1320 Ma Moss-Filtvet orthogneiss. Berthelsen's (1980, Fig. 2) structural map from southeast Norway and adjacent parts of Sweden which shows the Värmland axes and axial trends, further illustrates the difficulty of a possible correlation between the two segments, as the Värmland axes/axial trends in the Østfold segment are parallel not only to  $F_2$  fold axes, but also to  $F_1$  and  $F_3$  fold axes/axial trends (cf. Plate 3) in this multiply folded area.

A folding and metamorphic episode is established in the median segment between the 1631 Ma intrusive age of foliated grey orthogneisses (Langvass gneiss) and the ca. 1400 Ma sill-like layers of light grey granodioritic orthogneiss (Loppeholl gneiss) which cut the foliation (Pedersen 1979, Skjernaa & Pedersen 1982). This event in the median segment might be correlated with the (?) 1500 Ma event to the north in the Østfold segment which corresponds to the  $F_2$  deformation and metamorphism in the Oslofjord-Øyeren area. Possible equivalents of the  $F_1$  and  $F_0$  fold episodes in the Oslofjord-Øyeren area may also be present in the median segment where possibly one or more phases of folding and metamorphism predate the intrusion of the grey orthogneisses (1631 Ma) (Skjernaa & Pedersen 1982).

## Discussion of the results and aspects of the regional geology

The earliest recognized event of the Precambrian geological evolution of the Oslofjord-Øyeren area, and the Østfold area in general, is the deposition of supracrustal rocks of mainly sedimentary origin. Several orogenic episodes subsequently affected the area. The orogenic evolution has been inferred from the repeated intrusion of granitic rocks which are separated by regionally developed deformation episodes accompanied by amphibolite facies metamorphism. Dating of the later events was facilitated by radiometric whole-rock age determinations of the younger intrusive gneisses.

## STRUCTURAL CONSIDERATIONS

The structural analysis is based on stratiform intrusive bodies which outcrop in the supracrustal gneiss. These stratiform layers, however, may originally have been irregular intrusive bodies which were later modified by deformation such that their contacts are now parallel with the structure of the surrounding rock. The interpreted structures thus represent tectonic, intrusive levels which do not necessarily coincide with specific stratigraphic levels in the supracrustal sequence.

The age relationships of the intrusive granitic rocks have been deduced from their mesoscopic and microscopic structural and metamorphic evolution, combined with observed contact relations and the absence of presence of certain metabasic rocks. On an outcrop scale foliation in all the granitic rocks appears parallel to their contacts and to the foliation in the surrounding gneiss. However, on a regional scale the contacts of the intrusions have slightly discordant relationships, a feature more clearly seen in the younger intrusions.

A structural age relationship (i.e. the relative age of a rock unit in relation to structural episodes) of the intrusive gneisses has been established through geometrical analysis of the regional structure. The intrusion of the augen gneiss is thus separated from the older biotite gneiss by the proposed  $F_0$  fold episode, while during the  $F_1$  deformation both

rock units were folded together with the supracrustal gneiss. This deformation ( $F_1$ ) was succeeded by the intrusion of the tonalite/granite complex which in turn was folded during the  $F_2$  and  $F_3$ - $F_3'$  fold episodes. The southern and western granitic orthogneisses cut the regionally developed  $F_2$  folds in the southern part of the area and are thus separated from the metatonalite/granite complex by the  $F_2$  deformation. This macroscopic structural evolution of the individual intrusive gneiss units corroborates the succession established by the contact relationships and the mesoscopic and microscopic structures. The intrusion of the granitic gneiss units is thus separated by major deformation episodes and the most intensely reworked gneisses correspondingly display the least discordant contact relationships. The total thickness of the tectonostratigraphic sequence was estimated from the map (Plate 1) and the cross-sections in Plate 2 at about 2.5 km.

The style of folding which developed during each deformation phase (Fig. 31) indicates changing tectonic regimes governed mainly by subhorizontal stress fields. This, together with the repeated intrusion of granitic rocks as well as dolerite dykes, which were both separated by the regionally developed fold systems, indicates that the times of intrusion/folding constituted major breaks in the geological evolution of the area. The superimposed fold systems thus demonstrate diachronous refolding and a recycling of the older rocks.

#### OROGENIC EVOLUTION

The Østfold area is situated in the eastern subprovince (Berthelsen 1980) or marginal zone (Falkum & Petersen 1980) of the Sveconorwegian orogenic belt in the southwestern part of the Baltic Shield. The proposed interpretation of the structural evolution of the Oslofjord-Øyeren area places the  $F_3$  and  $F_3'$  events in the Sveconorwegian orogeny. These events are separated from  $F_2$  deformation by the Moss-Filtvet orthogneiss which has a 1320 Ma old intrusion age (Hageskov & Pedersen 1980). An older deformation episode around 1500 Ma ago is suggested by minimum reference ages of 1525 Ma and 1480

Ma (? metamorphism) obtained from two localities around Kolbotn in the Sørmarka metatonalite/granite complex (Pedersen 1979). This complex was emplaced subsequent to  $F_1$ , while the first deformation and metamorphism affecting the complex occurred during  $F_2$ . The possible metamorphism around 1500 Ma ago is therefore linked to the  $F_2$  deformation. These results indicate that the major tectonic-metamorphic evolution of the Oslofjord-Øyeren area took place in pre-(Grenville-) Sveconorwegian times. As the  $F_2$  deformation and metamorphism appear to have taken place 1500 Ma ago, the  $F_1$  and  $F_0$  deformations presumably relate to a pre-1500 Ma history. Incorporation of Svecokarelian elements in the early evolution cannot be excluded until results of further geological and radiometric work are available.

#### *Sveconorwegian deformation in the northern Østfold segment*

In the northern part of the Østfold segment (Figs 1 & 2) it is possible to distinguish a Sveconorwegian deformation zone to the east superimposed on the  $F_2$  (and older) fold systems occurring in a pre-Sveconorwegian area preserved around Bunnefjorden to the west (Fig. 32). The structural distinction between a stable western zone and a younger regeneration zone to the east was first established by Graversen & Hageskov (1976). The eastern zone is equivalent to the Enebakk-Rakkestad zone, and the western zone to the Vannsjø-Bunnefjorden zone established by Hageskov (1980).

The Sveconorwegian shear zones, the Oslofjord high-strain zone and the Dalsland boundary thrust (Fig. 32), define the boundaries of the Østfold segment and played an active role in the deformation pattern during the later stage of the Sveconorwegian orogeny. The Dalsland boundary thrust to the east is parallel to the main trend of the  $F_3$  folds in the northeastern part of the Østfold segment (Fig. 32). The later, large-scale,  $F_3'$  flexures in the Mjæren-Lyseren area, as well as a similar flexure suggested to the north in the Oslo area (Fig. 32), most probably developed along the margin of the Østfold segment during eastward thrusting. The Øst-

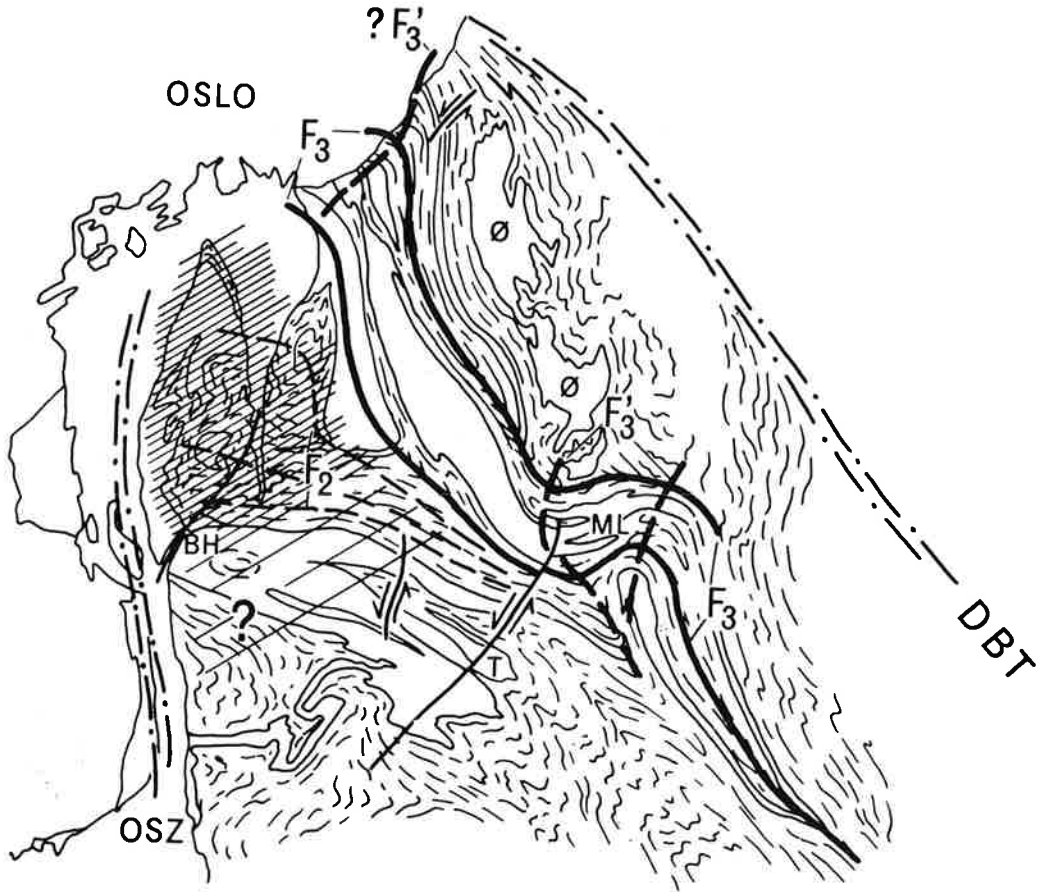


Fig. 32. Sveconorwegian structures in the northern Østfold segment (the Oslofjord-Øyeren area). The resistant pre-Sveconorwegian area (cross-hatched) to the northwest is bounded to the east by major Sveconorwegian folds ( $F_3$ ) that lie parallel to the Dalsland boundary thrust (DBT). See text for further explanation. Ø: Østmarka metatonalite complex, OSZ: Oslofjord strain zone, T: Tomter fault, BH: Bunnefjorden-Hallangspollen fault, ML: Mjæren-Lyseren area.

marka metatonalite complex may have acted as a competent body during this movement. Several major NE-SW-trending steep faults with sinistral displacement (e.g. the Tomter fault, Fig. 32) occur in connection with the flexures, and were probably the last movements associated with the thrusting. The Bunnefjorden-Hallangspollen fault in the southern part of Nesodden (BH, Fig. 32) may have also been active at this stage. The joints of the augen gneiss, as well as the faults which delineate the down-faulted Palaeozoic strata both in the Oslo area and along Lake Øyeren (Holtedahl 1907), also have NE-SW trends.

#### *Pre-Sveconorwegian evolution in the marginal zone of the Sveconorwegian orogenic belt*

The results obtained from the northern part of the Østfold segment concur with the major trends in the Kongsberg-Bamble segment to the west and with the Swedish part of both the Østfold and the median segments to the south.

In the Kongsberg and Bamble areas (Bugge 1936), the pre-Sveconorwegian evolution has been established mainly by Starmer (1972, 1977 & 1979) and supported by geochronological studies (O'Nions & Baadsgaard 1971,



O'Nions & Heier 1972, Jacobsen & Heier 1978, Field & Råheim 1979 a, b, 1980). Although a direct correlation is difficult, the sequence of events established by Starmer is similar to the evolution presented here.

In southwest Sweden 1600–1700 Ma old tonalitic to granodioritic intrusions were folded and metamorphosed prior to a period of plutonism at around 1400–1350 Ma (Samuelsson 1978, 1980, Daly et al. 1979, Gorbatshev & Welin 1980). It is thus evident that widespread orogenic activity (folding and metamorphism) occurred around 1500–1400 Ma ago in the southwestern part of the Baltic Shield.

In Sweden the 1600–1700 Ma old intrusions were emplaced into already folded, metamorphosed and migmatized St. Le-Marstrand rocks on Tjørn northwest of Göteborg (Welin & Gorbatshev 1978 c). In the Østfold-Øyeren area in the north of the Østfold segment, the main migmatization of the St. Le-Marstrand 'series' (the supracrustal gneiss unit) occurred during the  $F_1$  deformation. Thus, if early migmatization of the St. Le-Marstrand 'series' was simultaneous throughout the Østfold segment, then both the  $F_1$  and  $F_0$  fold episodes may conceivably have preceded the 1600–1700 Ma intrusive events.

*Acknowledgements.* – I thank professor S. Skjeseth, formerly Norges Landbrukshøyskole, Ås, who introduced me to the area. The study is part of the Østfold project initiated and guided by professor A. Berthelsen, Institut for almen Geologi, University of Copenhagen. The fieldwork was supported by Norges geologiske Undersøkelse and the Danish Natural Science Research Council, who also subsidized a revision of the English language and publication costs (J.nr. 11-0958 & 11-3345).

To my colleagues in the Østfold project, professor A. Berthelsen and drs B. Hageskov, S. Pedersen and L. Skjærnaa, I express my sincere thanks for valuable discussions during various stages of the work, and they have all critically reviewed an early draft of the manuscript.

Useful suggestions were also provided by Dr. H. P. Zeck, and valuable comments concerning the presentation were received from dr. phil. M. Ghisler. Dr. A. K. Higgins revised the English language and suggested several improvements in the text. Preparation of the illustrations for publication was undertaken by lithographer M. Schierling while P. Andersen typed the manuscript. To all I express my sincere thanks.

## References

- Barth, T. F. W. 1960: Southeastern Norway. In Høltedahl, O. (ed.) *Geology of Norway*. Norges geol. Unders. 208, 22–23.
- Barth, T. F. W. 1963: Southeastern Norway (the Østfold–Trysil area). In Rankama, K. (ed.) *The Precambrian*, vol. 1, 29–64. Interscience Publishers, New York.
- Becke, F. 1904: Über Mineralbestand und Struktur der kristallinen Schiefer. Congr. Geol. Internat. Compte Rendu de la IX Sess. Vienne 1903, 553–570.
- Berthelsen, A. 1960 a: Structural Studies in the Pre-Cambrian of Western Greenland. II Geology of Tovoquassap Nunå. *Bull. Granlands geol. Unders.* 25, 226 pp.
- Berthelsen, A. 1960 b: Structural Contour Maps Applied in the Analysis of Double Fold Structures. *Geol. Rundschau* 49, 459–466.
- Berthelsen, A. 1967: Grundfeldstektoniske studier omkring Moss (SØ-Norge). En foreløbig meddelelse. *Norges geol. unders.* 247, 51–56.
- Berthelsen, A. 1970: Globulith, a new type of intrusive structure, exemplified by metabasic bodies in the Moss area, SE Norway. *Nor. geol. unders.* 266, 70–85.
- Berthelsen, A. 1974: Methods used in the study of deep level tectonics. In Belliere, J. & Duchesne, J. C. *Géologie des domaines cristallins*. Société Géologique de Belgique, Liège.
- Berthelsen, A. 1977: Himalayan tectonics: A key to the understanding of Precambrian shield patterns. In *Colloques internationaux du C.N.R.S. No 268. Écologie et géologie de l'Himalaya*, 61–67. Centre National de la Recherche Scientifique, Paris.
- Berthelsen, A. 1978: Himalayan and Sveconorwegian tectonics – a comparison. In Saklani, P. S. (ed.) *Tectonic geology of the Himalaya*, 287–294. Today and Tomorrow's Printers & Publishers, New Delhi.
- Berthelsen, A. 1980: Towards a palinspastic tectonic analysis of the Baltic Shield. International Geological Congress, Paris, Colloquium C 6, 5–21.
- Broch, O. A. 1926: Ein suprakrustaler gneiskomplex auf der halbinsel Nesodden bei Oslo. *Norsk geol. Tidsskr.* IX, 81–223.
- Broch, O. A. 1964: Age determinations of Norwegian minerals up to March 1964. *Nor. geol. unders.* 228, 84–113.
- Brøgger, W. C. & Schetelig, J. 1900: Kristiania. Geologisk kart 1:100000. *Nor. geol. unders.* Published by Norges Geografiske Opmaaling.
- Bugge, A. 1936: Kongsberg–Bamble Formation. *Nor. geol. unders.* 146, 1–117.
- Daly, J. S., Park, R. G. & Cliff, R. A. 1979: Rb–Sr ages of intrusive plutonic rocks from the Stora Le–Marstrand belt in Orust, SW Sweden. *Precambrian Res.* 9, 189–198.
- Eskola, P. 1922: On contact phenomena between gneiss and limestone in western Massachusetts. *J. geol.* 30, 265–294.
- Falkum, T. & Petersen, S. 1980: The Sveconorwegian Orogenic belt, a case of Late–Proterozoic Plate–Collision. *Geol. Rundschau* 69, 622–647.
- Field, D. & Råheim, A. 1979 a: Rb–Sr total rock isotope studies on Precambrian charnockitic gneisses from south Norway: evidence for isochron resetting during a low-grade metamorphic-deformational event. *Earth Planet. Sci. Lett.* 45, 32–44.
- Field, D. & Råheim, A. 1979 b: A geologically meaningless Rb–Sr total rock isochron. *Nature* 282, 497–499.
- Field, D. & Råheim, A. 1980: Secondary geologically meaningless Rb–Sr isochrons, low  $^{87}\text{Sr}/^{86}\text{Sr}$  initial ratios and crustal residence times of high-grade gneisses. *Lithos* 13, 295–304.

- Gleditsch, C. 1952: Oslofjordens Prekambriske områder I. Indledende oversikt. Hurum. *Nor. geol. unders.* 181, 118 pp.
- Gorbatshev, R. 1980: The Precambrian development of southern Sweden. *Geol. För. Stockholm Förh.* 102, 129-136.
- Gorbatshev, R. & Welin, E. 1980: The Rb-Sr age of the Varberg chamoctite, Sweden: a reply and discussion of the regional contexts. *Geol. För. Stockholm Förh.* 102, 43-48.
- Graversen, O. 1973: Structural Interpretation of a Double-folded Gneiss-amphibolite Sequence, Bunnefjorden, Akershus. *Nor. geol. unders.* 300, 73-82.
- Graversen, O. 1974: Contemporaneous development of multilions and hornblende lineations in divergent directions. *Geol. Rundschau* 63, 335-340.
- Graversen, O. 1980: Intrusive meta-anorthosite/leucodiorite from the Precambrian of Akershus, SE Norway. *Norsk geol. Tidsskr.* 60, 131-137.
- Graversen, O. & Hageskov, B. 1971: Basic magma tectonics contrasted to folding of basic rocks. *Geol. Rundschau* 60, 1442-1455.
- Graversen, O. & Hageskov, B. 1976: Østfolds grundfjeld vest for Glomma. Abstract, XII Nordiska Geologvintermøtet, Göteborg.
- Hageskov, B. 1972: Shear-fold-like structures developed by progressive deformation of initial buckle folds. *Norsk geol. Tidsskr.* 52, 203-207.
- Hageskov, B. 1978: On the Precambrian structures of the Sandbukta-Mølen inlier in the Oslo graben, SE Norway. *Norsk geol. Tidsskr.* 58, 69-80.
- Hageskov, B. 1980: The Sveconorwegian structures of the Norwegian part of the Kongsberg-Bamble-Østfold segment. *Geol. För. Stockholm Förh.* 102, 150-155.
- Hageskov, B. & Jorde, K. 1980: Drøbak, berggrunnsgeologisk kart 1814 II - M. 1:50000. Foreløbig utgave. *Nor. geol. unders.*
- Hageskov, B. & Pedersen, S. 1980: Rb/Sr whole rock age determinations from the western part of the Østfold basement complex, SE Norway. *Bull. geol. Soc. Denmark* 29, 119-128.
- Hentschel, H. 1943: Die kalksilikatischen Bestandmassen in den Gneisen des Eulengebirges (Schlesien). *Mineral. Petrog. Mitt.* 55, 1-136.
- Holtedah, O. 1907: Alunskiferfeltet ved Øieren. *Nor. geol. unders.* 45, V. 1-16.
- Holtedah, O. & Dons, J. A. 1960: Geological map of Norway (Bedrock), 1:1.000.000. *Nor. geol. unders.*
- Jacobsen, S. B. & Heier, K. S. 1978: Rb-Sr isotope systematics in metamorphic rocks, Kongsberg sector, south Norway. *Lithos* 11, 257-276.
- Kalsbeek, F. 1970: The petrography and origin of gneisses, amphibolites and migmatites in the Quasigialik area, south-west Greenland. *Bull. Grønlands geol. Unders.* 83, 70 pp.
- Keilhau, B. M. 1850: *Gæa Norwegica*, 516 pp. Kristiania.
- Killeen, P. G. & Heier, K. S. 1975: A uranium and thorium enriched province of the Fenoscandian shield in southern Norway. *Geochim. Cosmochim. Acta* 39, 1515-1524.
- Kjerulf, T. 1857: Ueber die Geologie des südlichen Norwegens (mit Beiträgen von T. Dahll). *Nyt magasin for Naturvidenskaberne* 9, 193-333.
- Kjerulf, T. 1879: Udsigt over det sydlige Norges geologi, 262 pp. Den Kongelige Norske Regjerings Departement for det Indre, Christiania.
- Kjerulf, T. & Dahll, T. 1858-1865: Geologisk kart over det søndenfeldske Norge I. Christiania og Hamars Stifter i 6 blade 1:400000. Den Kongelige Norske Regjerings Departement for det Indre, Christiania.
- Kratz, K. O., Gerling, E. K. & Lobach-Zhuchenko, S. B. 1968: The isotope geology of the Precambrian of the Baltic Shield. *Can. J. Earth Sci.* 5, 657-660.
- Larsson, W. 1956: Beskrivning till kartbladet Värвик. Berggrunden. *Sveriges geol. Unders. Ser. Aa* 187, 10-127.
- Lundegårdh, P. H. 1958: Göteborgstraktens berggrund. *Sveriges geol. Unders. Ser. C*, 553, 82 pp.
- Lundqvist, T. 1979: The Precambrian of Sweden. *Sveriges geol. Unders. Ser. C*, 768, 87 pp.
- Magnusson, N. H. 1958: Karta över Sveriges Berggrund 1:1 mill., södra bladet. *Sveriges geol. Unders. Ser. Ba*, 16.
- Magnusson, N. H. 1960: Age determinations of Swedish Precambrian rocks. *Geol. För. Stockholm Förh.* 82, 407-432.
- Marker, M. 1977: Linnekleppen Massivet i SØ-Norges Prækambrium. Unpublished M.Sc.-thesis, 253 pp., Institut for almen Geologi, University of Copenhagen.
- Marker, M. 1979: Linnekleppen massivet med omgivende gneiser - tektonik i og omkring et granulitfacies massiv i Østfolds Prækambrium, SØ Norge. Abstract, 14. Nordisk geol. vintermøte 1980, Norsk geol. Forening, *Geolognytt* 13, 45.
- Mehnert, K. R. 1968: Migmatites and the origin of granitic rocks, 393 pp. Elsevier Publishing Company, Amsterdam 1968.
- Oftedah, C. 1974: Norges geologi. En oversikt over Norges regionalgeologi, 171 pp. Tapir, Trondheim 1974.
- O'Nions, R. K. & Baadsgaard, H. 1971: A radiometric study of polymetamorphism in the Bamble region, Norway. *Contr. Mineral. petrol.* 34, 1-21.
- O'Nions, R. K. & Heier, K. S. 1972: A reconnaissance Rb-Sr geochronological study of the Kongsberg area, south Norway. *Norsk geol. Tidsskr.* 52, 143-150.
- Pedersen, S. 1979: Geologisk og tektonisk udvikling i Syd-norge i den sidste del av Proterozoikum belyst ved Rb/Sr-aldersbestemmelser fra Østfold og Agder-Rogaland. Unpublished Ph.D.-thesis, 184 pp., Institut for almen Geologi, University of Copenhagen.
- Pedersen, S., Berthelsen, A., Falkum, T., Graversen, O., Hageskov, B., Maaløe, S., Petersen, J. S., Skjermå, L. & Wilson, J. R. 1978: Rb/Sr-dating of the plutonic and tectonic evolution of the Sveconorwegian Province, Southern Norway. In Zartman, R. E. (ed.) Short papers of the fourth international conference, geochronology, cosmochronology, isotope geology 1978. U.S. Geol. Surv. open-file report 78-701, 329-331.
- Pedersen, S., Skjermå, L. & Berthelsen, A. 1979: Rb/Sr age patterns in a multiple folded and metamorphosed plutonic complex: An example from SE-Norway. Abstract, ECOG VI, Lillehammer.
- Ramsay, J. G. 1958 a: Superimposed folding at Loch Monar, Inverness-Shire and Ross-Shire. *Q. Jl. geol. Soc. Lond.* CXIII, 271-305.
- Ramsay, J. G. 1958 b: Moine-Lewisian relations at Glenelg, Inverness-Shire. *Q. Jl. geol. Soc. Lond.* CXIII, 487-520.
- Ramsay, J. G. 1962: Interference patterns produced by the superposition of folds of similar type. *J. Geol.* 70, 466-481.
- Rankama, K. & Welin, E. 1972: Joint meeting of the Precambrian stratigraphy groups of Denmark, Finland, Norway, and Sweden in Turku, Finland, March 1972. *Geol. News* 4, 265-267.
- Rekstad, J. 1921: Eidsberg. De geologiske forhold innen rektangelkartet Eidsbergs område. *Nor. geol. unders.* 88, 1-76.
- Samuelsson, L. 1978: Beskrivning till berggrunskartan Göteborg SO, 1:50 000. *Sveriges geol. Unders. Ser. Af*, 177, 85 pp.
- Samuelsson, L. 1980: Major features of the Proterozoic of the Göteborg region, Sweden. *Geol. För. Stockholm Förh.* 102, 141-144.

- Sander, B. 1948: Einführung in die Gefügekunde der Geologischen Körper. Erster Teil: Allgemeine Gefügekunde und Arbeiten im Bereich Handstück bis Profil, 215 pp. Springer-Verlag, Wien.
- Sigmond, E. M. O., Gustavson, M. & Roberts, D. 1984: Berggrunnskart over Norge - M. 1:1 million. *Nor. geol. unders.*
- Skiöld, T. 1976: The interpretation of the Rb-Sr and K-Ar ages of late Precambrian rocks in south-western Sweden. *Geol. För. Stockholm Förh.* 98, 3-29.
- Skjerna, L. 1972: The discovery of a regional crush belt in the Ørje area, southeast Norway. *Norsk geol. Tidsskr.* 52, 459-461.
- Skjerna, L. & Pedersen, S. 1982: The effects on penetrative Sveconorwegian deformations on Rb-Sr isotope systems in the Rømskog-Aurskog-Høland area, SE-Norway. *Precambrian Res.*, 17, 215-243.
- Skjerna, L., Berthelsen, A. & Pedersen, S. 1979: Relationer mellem Rb/Sr dateringer og deformationsmønstre: et eksempel fra SØ-Norge. Abstract, 14. Nordiske geol. vintermøte 1980, Norsk geol. Forening. *Geologymitt* 13, 66.
- Starmer, I. C. 1972: The Sveconorwegian regeneration and earlier orogenic events in the Bamble series, South Norway. *Nor. geol. unders.* 277, 37-52.
- Starmer, I. C. 1977: The geology and evolution of the south-western part of the Kongsberg series. *Norsk geol. Tidsskr.* 57, 1-22.
- Starmer, I. C. 1979: The Kongsberg Series margin and its major bend in the Flesberg area, Numedal, Buskerud. *Nor. geol. unders.* 351, 99-120.
- Steiger, R. H. & Jäger, E. 1977: Convention on the use of decay constants in geo- and cosmochronology. *Earth Planet. Sci. Lett.* 36, 359-362.
- Streckeisen, A. 1974: Classification and Nomenclature of Plutonic Rocks. *Geol. Rundschau* 63, 773-786.
- Tröger, W. E. 1971: Optische Bestimmung der gesteinsbildenden Minerale, Teil 1: Bestimmungstabellen, 4. Auflage. E. Schweizerbartsche Verlagsbuchhandlung, Stuttgart.
- Turner, F. J. 1968: *Metamorphic petrology*, 403 pp. McGraw-Hill Book Company, New York.
- Turner, F. J. & Weiss, L. E. 1963: *Structural analysis of metamorphic tectonites*, 545 pp. McGraw-Hill Book Company, New York.
- Verstevee, A. J. 1975: Isotope geochronology in the high-grade metamorphic Precambrian of southwestern Norway. *Nor. geol. Unders.* 318, 1-50.
- Wegmann, C. E. 1930: Über Diapirismus (besonders im Grundgebirge). *Bull. Comm. géol. Finlande* 92, 58-76.
- Welin, E. & Gorbatschev, R. 1976 a: A Rb-Sr geochronological study of the older granitoids in the Åmål tectonic mega-unit, south-western Sweden. *Geol. För. Stockholm Förh.* 98, 374-377.
- Welin, E. & Gorbatschev, R. 1976 b: Rb-Sr age of granitoid gneisses in the «Pregothian» area of south-western Sweden. *Geol. För. Stockholm Förh.* 98, 378-381.
- Welin, E. & Gorbatschev, R. 1978 a: Rb-Sr age of the Lane granites in south-western Sweden. *Geol. För. Stockholm Förh.* 100, 101-102.
- Welin, E. & Gorbatschev, R. 1978 b: The Rb-Sr age of the Varberg charnockite, Sweden. *Geol. För. Stockholm Förh.* 100, 225-227.
- Welin, E. & Gorbatschev, R. 1978 c: Rb-Sr isotopic relations of a tonalitic intrusion on Tjörn Island, south-western Sweden. *Geol. För. Stockholm Förh.* 100, 228-230.
- Welin, E. & Gorbatschev, R. 1978 d: A Rb-Sr age of the Åmål granite at Åmål, Sweden. *Geol. För. Stockholm Förh.* 100, 401-403.
- Wielens, J. B. W., Adriessen, P. A. M., Boelrijk, N. A. I. M., Hebeda, E. H., Priem, H. N. A., Verdurmen, E. A. Th. & Verschure, R. H. 1980: Isotope geochronology in the high-grade metamorphic Precambrian of southwestern Norway: new data and reinterpretations. *Nor. geol. unders.* 359, 1-30.
- Wynne-Edwards, H. R. 1972: The Grenville Province. In Price, R. A. & Douglas, R. J. W. (eds.) Variations in tectonic styles in Canada. *Geol. Assoc. Canada, Spec. Paper No. 17*, 263-334.
- Wynne-Edwards, H. R. & Hassan, Z.-ul 1970: Intersecting orogenic belts across the North Atlantic. *Amer. J. Sci.* 268, 289-308.
- Zetterström, C. 1974: Dome-bassin strukturer i grundfeltet mellem Kolbotn og Bunnefjorden, Akershus. *Nor. geol. unders.* 304, 47-54.
- Zwart, H. J. & Domsiepen, U. F. 1978: The tectonic framework of Central and Western Europe. In van Loon, A. J. (ed.) Key-notes of the MEGS-11 (Amsterdam). *Geol. Mijnb.* 57, 627-654.

TABLE 1. CHRONOLOGY OF THE PRECAMBRIAN GEOLOGICAL EVENTS IN THE OSLOFJORD - ØYEREN AREA				
MAIN OROGENIC EVENTS	DEFORMATION AND AGE / PERIOD OF INTRUSION / METAMORPHISM	INTRUSION OF GRANITIC ROCKS	INTRUSION OF BASIC DYKES	REGIONAL METAMORPHISM
	(PERMIAN)		(RHOMB - PORPHYRY DYKES AND MINOR DOLERITE DYKES)	
(GREENVILLE - ) SVECONORWEIGIAN OROGENY	900 Ma	BOHUSLEN - IDDEFJORD PEGMATITES		
	F <sub>3</sub> FOLDING AND SHEARING			GREENSCHIST - AMPHIBOLITE TRANSITION FACIES
	F <sub>3</sub> FOLDING (NNW - AXES)			MEDIUM - LOW AMPHIBOLITE FACIES
	1320±22 Ma	GRANITIC ORTHOGNEISS	BASIC DYKES	
	F <sub>2</sub> FOLDING (NW - AXES)			MEDIUM AMPHIBOLITE FACIES
	( ? ) 1500 Ma	METATONALITE / GRANITE COMPLEX	BASIC DYKES	
	F <sub>1</sub> FOLDING (NNE - SSW AXES)			MEDIUM - HIGH AMPHIBOLITE FACIES WITH INTENSE MIGMATIZATION
		AUGEN GNEISS		
SVECKARELIAN OROGENY ?			GARNET AMPHIBOLITES / META - ANORTHOSITE / LEUCODIORITE	
	F <sub>0</sub> FOLDING (N - S AXES)			?
		BIOTITE GNEISS		
	?			?
	DEPOSITION OF SEDIMENTS, NOW THE SUPRACRUSTAL GNEISS			



# RECENT MAPS PUBLISHED BY NGU

(A list of earlier maps appears on the inside back cover of all Bulletins and Skrifter from and including Bulletin 20, NGU nr. 300)

MAPS PRINTED IN COLOUR (On sale from Universitetsforlaget, N.kr. 30,-).

1:250 000	Mandal		Bedrock geology 1: 50 000	1117 IV	Askvoll	Quaternary geology
	Mosjøen		→→	2016 IV	Elverum	→→
	Nordkapp		→→	1917 I	Evenstad	→→
				1815 I	Gran	→→
1: 50 000	2028 I	Beiardalen	Bedrock geology	1817 II	Lillehammer	→→
	1413 IV	Botsvatn	→→	1713 IV	Nordagutu	→→
	1720 II	Brekken	→→	1935 I	Repparfjorden	→→
	1716 I	Bruflat	→→	1417 IV	Solvorn	→→
	1719 II	Elgå	→→	1917 III	Åsmarka	→→
	1916 IV	Hamar	→→			
	1214 IV	Husnes	→→	1816 I	Gjøvik	Sand and gravel resources
	1916 I	Løten	→→			
	1720 III	Røros	→→			
	1918 III	Stor-Elvdal	→→			
	1918 II	Storsjøen	→→			
	1414 II	Sæsvatn	→→			
1: 20 000	Brandbu	CKL 057058-20	Lunner	CMN 053054-20		Quaternary geology
	Brattli	HUV 269370-20	Lygna	CMN 057058-20		→→
	Drammen	CHJ 041042-20	Mosjøen	DMN 181182-20		→→
	Gran	CMN 055056-20	Olderskog	DOP 181182-20		→→
	Grymyr	CKL 055056-20				
	Jømna	CWX 065066-20	Skei	BQR 115116-20		→→
	Kulstad	DMN 183184-20	Stiklestad	CUV 135136-20		→→
	Langvasseid	HST 269270-20	Tromsdalen	CUV 133134-20		→→
	Levanger	CST 133134-20	Vardefjell	DOP 183184-20		→→
1: 10 000	Helgja	BW 030-10				Quaternary geology

MAPS IN BLACK AND WHITE (on sale direct from NGU either as paper-copies (N.kr. 12,-) or as transparent-copies (N.kr. 100,-)).

1:250 000	Bodø		Bedrock geology	(preliminary)
	Lillehammer		→→	→→
	Røros		→→	→→
	Stavanger		→→	→→
	Sveg		→→	→→
	Tromsø		→→	→→
	Vega		→→	→→
1: 50 000	2135 I	Adamsfjord	Bedrock geology	(preliminary)
	1611 IV	Arendal	→→	→→
	1517 III	Borgrund	→→	→→
	1318 III	Breim	→→	→→
	1218 II	Fimlandsgrend	→→	→→
	1817 III	Follebu	→→	→→
	1927 I	Mo i Rana	→→	→→
	1418 II	Mørkrisdalen	→→	→→
	1824 I	Namskogen	→→	→→
	1818 I	Sollia	→→	→→
	2029 III	Strømøen	→→	→→
	1518 III	Sygnefjell	→→	→→
	1533 III	Takvatnet	→→	→→
	2135 II	Ul'lugai'sa	→→	→→
	1316 II	Ulvik	→→	→→
	1316 III	Voss	→→	→→
	1521 II	Hølonda	Natural environmental potential (GMNEP)	
	1521 I	Orkanger	→→	
	1612 III	Støren	→→	
	1612 IV	Trondheim	→→	

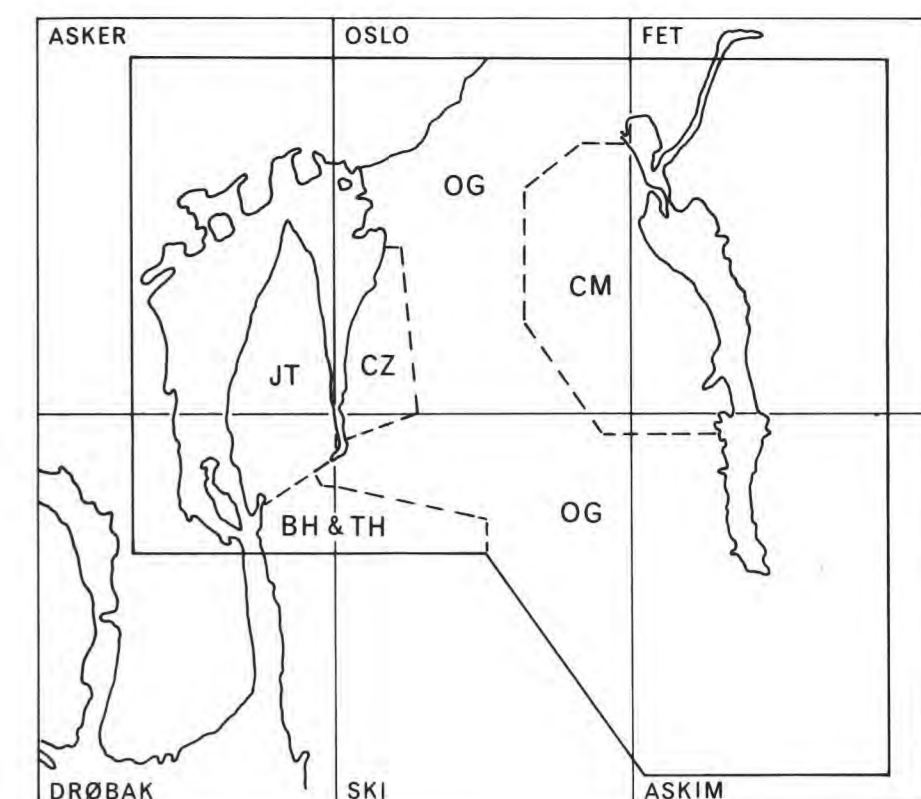
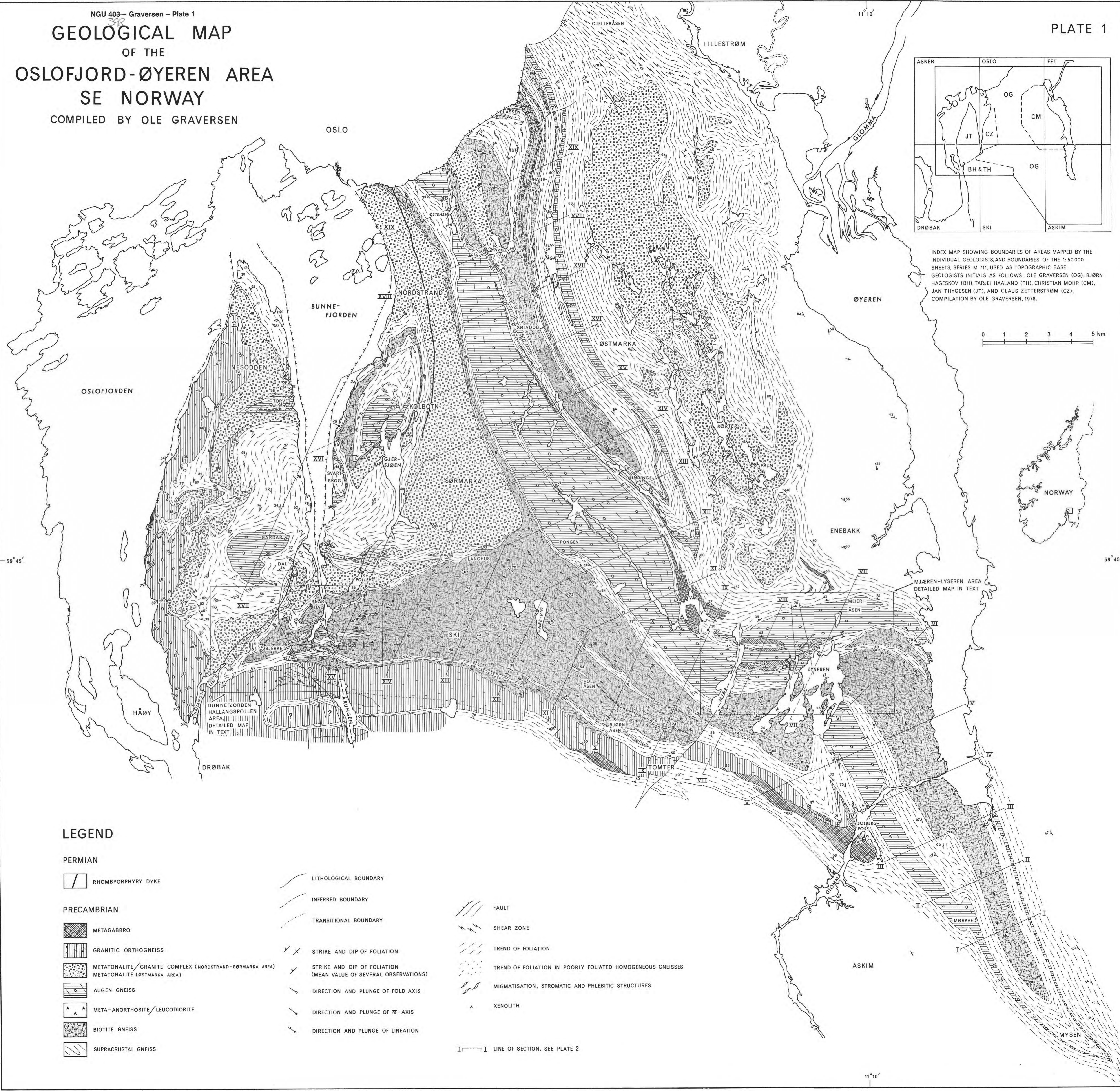
A list of other maps (hydrogeology, geochemistry, geophysics) issued by the Geological Survey is available upon request.

# GEOLOGICAL MAP

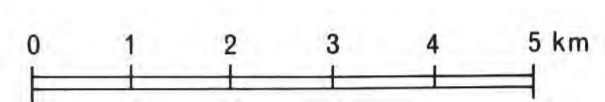
OF THE

## OSLOFJORD-ØYEREN AREA SE NORWAY

COMPILED BY OLE GRAVERSEN



INDEX MAP SHOWING BOUNDARIES OF AREAS MAPPED BY THE INDIVIDUAL GEOLOGISTS, AND BOUNDARIES OF THE 1:50 000 SHEETS, SERIES M 711, USED AS TOPOGRAPHIC BASE. GEOLOGISTS INITIALS AS FOLLOWS: OLE GRAVERSEN (OG), BJØRN HAGESKOV (BH), TARJEI HAALAND (TH), CHRISTIAN MOHR (CM), JAN THYGESSEN (JT), AND CLAUD ZETTERSTRØM (CZ). COMPILATION BY OLE GRAVERSEN, 1978.



59°45'

59°45'

### LEGEND

#### PERMIAN

RHOMBPORPHYRY DYKE

#### PRECAMBRIAN

- METAGABBRO
- GRANITIC ORTHOGNEISS
- METATONALITE/GRANITE COMPLEX (NORDSTRAND-SØRMARKA AREA)  
METATONALITE (ØSTMARKA AREA)
- AUGEN GNEISS
- META-ANORTHOSITE/LEUCODIORITE
- BIOTITE GNEISS
- SUPRACRUSTAL GNEISS

LITHOLOGICAL BOUNDARY

INFERRED BOUNDARY

TRANSITIONAL BOUNDARY

STRIKE AND DIP OF FOLIATION

STRIKE AND DIP OF FOLIATION (MEAN VALUE OF SEVERAL OBSERVATIONS)

DIRECTION AND PLUNGE OF FOLD AXIS

DIRECTION AND PLUNGE OF  $\pi$ -AXIS

DIRECTION AND PLUNGE OF LINEATION

FAULT

SHEAR ZONE

TREND OF FOLIATION

TREND OF FOLIATION IN POORLY FOLIATED HOMOGENEOUS GNEISSES

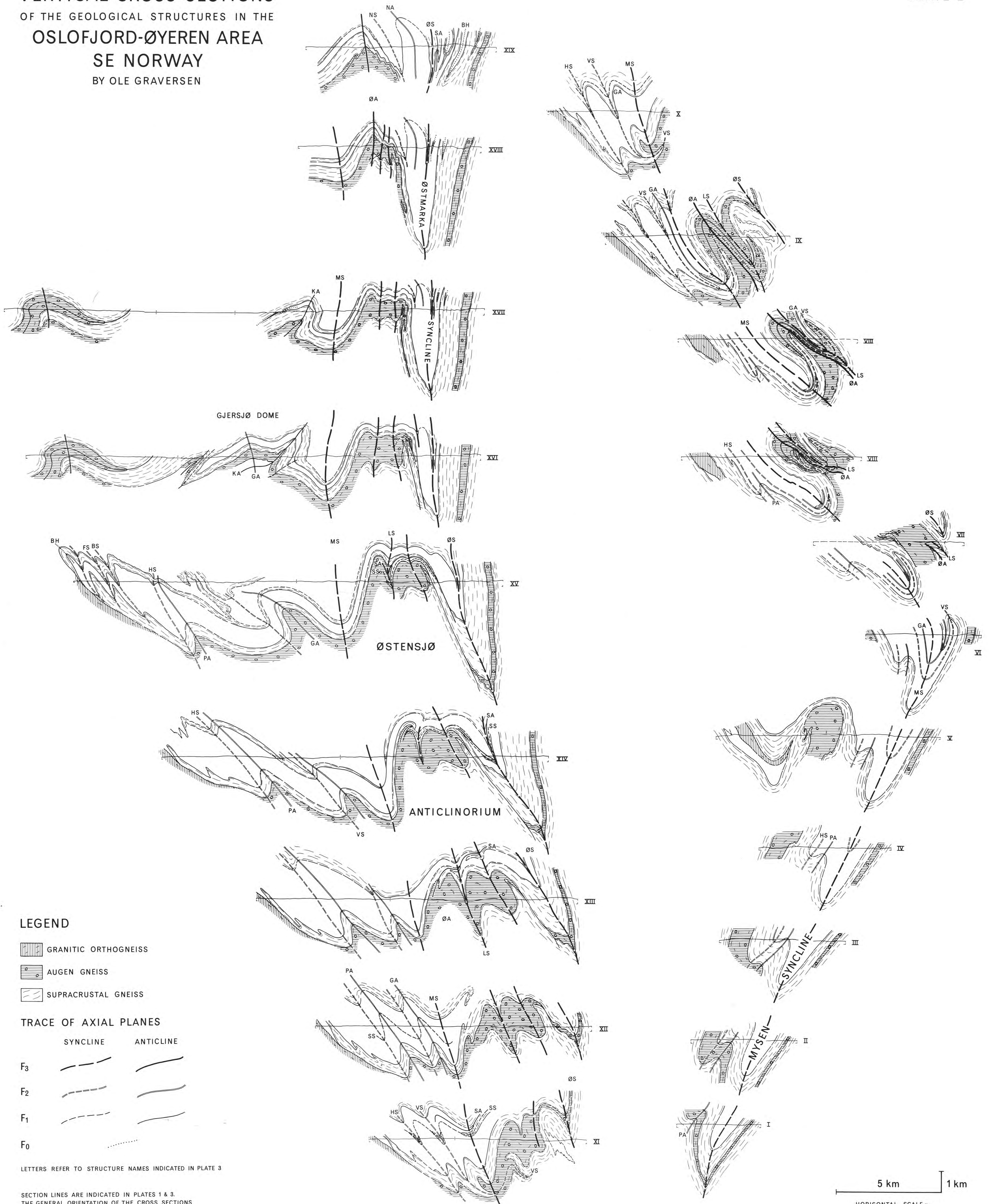
MIGMATISATION, STROMATIC AND PHELBIC STRUCTURES

XENOLITH

LINE OF SECTION, SEE PLATE 2

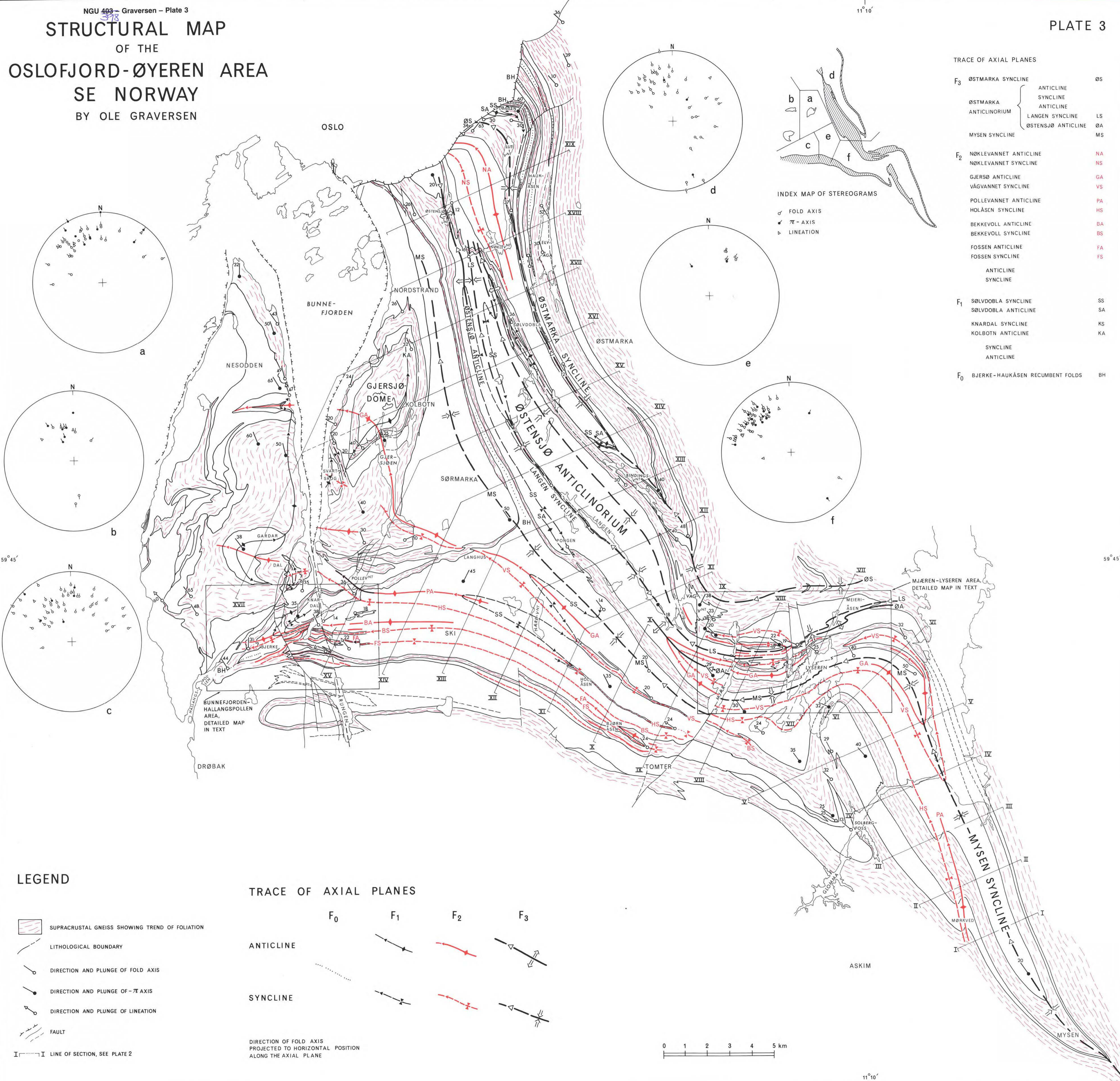
11°10'

# VERTICAL CROSS SECTIONS OF THE GEOLOGICAL STRUCTURES IN THE OSLOFJORD-ØYEREN AREA SE NORWAY BY OLE GRAVERSEN



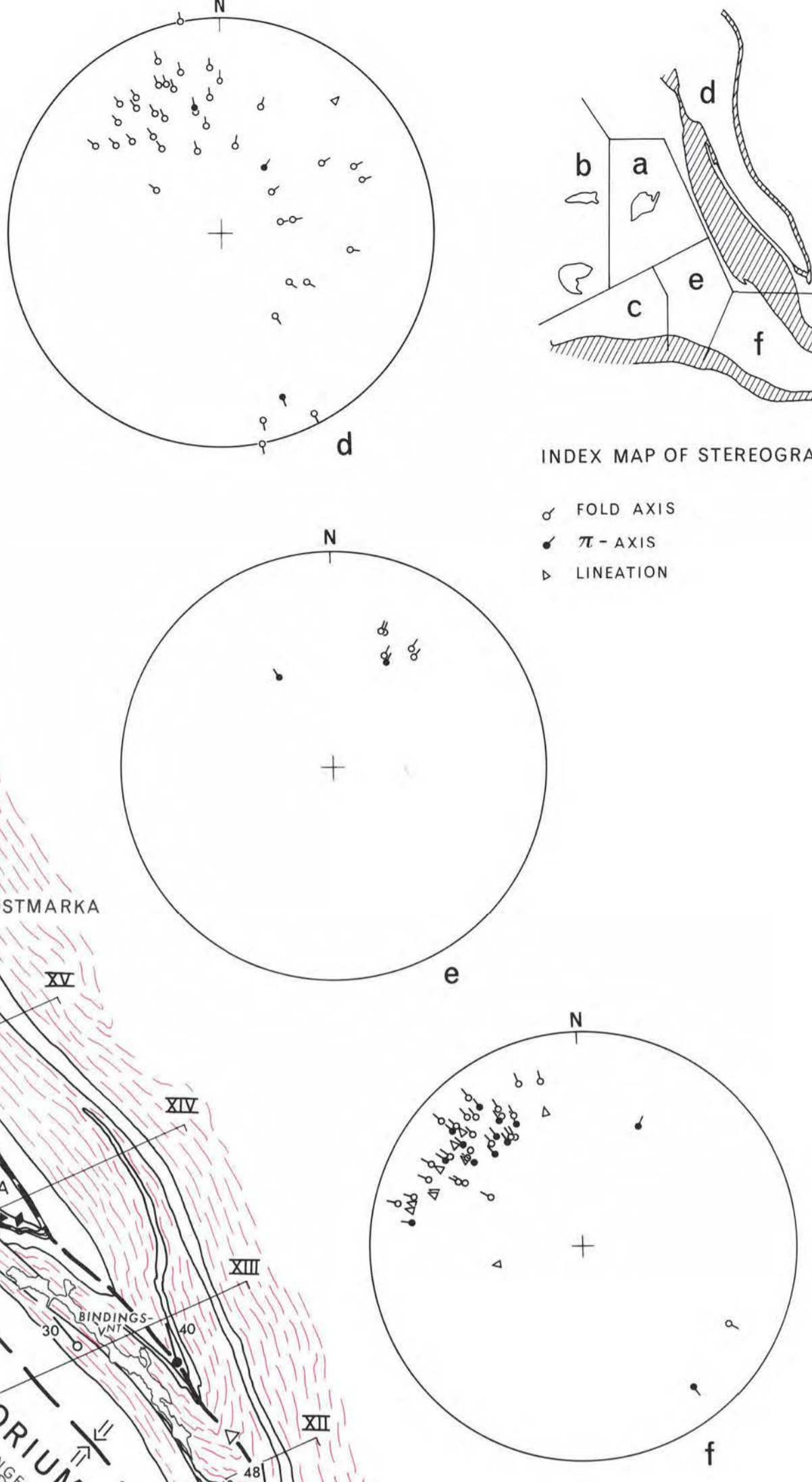
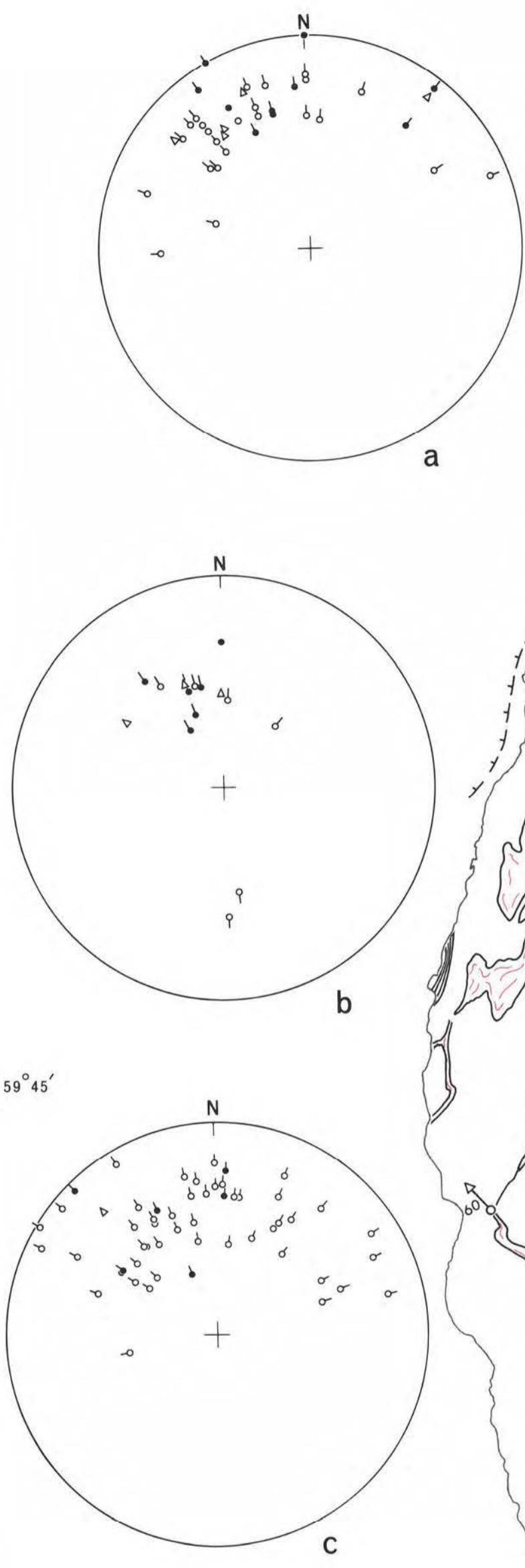
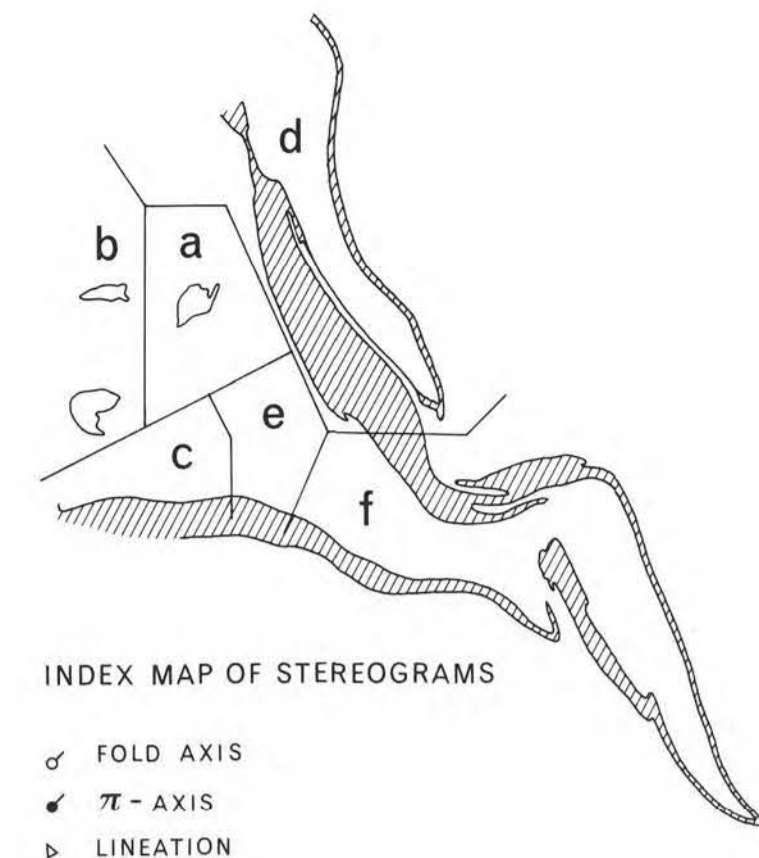


# STRUCTURAL MAP OF THE OSLOFJORD-ØYEREN AREA SE NORWAY BY OLE GRAVERSEN



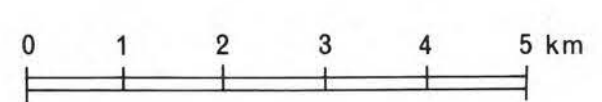
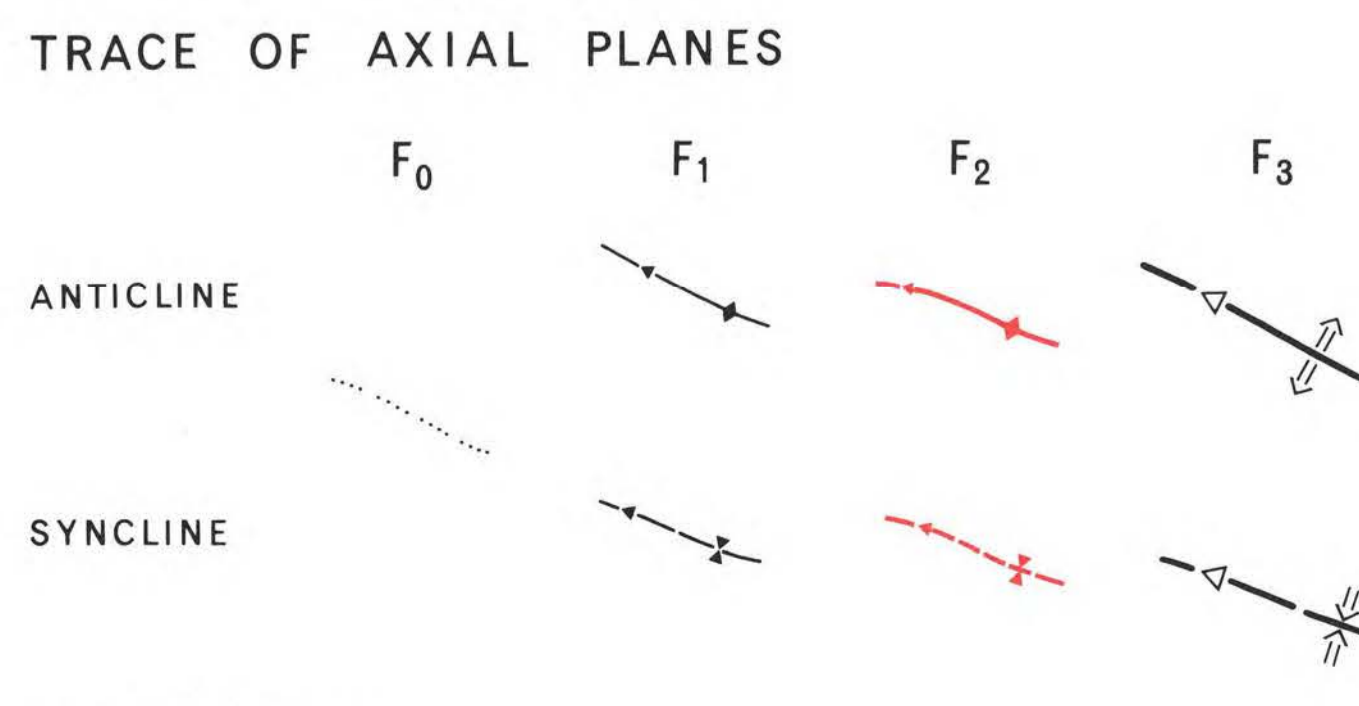
TRACE OF AXIAL PLANES

F <sub>3</sub>	ØSTMARKA SYNCLINE	ØS
F <sub>3</sub>	ØSTMARKA ANTICLINORIUM	LS
	ANTICLINE	
	SYNCLINE	
	LANGEN SYNCLINE	ØA
	ØSTENSJØ ANTICLINE	MS
	MYSEN SYNCLINE	
F <sub>2</sub>	NØKLEVANNET ANTICLINE	NA
	NØKLEVANNET SYNCLINE	NS
	GJERSJØ ANTICLINE	GA
	VÅGVANNET SYNCLINE	VS
	POLLEVANNET ANTICLINE	PA
	HOLLÅSEN SYNCLINE	HS
	BEKKEVOLL ANTICLINE	BA
	BEKKEVOLL SYNCLINE	BS
	FOSSEN ANTICLINE	FA
	FOSSEN SYNCLINE	FS
	ANTICLINE	
	SYNCLINE	
F <sub>1</sub>	SØLVDOBLA SYNCLINE	SS
	SØLVDOBLA ANTICLINE	SA
	KNARDAL SYNCLINE	KS
	KOLBOTN ANTICLINE	KA
	SYNCLINE	
	ANTICLINE	
F <sub>0</sub>	BJERKE-HAUKÅSEN RECUMBENT FOLDS	BH

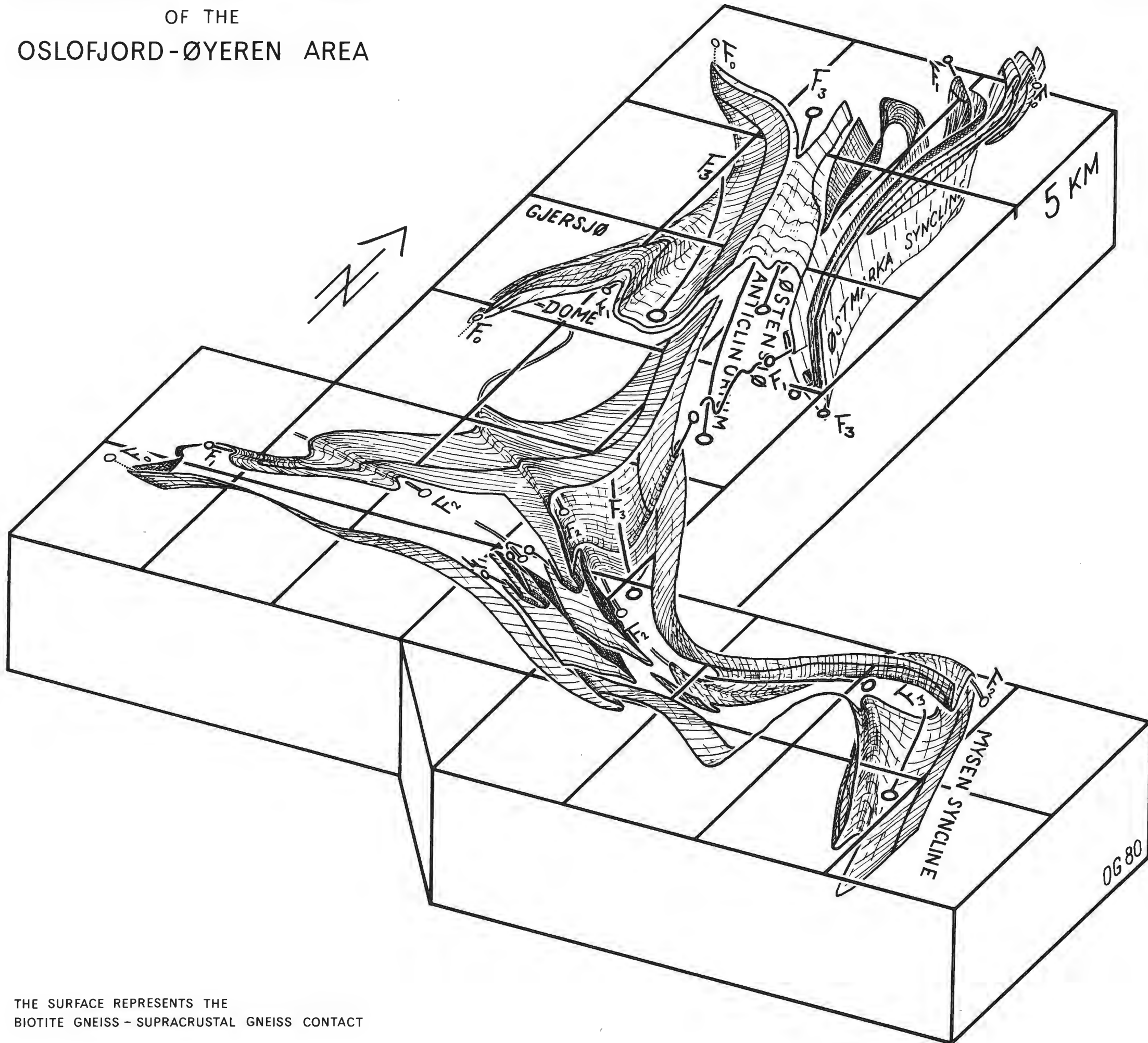


## LEGEND

- SUPRACRUSTAL GNEISS SHOWING TREND OF FOLIATION
- LITHOLOGICAL BOUNDARY
- DIRECTION AND PLUNGE OF FOLD AXIS
- DIRECTION AND PLUNGE OF π - AXIS
- DIRECTION AND PLUNGE OF LINEATION
- FAULT



STRUCTURAL STEREOGRAM  
OF THE  
OSLOFJORD-ØYEREN AREA



THE SURFACE REPRESENTS THE  
BIOTITE GNEISS - SUPRACRUSTAL GNEISS CONTACT